ABSTRACT

This thesis describes experiments on the thermal conductivity of some two-phase composites between 2 K and room temperature. The composites are made from particulate, non-metallic fillers of glass, crystalline quartz and alumina, and diamond embedded in a matrix of a thermosetting epoxy resin, Araldite MY 740. Filler particles, ranging from a size of 2 to 150 microns have been used in this work.

Chapter 2 gives a review of the theory of heat transport in insulating crystals and amorphous glasses and polymers. There is also an account of the various methods predicting the thermal conductivity of two-phase composites with particulate fillers.

Chapter 3 gives a general account of epoxy resins, the type of fillers used in epoxy resins and the effect of fillers on various physical properties of the system. A description of the specimen preparation is also given. The specimens were all prepared in the same way and the same epoxy has been used throughout this work.

Chapter 4 describes the experimental techniques and apparatus. The thermal conductivity was measured by the conventional steady-state method using cryostats of straight-forward design. Differential gold-iron (0.03 at %) versus chromel thermocouples were used for temperature measurement from liquid hydrogen temperatures down to 2 K. Above these temperatures differential copper versus constantan thermocouples were used. Great care was taken to minimize errors due to radiation from the sides of specimen at temperatures of 76 K and

above.

Chapter 5 describes some experiments on the unfilled epoxy and chapter 6 some experiments on the filled epoxies. The effect on the composite thermal conductivity of the filler thermal conductivity, filler volume concentration and filler particle size and shape has been studied.

Above helium temperatures the thermal conductivity of the two phase composites is dependent on the thermal conductivities of the epoxy matrix and filler, the volume concentration of the filler and the shape of the filler particles. The size of the particles is also important for crystalline filling materials when their thermal conductivity becomes size dependent due to the frequency independent phonon mean free path of boundary scattering.

At helium temperatures a pronounced size effect is found in which the smaller the particle size the lower is the resulting composite thermal conductivity, all other things being equal. This size dependence is found to b much greater than would be expected from considerations of the size dependent thermal conductivity of crystalline filler materials in the boundary scattering region. This discrepancy is believed to be a result of the presence of a thermal contact resistance at the filler-epoxy interface due to phonon mismatch at the interface.

Generally, bulk displacement of the epoxy with a filler whose thermal conductivity is higher than that of the matrix produces composites whose thermal conductivity is higher than that of the

epoxy, and increasing filler volume concentration results in increasing composite conductivity. At helium temperatures this may not be so. The presence of a thermal contact resistance between the matrix and filler can result in composites whose thermal conductivities are substantially lower than that of the matrix and an increase in the filler concentration produces a decrease in the composite thermal conductivity.

The experimental results have been compared with the various predictions of the thermal conductivity of two-phase composites. At liquid hydrogen temperatures and above predictions using the theory of Maxwell and Rayleigh to which an extra factor to take account of the shape of the particle are in reasonable agreement with the experimental results. At liquid helium temperatures the presence of a thermal contact resistance will result in this theory predicting values which are much higher than those found by experiment. An attempt has been made to include the effect of this thermal contact resistance in the theoretical predictions and this does enable a fairly satisfactory explanation to be given of the low temperature measurements.

BODLEIAN LIBRARY OXFORD
DEPOSITED THESIS
17.1.73

THE THERMAL PROPERTIES OF COMPOSITE MATERIALS

by

K. W. GARRETT
Brasenose College
Oxford

A thesis submitted for the degree of Doctor of Philosophy in the University of Oxford.

September 1972

A C K N O W L E D G E M E N T S

It is a pleasure to offer my particular thanks to the following:

Professor B. Bleaney, F.R.S. for making the facilities of the Clarendon Laboratory available to me.

Dr. H. M. Rosenberg for his encouragement and enthusiastic supervision.

Dr. D. K. Carrod and Dr. M. Metcalfe for the introduction to low temperature physics.

Dr. J. Wilks, Dr. D. Driver and Mr. C. M. Lanigham for extending to me the use of the scanning electron microscope.

Mr. E. S. Look and all other workshop staff who have helped in building and maintaining apparatus.

My mother-in-law and father-in-law for the typing and binding of the thesis, so patiently undertaken.

Finally to the Rutherford High Energy Laboratory for a maintenance grant.

C O N T E N T S

		Page
CHAPTER 1	INTRODUCTION	1.1
CHAPTER 2	THEORY	
	2.1 Lattice vibrations and thermal conductivity	2.1
	2.2 Phonon-phonon interactions	2.3
	2.3 Boundary scattering	2.5
	2.4 The thermal conductivity of glasses and polymers	2.6
	2.5 Contact resistance at low temperatures	2.14
	2.6 Theoretical equations for predicting the thermal conductivity of two-phase composites	2.16
	a) Introduction	2.16
	b) Exact solutions	2.17
	c) Simplified solutions	2.20
CHAPTER 3	EPOXIES, FILLERS AND SAMPLE PREPARATION	
	3.1 Introduction	3.1
	3.2 The cure and properties of the cured epoxies	3.3
	3.3 The use of modifying agents in epoxy systems	3.4
	3.4 The effect of fillers on the viscosity of the epoxy system and the settling properties of fillers	3.7

		Page
	3.5 Specimen preparation	3.8
	3.6 Particle size of fillers and test sieving	3.10
	3.7 Precautions for handling epoxy resins and mineral powders	3.13
CHAPTER 4	EXPERIMENTAL TECHNIQUES	
	4.1 Outline of the method	4.1
	4.2 The cryostats	4.2
	a) Cryostat I for temperatures below 20 K	4.2
	b) Cryostat II for temperatures above 77 K	4.2
	4.3 Specimen mounting and heater arrangement	4.3
	a) Specimens for measurements below 20 K	4.3
	b) Specimens for measurements above 77 K	4.4
	4.4 Specimens for measuring the thermal contact resistance	4.6
	4.5 Thermometry	
	a) Choice of the gold-iron versus chromel thermocouple	4.7
	b) Calibration	4.9
	c) The thermocouple circuitry and voltage measurement	4.10
	4.6 Experimental details	4.12
	4.7 Possible sources of error in the measurement	4.14

		Page
	a) Error in the form factor	4.14
	b) Heat flow along thermometer leads	4.14
	c) Errors in measured specimen heater power	4.15
	d) Error in calibration of the thermocouples	4.16
	e) Error in the thermocouple voltage measurement	4.16
4.8	Summary of the accuracy of the experiment	4.16
	a) Errors in the determination of the absolute magnitude of the thermal conductivity	4.16
	b) Relative errors in the thermal conductivity measured at different temperatures	4.17
CHAPTER 5	EXPERIMENTS ON THE UNFILLED EPOXY	
	5.1 Experimental results and discussion	5.1
CHAPTER 6	EXPERIMENTS WITH FILLED EPOXIES	
	GLASS FILLED EPOXIES	
	6.1 Specimens	6.1
	6.2 Results	6.2
	6.3 Comparison between theory and experiment	6.4
	QUARTZ FILLED EPOXIES	
	6.4 Samples	6.8

		Page
6.5	Experimental results	6.9
6.6	Comparison of the high temperature results with theorh	6.12
6.7	Comparison of the low temperature results with theory	6.16
ALUMINA FILLED EPOXIES		
6.8	Specimens	6.20
6.9	Experimental results	6.21
6.10	Comparison of high temperature results with theory	6.23
6.11	Comparison between theory and experimental results at helium temperatures	6.25
DIAMOND FILLED EPOXIES		
6.12	Specimens	6.31
6.13	Experimental results and discussion	6.32
CHAPTER 7	CONCLUSIONS	7.1
REFERENCES		

CHAPTER 1

INTRODUCTION

Introduction

The addition of inorganic fillers to thermosetting compounds can produce composites with enhanced physical properties. Composite materials, especially those with an epoxy resin matrix, are being increasingly used in industry, and several low temperature applications of loaded epoxy resins have been reported, e.g. Ashworth et al. (1968). Fillers can be in the form of particles, fibres and short chopped strands. In this thesis particulate fillers have been studied.

Interest in the transport of heat in composite materials began as early as 1892 when Rayleigh and Maxwell studied the effect of a cubic array of spherical particles dispersed in a uniform matrix. Fricke (1924) and Hamilton and Crosser (1962) extended Maxwell's theory to include the effect of particle shape and many other theoretical solutions have been proposed.

There has been a large amount of research on the room temperature thermal conductivity of composite materials (e.g. Kline 1961, Hirsch and Koved 1964, Sundstrom and Chen 1970) and Ashworth et al. (1969) have measured the thermal conductivity of an alumina loaded epoxy down to 77 K. Anderson and Rauch (1971) have measured the thermal conductivity of a copper grease composite at temperatures below 1 K but there has been no systematic study undertaken at low temperatures

In this thesis some measurements of the thermal conductivity

of two-phase composites, comprising particulate fillers of glass, crystalline quarts and alumina, and diamond, embedded in a matrix of a thermosetting epoxy resin, Araldite MY740, are described. Glass, quarts and alumina are widely used fillers in thermosetting plastics. Diamond is of interest because of its rather extreme thermal properties. The measurements were performed in the temperature range 2 K to room temperature and the effect of particle concentration, particle thermal conductivity and particle size and shape has been studied.

The first evidence that the low temperature thermal conductivity of composites might present rather special features was provided by Anderson and Rauch (1970) who showed that the thermal transport was influenced by the presence of a thermal contact resistance at the filler-matrix interface. Their experiments were made on a composite of grease and copper spheres. They found that as the temperature is reduced, acoustic mismatch limits the transmission of phonons between the grease and the copper, and there results a decrease in the effective thermal conductivity of the composite. The acoustic mismatch results in some phonons being reflected at the interface and some being refracted into the second medium.

The thermal contact resistance between bulk specimens of the epoxy and the filler materials has been measured and its effect on the low temperature thermal conductivity of the composites, with relation to filler particle size, has been studied.

Chapter 2 of this thesis is a review of the theory of the thermal conductivity of amorphous glasses and polymers, and the theoretical predictions of the thermal conductivity of two-phase composites; chapter 3 gives a general account of epoxy resins and the use of fillers; chapter 4 described the experimental methods, and the remaining chapters deal with the experiments on the filled epoxy resins and t eir interpretation.

CHAPTER 2

THEORY

2.1 Lattice vibrations and Thermal Conductivity

The atoms in a crystal vibrate about their equilibrium position and since they are bound to their neighbouring atoms they form a coupled system of vibrators. The motion of the atoms can be described in terms of travelling waves which are the normal modes of vibration of a crystal lattice assuming the restoring forces between the atoms is proportional to their relative displacement.

The energy of each normal mode is quantised in units of $\hbar\omega$ where ω is the frequency of the mode. These quanta are called phonons and they obey Bose-Einstein statistics.

A phonon of frequency $\omega_{\underline{q}s}$ carries a quantum of energy $\hbar\omega_{\underline{q}s}$ at the group velocity $\partial\omega_{\underline{q}s}/\partial\underline{q}$ ($\underline{q}$ is the wavevector and s the polarization) and therefore the net flow of heat in a crystal can be written

$$\dot{Q} = \sum_{\underline{q}s} N_{\underline{q}s} \cdot \hbar\omega_{\underline{q}s} \cdot \frac{\partial\omega_{\underline{q}s}}{\partial\underline{q}} \qquad 2.1$$

where $N_{\underline{q}s}$ is the number of phonons in mode of wavevector $\underline{q}$ and polarization s.

Normally $N_{\underline{q}s} = N_{-\underline{q}s}$ and so there is no net heat flow. If the distribution of phonons is asymmetrical a heat current will flow. In real crystals when the restoring forces are not perfectly harmonic there are processes which tend to restore thermal equilibrium. Assuming this return to equilibrium follows an exponential law we may write

$$\frac{dN_{\underline{q}s}}{dt} = -\frac{n_{\underline{q}s}}{\tau_{\underline{q}s}} \qquad 2.2$$

where $n_{\underset{\sim}{q}s}$ is the deviation of the population from its equilibrium value and $\tau_{\underset{\sim}{q}s}$ defines a relaxation time.

A Boltzmann equation can now be set up. In the presence of a temperature gradient under steady state conditions we have

$$\frac{dN_{\underset{\sim}{q}s}}{dt} = - \left(\underset{\sim}{v}_{\underset{\sim}{q}s} \cdot \text{grad } T \right) \frac{dN_{\underset{\sim}{q}s}}{dT} \qquad 2.3$$

where $\underset{\sim}{v}_{\underset{\sim}{q}s} = \frac{\partial \omega_{\underset{\sim}{q}s}}{\partial \underset{\sim}{q}}$

Combining equations 2.1, 2.2 and 2.3 and assuming $v_{\underset{\sim}{q}s}$, $\tau_{\underset{\sim}{q}s}$ are functions of $|\underset{\sim}{q}|$ only, the thermal conductivity (Klemens 1958) is

$$K = \frac{1}{3} \sum_s \int d\underset{\sim}{q}\, v_{\underset{\sim}{q}s}\, \tau_{\underset{\sim}{q}s}\, C_{\underset{\sim}{q}s} \qquad 2.4$$

where $C_{\underset{\sim}{q}s}$ is the contribution to the specific heat from phonons with wavenumbers in the interval q to q + dq.

The Debye theory of specific heat can be used to evaluate equation 2.4. This gives

$$K = 3Nk \left(\frac{T}{\Theta}\right)^3 v^2 \int_0^{\Theta/T} \frac{x^4 e^x \tau(x)}{(e^x - 1)^2} dx \qquad 2.5$$

where $x = \frac{\hbar \omega}{kT}$, v is the average velocity of sound, Θ is the Debye temperature and $\sum_s$ is replaced by a factor of 3 to allow for the three polarisation branches of the phonon spectrum.

Normally there are a number of scattering mechanisms which determine the thermal conductivity and the net relaxation time is

$$\frac{1}{\tau} = \sum_i \frac{1}{\tau_i} \qquad 2.6$$

where τ_i is the relaxation time of each of the scattering processes.

2.2 Phonon-Phonon Interactions

In a real crystal anharmonicities in the interatomic forces give rise to phonon-phonon interactions. They serve to establish thermal equilibrium between the modes and give rise to a thermal resistance.

Three-phonon interactions are discussed here, higher order interactions can occur but are only important at temperatures high compared with the Debye temperature.

The conditions that govern the three-phonon processes are

$$\omega_1 + \omega_2 = \omega_3$$

$$\underset{\sim}{q}_1 + \underset{\sim}{q}_2 = \underset{\sim}{q}_3 + n\underset{\sim}{G} \qquad 2.7$$

where $\underset{\sim}{G}$ is a basic vector of the reciprocal lattice and n is an integer defined that $\underset{\sim}{q}_1, \underset{\sim}{q}_2, \underset{\sim}{q}_3$ are wavevectors within the first

Brillouin zone. The first equation ensures conservation of energy and the second conservation of wavevector when n = 0.

When n = 0 the process is called a Normal or N-process. The net flow of energy is unchanged and so N-processes do not give rise to a thermal resistance. However it has an indirect influence on the thermal conductivity because the N-processes transfer energy between different parts of the frequency spectrum and so influence scattering processes that are frequency dependent. When $n \neq 0$ the process is called an Umklapp or U-process. For U-processes the direction of energy flow is changed and so a thermal resistance results.

From theory U-processes give rise to a thermal resistance which varies exponentially. At high temperatures the majority of phonons have a wavevector near the boundary of the Brillouin zone and so there is a high probability of a U-process taking place. At lower temperature only phonons of small wavevector are excited and the probability of a U process occurring is small.

2.3 Boundary scattering The infinite conductivity predicted by the theory of U-processes at absolute zero is not realized because at sufficiently low temperatures, as pointed out by Peierls (1939), the phonon mean free path becomes comparable with the specimen dimensions and scattering from the crystal boundaries limits the heat flow. Thus the conductivity of the crystal is dependent on the size of the crystal.

The relaxation time for this boundary scattering is

$$\tau_B = \frac{L}{v} \qquad 2.8$$

where L is a length of the order of the crystal dimensions and v is the average velocity of sound. Putting this relaxation time into the equation 2.5 we have

$$K = 3Nk\left(\frac{T}{\theta}\right)^3 v^2 \frac{L}{v} \int_0^{\theta/T} \frac{x^4 e^x}{(e^x-1)^2}\, dx \qquad 2.9$$

If $T \ll \theta$ we have $K \propto T^3$ Therefore pure, defect free crystals will have a conductivity that increases as a function of T^3 up to a maximum whence it falls exponentially as U-processes have a high probability of occurring.

Boundary scattering will be very important in determining the effective conductivity, at low temperatures, of the crystalline filling materials used in this work as their particle sizes are quite small, < 100 micron.

The occurrence of crystal defects, impurities and isotopes will greatly affect the conductivity at or above the maximum. See, for example, Rosenberg (1963).

The general shape of the heat conductivity curve of a crystal is shown in fig. 6.19 where the heat conductivity of a quarts crystal is given.

2.4 The Thermal Conductivity of Glasses and Polymers

There are profound differences between the thermal conductivity of a glass and a crystal. The conductivity of a glass always decreases monotonically with temperature, whereas that of a crystal increases with decreasing temperaturing reaching a maximum when boundary scattering becomes important. The range of glass conductivities is much smaller than that of crystals, and, most important of all, the glass conductivities are much less than those of crystals.

Glass is a disordered solid whose lattice lacks both symmetry and periodicity. There will be a short range order. For example in quarts glass this will be of the size of the oxygen tetrahedra.

Kittel (1949) showed that substitution of measured values of the specific heat C into the simple Debye Formula

$$K = \frac{C v l}{3} \qquad 2.10$$

gave, for a glass, an average mean free path l which is constant at room temperature and above and of the same size as the oxygen tetrahedra. Also for high temperatures the glass conductivity will be approximately proportional to its specific heat. At lower temperatures, however, the average mean free path l increases. This increase is to be expected at lower temperatures as the disorder of the glass becomes less important when the phonon wavelength is large compared with the lattice constant.

From the experiments of Berman (1951) on fused silica, Klemens (1951) developed a semi-empirical theory that could explain the results from helium temperatures up to 100 K.

The thermal vibration of the atoms in a glass can be resolved into normal modes but because of the disorder of the lattice these will not be plane waves. However the instantaneous atomic displacements can be resolved in terms of plane waves but there will be a strong interchange of energy between them. Klemens called these interactions "structure scattering". He derived an expression for the relaxation length for structure scattering and found for longitudinal waves

$$l_I = A a \left(\frac{1}{aq}\right)^2 \quad \text{if} \quad aq < 1$$
$$= A a \quad \text{if} \quad aq \gg 1 \qquad 2.11$$

and for transverse waves

$$l_{II} = B a \left(\frac{1}{aq}\right)^2 \quad \text{if} \quad aq < 1 \qquad 2.12$$
$$= B a \quad \text{if} \quad aq \gg 1$$

where A and B are constants and the suffices I and II refer to longitudinal and transverse modes respectively.

Klemens pointed out that transverse waves could be scattered much more easily than longitudinal ones (i.e. $A \gg B$) and so the process in which longitudinal waves are converted into transverse waves and subsequently scattered must be taken into account when calculating the contribution of the longitudinal waves to the thermal conductivity. He obtained

$$K_I = \frac{A k^2 T}{3\pi a h} \int_0^\infty \frac{x^2 e^x}{(e^x-1)^2} \left[1+\left(\frac{T}{T_0}\right)^3 x^2\right]^{-1} dx \qquad 2.13$$

where $x = \hbar\omega/kT$

and $\left(\frac{1}{T_0}\right)^3 = \frac{A a^2}{C}\left(\frac{2\pi k}{h v_I}\right)^2$

C is a constant.

T_0 is a parameter of temperature characterising the process in which longitudinal waves are converted into transverse waves.

At the lowest temperatures $K_I(T)$ is proportional to T. At slightly higher temperatures where the interaction of longitudinal phonons with transverse phonons becomes important, the slope of $K_I(T)$ flattens out and reaches a maximum at $T = 0.8\ T_0$, and for high temperatures $K_I(T)$ is proportional to $T^{-\frac{1}{2}}$.

The contribution of the transverse waves to the thermal conductivity is more complicated. However, at high temperatures

$$K_{II}(T) = \frac{1}{3} B a v_{II} C(T) \qquad 2.14$$

and at low temperatures

$$K_{II}(T) = 3{\cdot}29 \cdot \frac{2Bk^2T}{3\pi a h} \qquad 2.15$$

At intermediate temperatures an approximate expression for K_{II} can be obtained by adding equations 2.14 and 2.15, though this will overestimate K_{II}.

The total conductivity K will be given by

$$K = K_I + K_{II} \qquad 2.16$$

At high temperatures $K_I(T)$ will be small and we have $K(T) \propto C(T)$ as predicted by Kittel. At low temperatures $K(T) \propto T$ as found by Berman on fused silica.

The conductivity of a glass thus depends on three constants A, B and T_o and Klemens obtained the values of these constants for fused silica by fitting his formula to Berman's results. B can be obtained from the high temperature values where K_I is small, (A + 2B) from the linear region at low temperature and T_o from the position of the flat region where K_I reaches a maximum.

A very good fit between Klemens theory and Berman's results on fused silica was obtained for A = 180, B = 2.4 and T_o = 9.8 K.

Reese (1966[a]) applied Klemens theory to the amorphous polymers perspex and polystyrene. He concluded that his thermal conductivity results on polystyrene and perspex samples gave "considerable encouragement that, in the main, Klemens theory is applicable to amorphous polymers."

In a later paper Reese (1966[b]) slightly modified Klemens' theory

to take account of the fibrous nature of polymers. He split the heat capacity into two parts following the Tarasov model of the vibration spectrum of polymers (1950), and assigned different constant mean free paths to each. One part of the heat capacity (C_3) is due to three dimensional vibrations for frequencies from 0 to a frequency characterised by an equivalent temperature θ_3, and the other (C_1) is due to one dimensional vibrations for frequencies between θ_3 and a second characteristic temperature θ_1.

Equation 2.14 is split into two parts,

$$K_3 = \frac{1}{3} v_3 C_3 B a \qquad 2.17$$

for 3 dimensional vibrations

$$K_1 = \alpha_1 v_1 C_1 \Lambda \qquad 2.18$$

for 1 dimensional vibrations

where α is a number, taken to be $\frac{1}{2}$, reflecting the orientation of the polymer chains, v_1 is the velocity of one dimensional vibrations which can be found from θ_1 and Λ is a constant mean free path.

This modification of Klemens theory leads to better agreement between Reese's measurements on polymethyl methacrylate (perspex) but difficulty was experienced in the separation of the one and three dimensional heat capacities.

The existence of an excess specific heat in amorphous solids has been reported (e.g. Anderson 1959 , Reese 1966[c])which is assumed to be caused by localised non-acoustic modes. Rosenstock(1962) explained the presence of these localised modes in terms of micro-cavities in the disordered structure. The vibrational units con-

tained in, or adjacent to these cavities are bound only weakly to the rest of the lattice and so they vibrate independently and with low frequency. Although in his analysis Reese subtracted off this contribution before using the heat capacity in the thermal conductivity expressions, he assumed these modes would make a negligible contribution to the thermal conductivity.

Dreyfus et al. (1968) proposed a model of resonant scattering of the phonons by the band of localized modes $(\omega_R < \omega < \omega_2)$ responsible for the excess heat capacity to explain the thermal conductivity of amorphous solids. This model overcomes the difficulty of Klemens theory where it is possible to arrive at a minimum in the curve K(T) where the contribution of the longitudinal waves to the thermal conductivity is decreasing.

Dreyfus et al. treated the problem by splitting the range of frequencies into three parts:

(1) $\omega < \omega_R$

Following Klemens, the mean free path for phonon scattering is due to "structure scattering" and is

$$l = \frac{A}{a q^2}$$

This mean free path applies to both longitudinal and transverse waves. In this frequency range

$$k_1 = \frac{k^2}{2\pi^2 \hbar} \cdot \frac{A}{a} T \int_0^{\theta_R/T} \frac{x^2 e^x}{(e^x - 1)^2} dx \qquad 2.19$$

where $\theta_R = \frac{\hbar \omega_R}{k}$ and $x = \frac{\hbar \omega}{kT}$

(2) $\omega_R < \omega < \omega_2$

This is the region of resonant scattering and the mean free path is of the order of interatomic distances.

(3) $\omega_2 < \omega$

In this high frequency region the mean free path is constant and also of the order of interatomic distance, following Kittel (1949). In ranges (2) and (3) the same mean free path l is used and the contribution to the conductivity is given by

$$K_2 = \frac{1}{3} v l \int_{\theta_R/T}^{\theta_M/T} g(\omega) \frac{x^2 e^x}{(e^x-1)^2} dx. \qquad 2.20$$

where $g(\omega)$ is the spectral density of accoustical modes and ω_M is the maximum frequency of this distribution, $\theta_M = \frac{\hbar \omega_M}{k}$ and v is the average velocity of sound.

Following the acoustic spectrum from Tamasov (1967), Dreyfus et al. applied their theory to Berman's results on fused silica and a good fit was obtained.

Choy et al. (1970) have applied the Dreyfus model to amorphous polymers and have obtained a good fit above 1.2 K. Below 1.2 K a temperature dependence greater than the linear dependence expected was observed. This was also observed by Anderson et al. (1963) on an epoxy. This points to a second scattering mechanism becoming important at these temperatures.

Choy et al. suggested this was due to an additional internal boundary scattering following Chang and Jones (1962) on their work

on partly crystalline glasses, and applied by Reese and Tucker (1965) to partly crystalline polymers. Chang and Jones used a total mean free path

$$\frac{1}{l} = \frac{1}{l_1} + \frac{1}{l_\beta} \qquad 2.21$$

where $l_1 = \frac{A}{\omega q^2}$ the Klemens "structure scattering" mean free path and l_β is the mean free path due to the internal boundaries and is frequency independent. The thermal conductivity is then given by

$$K = \frac{k^2}{2\pi^2\hbar} \cdot \frac{A}{a} T \int_0^\infty \frac{x^4 e^x}{(e^x-1)^2} \cdot \frac{1}{x^2 + (A/\omega l_\beta)(\hbar v/kT)^2} dx. \qquad 2.22$$

Selected values of this integral may be found in a paper by Callaway (1961). Chang and Jones ascribed these internal boundaries to devitrified regions in the glass, and Reese and Tucker to the crystalline regions in their samples but apparently little quantitative significance can be given to l_β (Kelovsh and Brown 1968 and Choy et al. 1970).

2.5 Contact Resistance at low Temperatures When two dissimilar materials are joined together, a finite temperature difference will occur at very low temperature at the interface when a heat flux is maintained across the interface. Kapitza (1941) first observed this effect between helium II and a metal.

Little (1959) has presented a general explanation of this effect. Phonons incident at the interface between the two media will be refracted into the second medium or reflected at the interface. Using Snell's law of acoustic refraction and Rayleigh's transmission coefficients, Little obtained an expression for the heat flow across the interface for longitudinal phonons:

$$\frac{dQ}{dt} = \frac{2\pi k^4 \Gamma_l A}{h^3 c_l^2}\left(\frac{\pi^4}{15}\right)\left(T_1^4 - T_2^4\right) \qquad 2.23$$

$$= 5.01\times10^{16}\,\frac{\Gamma_l A}{c_l^2}\left(T_1^4 - T_2^4\right)\ \text{erg sec}^{-1}$$

where A is the area of the interface, c_l is the group velocity of the longitudinal phonons in medium one, T_1 and T_2 are the temperatures of the first and second media respectively and Γ_l is the transmission coefficient of longitudinal phonons and is a complicated function of the densities and acoustic velocities in the media.

Equation 2.23 can be generalized to add the contribution from transverse phonons;

$$\frac{dQ}{dt} = 5.01\times10^{16}\,A\left[\frac{\Gamma_l}{c_l^2} + \frac{2\Gamma_t}{c_t^2}\right]\left(T_1^4 - T_2^4\right)\ \text{erg sec}^{-1} \qquad 2.24$$

For small values of the ratio $T_1 - T_2 / T_1$ this becomes

$$\frac{dQ}{dt} = 4 \times 5.01 \times 10^{16} A \left[\frac{\Gamma_l}{c_l^2} + \frac{2\Gamma_t}{c_t^2} \right] T_1^3 \Delta T \text{ erg sec}^{-1} \quad 2.25$$

Little has computed values Γ_l and Γ_t for various densities and acoustic velocities.

From the graphs of Γ presented in his paper it can be seen that to obtain maximum heat flow across the interface the densities should be similar and the acoustic velocities similar. The matching of the specific acoustic impedance of each medium (i.e. $\rho_1 c_1 = \rho_2 c_2$) is not a sufficient condition for the maximum transfer of heat.

Equation 2.25 refers to a perfectly smooth interface. For a rough interface the heat flow will be modified. If the mean free path of the phonons is comparable to the mean amplitude of the roughness, then the effective area of the interface will differ for phonons of different frequencies but in general the effective area will be much greater than that for long lattice waves where the waves will be transmitted as though the interface was smooth. So for high energy phonons the heat transmitted across the interface will be greater than predicted by equation 2.25.

This contact resistance will play an important part in determining the low temperature thermal conductivity of the composite samples measured in this work. Generally the filling material and the epoxy matrix have widely differing densities and acoustic velocities and the resulting contact resistance at low temperatures will be high.

2.6 Theoretical equations for predicting the thermal conductivity of two-phase composites

(a) Introduction

There have been many attempts to predict the effective thermal conductivity K_e of two-phase composites where a uniform medium (matrix) of thermal conductivity K_m is interrupted by discrete regions (filler) of thermal conductivity K_f and volume concentration V_f.

In the limits, the matrix and the filler may be considered to be either in series or parallel with each other and the effective thermal conductivities in these two limiting cases are

$$K_e = (1 - V_f) K_m + V_f K_f \qquad 2.26$$

for parallel layers and

$$\frac{1}{K_e} = \frac{1 - V_f}{K_m} + \frac{V_f}{K_f} \qquad 2.27$$

for series layers. The effective thermal conductivity of a two-phase material with particulate filler should be between these limiting cases.

The theoretical expressions for predicting K_e fall into two main categories. One in which there are no assumptions made about the heat flow and temperature distributions for an assumed geometrical configuration, and the other which contains an assumption about the heat flow and temperature distribution. The former is termed an exact solution and the latter a simplified solution. Both forms

of solutions will be discussed in the following two sections.

(b) Exact Solutions

Most of the exact solutions discuss the electrical conductivity of two-phase materials, but they apply equally well to thermal conductivity.

Maxwell (1892) derived an expression for the effective conductivity of a two-phase composite consisting of spheres of one conductivity embedded in a matrix of another conductivity and it has the form

$$K_c = K_m \left[\frac{K_f + 2K_m - 2V_f(K_m - K_f)}{K_f + 2K_m + V_f(K_m - K_f)} \right] \qquad 2.28$$

It is assumed that the spheres are so far apart that they have no influence on one another.

Lord Rayleigh (1892) considered the case of a cubic array of uniform size spheres and essentially solved the Laplace equation for the potential inside and about a sphere by using the principle of superposition to take into account the effects of the surrounding spheres on the field in the neighbourhood of the central sphere. His equation is

$$K_M = \frac{(2+K_d)/(1-K_d) - 2V_f - 0.525\left[(3-3K_d)/(4+3K_d)\right]V_f^{10/3}}{(2+K_d)/(1-K_d) + V_f - 0.525\left[(3-3K_d)/(4+3K_d)\right]V_f^{10/3}} \qquad 2.29$$

where $K_M = K_c / K_m$ and $K_d = K_f / K_m$. This equation includes a numerical correction introduced by Runge (1925). For small values of V_f the Rayleigh equation is identical to the Maxwell equation.

Meredith and Tobias (1960) extended Rayleigh's analysis to higher powers and obtained

$$K_M = \frac{\frac{2+K_d}{1-K_d} - 2V_f + 0.409\ \frac{6+3K_d}{4+3K_d}\ V_f^{7/3} - 2.133\ \frac{3-3K_d}{4+3K_d}\ V_f^{10/3}}{\frac{2+K_d}{1-K_d} + V_f + 0.409\ \frac{6+3K_d}{4+3K_d}\ V_f^{7/3} - 0.906\ \frac{3-3K_d}{4+3K_d}\ V_f^{10/3}} \qquad 2.30$$

This modification is important when K_f tends to infinity or zero and V_f nears the value for maximum cubic packing ($V_f = 0.52$).

Fricke (1924) and Hamilton and Crosser (1962) modified Maxwell's analysis to include non-spherical particles. They concluded that particle shape becomes important when the ratio of the filler thermal conductivity to that of the matrix is over about a factor of 100, where non-spherical particle shapes will increase the thermal conductivity above that for spheres, all other things being the same. Hamilton and Crosser obtained

$$K_c = K_m \left[\frac{K_f + (n-1)K_m - (n-1)V_f(K_m - K_f)}{K_f + (n-1)K_m + V_f(K_m - K_f)} \right] \qquad 2.31$$

where $n = 3/\Psi$ and Ψ is the sphericity defined as the ratio of

surface area of a sphere, with a volume equal to that of the particle, to the surface area of the particle.

Hamilton and Crosser investigated the thermal conductivity of two phase composites of rubber and various shapes and sizes of aluminium filler. They concluded that for spheres the effective thermal conductivity is independent of the diameter of the spheres and good agreement with the Maxwell equation was obtained. For aluminium filler in the shape of cylinders and parallelepipeds a strong shape effect was observed which could be well accounted for by equation 2.31.

The Maxwell and Rayleigh equations usually predict thermal conductivities that correspond quite well to experimental results for two-phase composites whose components have nearly equal thermal conductivities. (Hamilton and Crosser, Sundstrom and Chen 1970, Knudsen and Wang 1958). For composites where the filler thermal conductivity is much higher than that of the matrix, the Maxwell and Rayleigh equations underestimate the effective thermal conductivity at high concentrations for spherical particles, and for all concentrations for non spherical particles.

Meredith and Tobias obtained good agreement at high concentrations between their electrical conductivity results, on a composite comprised of aluminium spheres in water, and their modified Rayleigh equation, although the equation still underestimated the effective conductivity at a filler concentration just below that for maximum cubic packing.

For non spherical particles equation 2.31 is applicable. The maximum filler concentration that Hamilton and Crosser used in their investigation was 27.5% by volume. For high concentrations it is possible that equation 2.31 will underestimate the effective conductivity as in the analysis it is assumed that the particles are so far apart that they will have no influence on each other.

(e) Simplified Solutions Many simplified solutions for the thermal conductivity of a two-phase material has been proposed and they generally fall into two categories, one in which the heat flow lines are assumed to be straight and parallel, and the other in which the isotherms are assumed to be planes perpendicular to the direction of heat flow. Generally, simplified solutions do not appear to be as relevant for filled plastics as do the exact solutions of the Maxwell-Rayleigh type. Babanow (1957), Gorring and Churchill (1961), Lamb ita (1959), Woodside and Messmer (1961) and Godbee and Ziegler (1966) review some of the schemes for predicting K_e.

One simplified solution which seems to be applicable at low temperatures to this work was proposed by Anderson and Rauch (1970) and included the effect of a thermal contact resistance (section 2.5) between the matrix and the filling material. Assuming the filler thermal resistance to be negligible compared with the thermal contact resistance, and the filler to be composed of spherical

particles in a cubic array they obtained, using an electrical analogue for the thermal resistance of the composite,

$$\frac{K_e}{K_m} = \frac{2a K_m R_k + \alpha d}{2b K_m R_k + cd} \qquad 2.32$$

where α is x/d where d is the diameter of the sphere x is the centre to centre separation of the spheres, R_k is the thermal contact resistance and a, b and c are functions of α only. For one approximation of the model a, b and c had the following form:

$$a = \frac{9\alpha}{2\pi}\left[\alpha^2 - \frac{\pi}{4}\right]$$

$$b = \frac{9}{2\pi}(\alpha-1)\left[\alpha^2 - \frac{\pi}{4}\right] + \frac{3\alpha^2}{\pi} \qquad 2.33$$

$$c = \alpha - 1$$

Anderson and Rauch investigated the thermal conductivity of a copper-grease composite at temperatures below 1 K. The copper was in the form of spheres of diameter about 60 micron. The required value of α to fit their results was 1.06, corresponding to a volume concentration of 43%, compared with the measured volume concentration of 26%. This discrepancy was explained in terms of particle aggregates short circuiting the thermal contact resistance between particles, consequently giving a higher measured thermal conductivity than that predicted by the model.

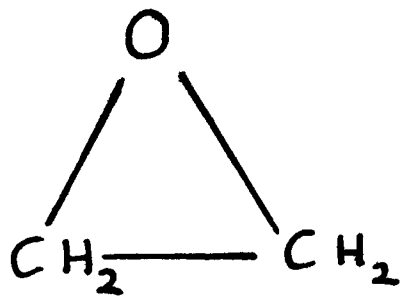
CHAPTER 3

EPOXIES, FILLERS AND SAMPLE PREPARATION

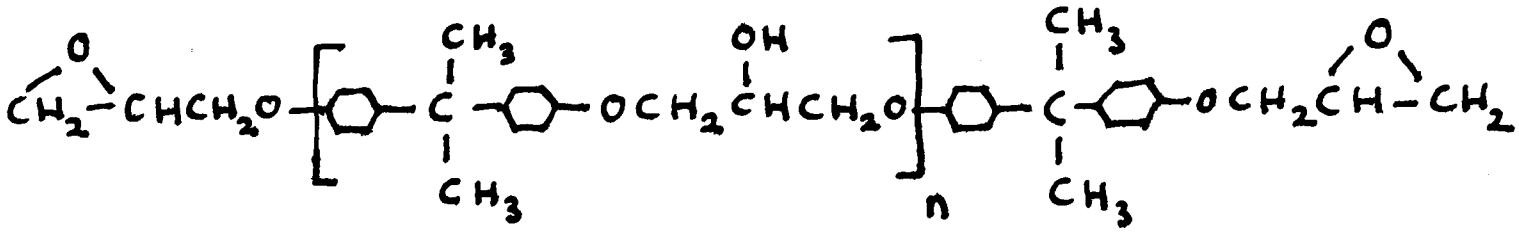
3.1 Introduction

Epoxy resins are synthetic materials made from petroleum derivatives. They may be reacted (cured) with various other chemicals (hardeners) to produce an infusible solid.

The term epoxy refers, broadly, to a chemical group consisting of an oxygen atom bonded with two carbon atoms already united in some other way. The simplest epoxy is a three-membered ring of which ethylene oxide is an example.



The most widely used epoxy resin is diglycoydyl ether of bisphenol A (DGEBA) manufactured by the reaction of epichlorohydrin with bisphenol A and has the following formula:



The resins range from liquids to brittle solids as 'n' increases from zero to about twelve. The major differences between various resins are in their molecular weight, their epoxide equivalent and their viscosity. The term epoxide equivalent indicates the number of grams of resin containing 1 gram-mole of epoxy groups.

The liquid or thermoplastic epoxy resin is converted to a hard solid by the addition of a chemically active compound called a curing agent or hardener. Depending on the choice of curing agent the cure can sometimes be achieved at room temperature with heat produced by exothermic reaction or it may require the application of external heat. The basic curing agents employed are Lewis bases, inorganic bases, primary and secondary amines, and amides. The use of accelerators is necessary when certain curing agents are used, to promote cure within a reasonable time.

An important consideration in the choice of resin and curing agent is pot life, defined as the time available for use of the epoxy system after the resin and curing agent a e mixed. Pot life of epoxy resin systems can vary from several seconds to several years.

3.2 The cure and properties of the cured epoxies

Predictions of optimum cure cycles for a given epoxy system are not possible and the usual procedure for determining cure cycles is to empirically optimise the desired end products. Cure cycles producing an optimum value for one physical property will not necessarily produce an optimum value for another. For commercial resins the manufacturers usually indicate the various curing cycles possible for optimising certain physical properties. In the epoxy resin molecule there are reactive sites that react with the curing agent. In the initial stages of the cure the resin becomes a thermoplastic. Here the epoxy groups are reacting with the curing agent producing linear chains. This is called conversion. With additional cure, cross-linking occurs. The molecules are coupled through reactive sites to form a three dimensional network. An epoxy resin is considered cured when sufficient cross linking has occurred to provide the desired optimum physical properties. Cured epoxy resins of the DGEBA type are rigid, amorphous, glass-like solids.

The properties that have made epoxies so successful are: high chemical resistance, good mechanical properties, high electrical insulation, high adhesive strengths with a variety of substrates and low shrinkage during cure. The versatility of epoxies is also important. There are many different resins available and, combined with the many different curing agents, a great diversity of properties

can be obtained.

Epoxy resins are used in many industrial applications. They are notably used as adhesives, for casting applications, for encapsulation of electric and electronic equipment, and as laminating resins.

3.3 The use of modifying agents in epoxy systems.

There is a wide range of additives which are compatible with the epoxy system which can extend, improve and modify the properties of the system. These modifying agents fall into three main categories, namely, dilutents, flexibilizers and fillers.

Dilutents are principally used to lower the viscosity of the system. Flexibilizers are additives which react with the resin during cure to impart flexibility to the epoxy by increasing the distance between the cross-linking points.

Fillers are used in epoxy systems for a variety of reasons and can be in the form of particles, fibres and short chopped strands. The main advantages are summarized below.

Fillers can:

1. Lower the cost of the product Epoxies are relatively expensive

and significant decrease in cost results by bulk displacement of the epoxy with a low cost filler.

2. Decrease the exothermic temperature rise in curing By absorbing heat fillers help to control the temperature rise of the system during polymerization which could impose a serious limitation on the use of epoxy systems in commercial large scale operations.

3. Reduce shrinkage on curing Significant decrease in shrinkage can result if an inert filler is used which does not undergo permanent dimensional change during the cure cycle.

4. Increase thermal conductivity Epoxies have very low thermal conductivities, about 2 mW cm $^{-1}K^{-1}$ at room temperature, and significant increases in thermal conductivity can be produced by bulk displacement of the resin by a filler of higher thermal conductivity.

5. Reduce the coefficient of thermal expansion Epoxies have a very high coefficient of thermal expansion, being about four times that of copper at room temperature. The general effect of fillers is to reduce the rate of expansion. For example, at room temperature a filler concentration of 50% by volume of crushed quartz in an epoxy system will give a coefficient of expansion comparable to that of copper. This reduction in expansion indirectly improves the adhesive strength of epoxy systems when materials of small coefficients of expansion are bonded together.

6. Higher deflection temperature The deflection temperature is

the temperature at which a standard size bar ½" x ½" x 5" long increases by 0.010" in length when subjected to a load of 264 p.s.i. Generally addition of fillers raise the deflection temperature of an epoxy system.

7. Reduce water absorption Fillers can reduce the amount of water absorption in epoxy systems although it should be noted that many fibrous fillers exhibit a wicking action and increase the water absorption.

8. Improve abrasion resistance The general effect of fillers is to increase the surface hardness and abrasive resistance of epoxy casting. Alumina for example causes substantial increases in these properties.

The machinability of various fillers will vary with the filler. Quartz and alumina fillers cause difficult machinability.

9. Increase Young's modules and compressive strength Particulate fillers generally decrease compressive fatigue but increase ultimate compressive strength and Young's modulus.

The main disadvantages of incorporating fillers in epoxy systems are increased viscosity, increased weight, loss of transparency, tendency to entrap air and decreased impact and tensile strength.

Fillers can be used to convert the epoxy insulator into an electrically conducting system. Particulate metallic fillers, metallic wools, and carbon black are used for this purpose.

Fillers are normally inert, finely divided inorganic powders.

Generally the greater the amount of filler in the epoxy system the greater the effect on the physical properties of the system. The amount of filler that can be incorporated into the system usually depends on the increase in viscosity that can be tolerated. This will be discussed in the next section.

3.4 <u>The effect of fillers on the viscosity of the epoxy system and the settling properties of fillers</u> Fillers increase the viscosity of epoxy resin systems. Particulate fillers cause the least increase, fibrous fillers the most. Finer particle sizes generally increase viscosity more than the same volume of larger size particles because of the larger surface area of smaller particles. When pourable systems are necessary the amount of filler that can be used is restricted and this has to be determined empirically. The viscosity of an epoxy system is reduced by raising its temperature. Filler concentrations may, in consequence, be increased if conditions allow the system to be heated for application. Due regard must be given to the shortening of usable life caused by heating. If a pastelike substance can be tolerated much higher filler concentrations can be obtained, the limit being imposed by

wettability considerations.

Fillers tend to settle from the resin on storage. The amount of settling is dependent upon the specific gravity of the filler, the particle size of the filler, and the viscosity of the filler system. The smaller the particle size the less the degree of settling. It is possible to retard the settling of coarse fillers by adding a small amount of filler of very small particle size.

High temperature cures of filled epoxy systems cause an initial decrease in viscosity before gelling takes place and so the settling tendency is accelerated. It is important that the filler is dispersed throughout the epoxy system and one way this can be achieved is to slowly rotate the epoxies when the cure takes place.

3.5 Specimen preparation In all specimens on which measurements were taken in this work, the same resin was used, and the samples were all prepared in the same way with the same cure cycle.

Araldite MY 740 was the epoxy resin used. This is a resin of type DGETA of medium viscosity. Mixed with hardener HY 906, a liquid anhydride of low viscosity, it produces a low-viscosity hot-

setting system suitable for casting and impregnation. An accelerator DY 062 a liquid modified tertiary amine which promotes rapid curing of small components was added to the mixture. The amounts of the resin, hardener and accelerator used were in ratio of 100 : 80 : 2 parts by weight respectively.

The resin, hardener and accelerator were mixed together in their correct proportions at room temperature and the required amount of filler was thoroughly stirred into the mixture. This procedure is satisfactory when small quantities are used. The resin-hardener mix has a lower viscosity than the resin alone and adding the filler in this way facilitates both the addition of the filler and escape of entrapped air. For large quantities the normal procedure is to add the filler to the resin and to use a mechanical mixer to disperse the filler. Vacuum treatment, to get rid of the entrapped air, may be lengthy and to ensure adequate usable life for the processing operations the hardener and accelerator are added afterwards. Before use the fillers are thoroughly dried.

The epoxy filler mix was degassed in a bell jar at about 40°C until bubbling of the mix ceased. The casting and curing was done in glass tubes of about 5 mm diameter and 30 mm long. As epoxy-resins have an affinity to glass an anti-stick agent must be applied to the glass surfaces. The inside of these tubes were coated with a PTFE aerosol spray, followed by a bake at 100°C for one hour to harden the coating, and as an added precaution a coat of silicone fluid

MS200 was added on top of the PTFE. The resin particle mix was poured into the tubes, or if very high filler concentrations were used the mix was "trowelled" into the tubes and was gelled at 100°C for one hour, followed by a cure at 180°C for two hours. The tubes were rotated at about 3 revolutions per minute during the curing process to prevent sedimentation of the particles. The resin mixture has a usable life of about 14 hours at 20°C and 1½ hours at 40°C.

The concentration of filler material in the samples was measured by measuring their density. Knowing the densities of the cured epoxy and the filler the volume concentration of filler can be deduced. As a check, the weighed samples can be ignited in a crucible, burning off the epoxy. The filler is left as residue, and weight concentration, hence volume concentration of filler can be determined. The difference between the density and ignition methods was less than 2%, indicating that the presence of voids is negligible.

3.6 Particle size of fillers and Test Sieving In this work particle fillers are used and it is necessary to grade the particle size of the fillers. If the particles are of a regular shape, for

example spheres, this is a fairly easy process. The particles can be sieved between sieves of aperture sizes that are close together and with the aid of a microscope a weighted diameter can be deduced.

The exact size of an irregular particle cannot be measured. Most of the fillers used in this work fall into this category. The terms length, breadth, thickness or diameter have little meaning because so many different values of these quantities can be determined. The equivalent diameter is often used in describing the size of particles. This refers to the diameter of a sphere that would behave in the same manner as the particle when submitted to some specific operation.

Several equivalent diameters are encountered. The Stokes' diameter is measured by sedimentation and elutriation techniques; the projected area diameter is measured microscopically; and the sieve aperture diameter is measured by test sieving. For any given irregular particle the magnitudes of these three diameters will not be equal.

The equivalent sieve aperture diameter of a particle is the diameter of a sphere equal to the width of the aperture through which the particle just passes. If the particles being tested are not true spheres this equivalent diameter refers only to their second largest dimension. Particle size as measured by test sieving may be specified by quoting the size of the two screens, one through which the particles have passed, and the other on which they are retained.

Where the filling material was obtained from the manufacturers in an ungraded form it was graded using test sieves. Scanning electron micrographs were then taken of the test sieve graded fillers. From the micrographs the projected areas of the particles were measured and, assuming the particles were randomly placed on the microscope specimen stubs, an average particle volume was deduced. Assuming the particles can be approximated to cubes, a volume weighted average cube length can be quoted. This figure was taken to be the average particle size of the filler in the case of random irregular particle shapes, unless otherwise stated.

Test sieving can be employed down to a sieve aperture size of 10 microns, but below about 60 microns a wet sieving technique must be employed as the sieve apertures may become "blind" or the particles may become electrostatically charged and "ball-up" when sieving is attempted.

The technique of wet sieving is as follows. The sieve is held over a bowl containing water (or another liquid if water is unsatisfactory) and the sample material is washed on to the mesh. The sieve is lowered into the liquid and held horizontally near the surface. A gentle "jigging" action is made until the fine particles cease to pass through the screen. The sieve is then inverted over another bowl and the oversize particles are back-washed into it. The particles are allowed to settle, most of the water is decanted off and then the particles are dried in an oven.

If a large quantity of unwanted very fine particles are present

in the sample, they should first be removed by first sieving the sample using a sieve of smaller aperture size than required in the particle size grading.

In practice a combination of dry and wet sieving was used to grade the fillers. For dry sieving a mechanical agitator was used.

3.7 Precautions for handling epoxy resins and mineral powders

It is important to note that precautions are necessary when handling epoxy resins. The uncured materials can cause severe skin irritation and rubber gloves or an effective barrier cream should be used. The working area should be well ventilated and the exhaust of vacuum pumps must be vented outside the room. Contact with the hot fumes when the resins are being cured should be avoided.

When using powdered fillers, especially in large quantities, the wearing of micron-particle dust respirators is necessary.

CHAPTER 4

EXPERIMENTAL TECHNIQUES

4.1 Outline of the method The thermal conductivity was measured by the conventional steady state method.

For temperatures below 20 K the specimen was in rod form and was mounted, in a vacuum, with one end in good thermal contact with a constant temperature bath. A steady temperature gradient, maintained along the specimen by means of a heater glued to its free end, was measured using a diffential gold + 0.03% at iron versus chromel thermocouple, whose junctions were attached to the specimen a known distance apart. The average temperature of the specimen was measured using another diffential gold-iron versus chromel thermocouple connected between the constant temperature bath and the top of the specimen.

A cryostat of fairly straightforward design was used for these measurements. It worked in the range 1.5 K to 4.2 K using liquid helium, and 10 K - 20 K using liquid hydrogen.

For temperatures of 77 K and above a miniature Lee's disc technique was used with a sample of thickness about 2 mm and about 5 mm in diameter. The high emissivity (about 0.9) and low thermal conductivity of the samples measured (< 10 mW cm^{-1} K^{-1} at room temperature) precluded the use of a Searle's Bar technique because of the loss of heat by radiation. The temperature gradient across the specimen was measured using a diffential copper versus constantan thermocouple.

A simple cryostat was used for these measurements above 77 K. Three temperature points were utilised, those of liquid nitrogen (77 K), dry ice (194 K) and room temperature.

4.2 The cryostats

(a) Cryostat I for temperatures below 20 K

The general arrangement of the cryostat is shown in fig. 4.1. The specimen chamber is bolted on to a copper can of volume about 400 c.c. which contains the reservoir of liquid helium or liquid hydrogen. Tube (a) is used for evacuating the specimen chamber and as a service tube for the heater and thermocouple leads. A radiation trap and a thermal anchoring point at 77 K for the leads are also provided in this tube. The cryogenic liquid in the reservoir can be pumped on through tube (b) and its vapour pressure measured through the static tube (c). The inner can and specimen chamber are surrounded by a brass vacuum jacket which has a demountable Woods metal seal. The vacuum jacket is evacuated through tube (d) which contains a radiation trap. The whole of the cryostat is immersed in liquid nitrogen contained in a glass dewar.

All the tubes are made of stainless steel to reduce heat conduction down the tubes and to give the cryostat added strength.

The liquid helium usually lasted for about seven hours and gave ample time for an uninterrupted experiment to be performed. The lowest temperature obtainable with liquid helium was about 1.5 K, using a rotary pump only.

(b) Cryostat II for temperatures above 77 K

The arrangement of the cryostat is shown in fig. 4.2. The specimen chamber is bolted on to a brass plate and the vacuum seal effected using an indium 'O' ring. The chamber is evacuated through

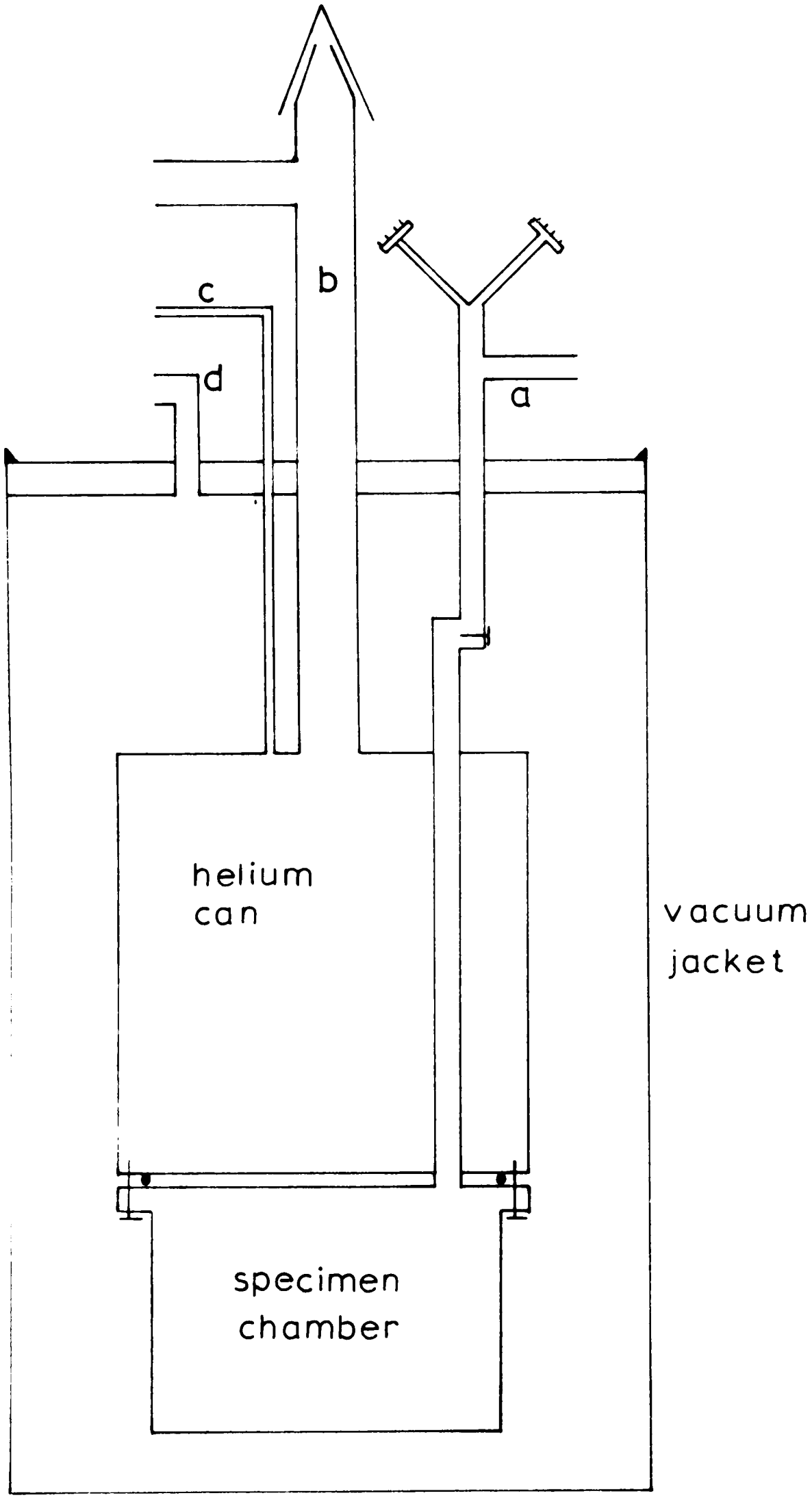


Fig 4.1 Schematic diagram of Cryostat I.

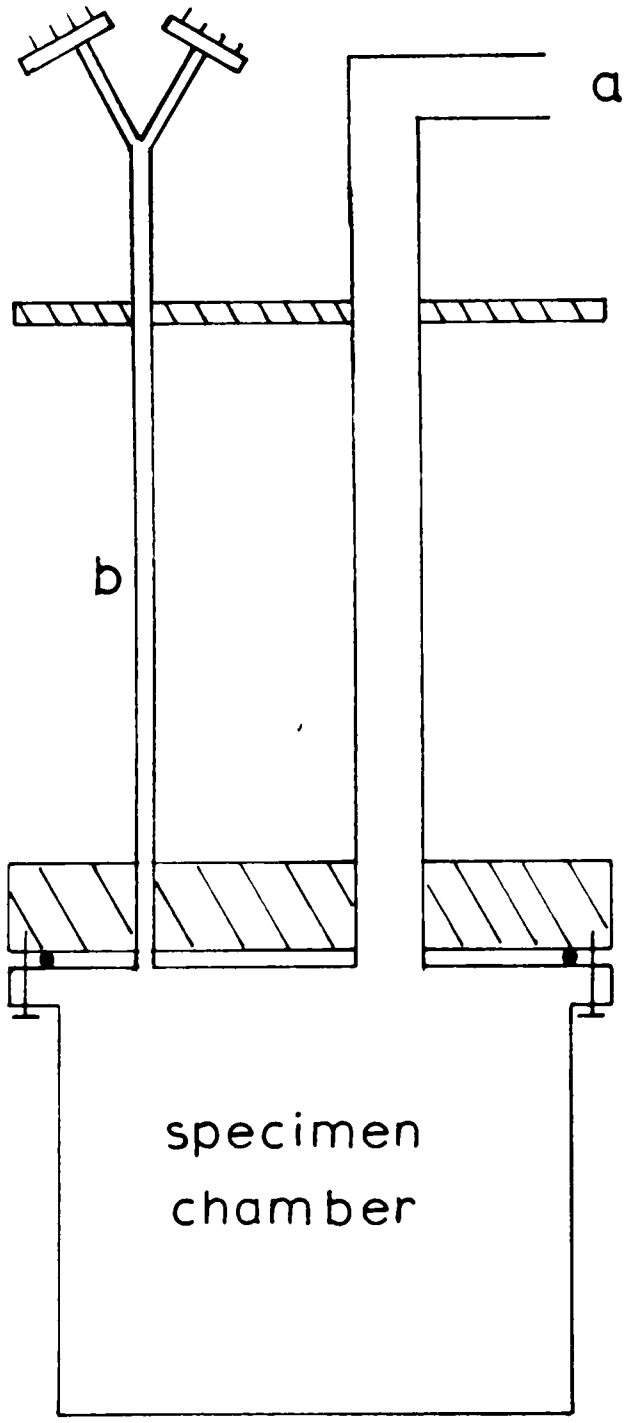


Fig 4.2.Schematic Diagram of Cryostat II.

tube (a) and tube (b) carries the heater and thermocouple leads. The specimen chamber is enclosed in a glass dewar which could contain liquid nitrogen, a freezing mixture of dry ice and acetone, or water, to give steady temperatures of 77 K, 194 K and room temperature respectively.

4.3 Specimen mounting and heater arrangement.

(a) Specimens for measurements below 20 K.

The general arrangement of a typical specimen mounting is shown in fig. 4.3

The specimens were cast in the form of rods of diameter about 5 mm and length about 15 mm. Two holes, diameter 0.8 mm and about 6 mm apart were drilled half way into the specimen. Two annealed copper pins about 6 mm long were araldited into these holes. These pins formed the thermometer contacts, and the thermocouple junctions were soldered directly on to them. Araldite type 1 was used to achieve thermal contact between the specimen and annealed copper specimen holder.

The heater was wound directly on to the specimen and consisted of about 2 metres of 47 swg constantan wire giving a resistance of about 500 ohms.

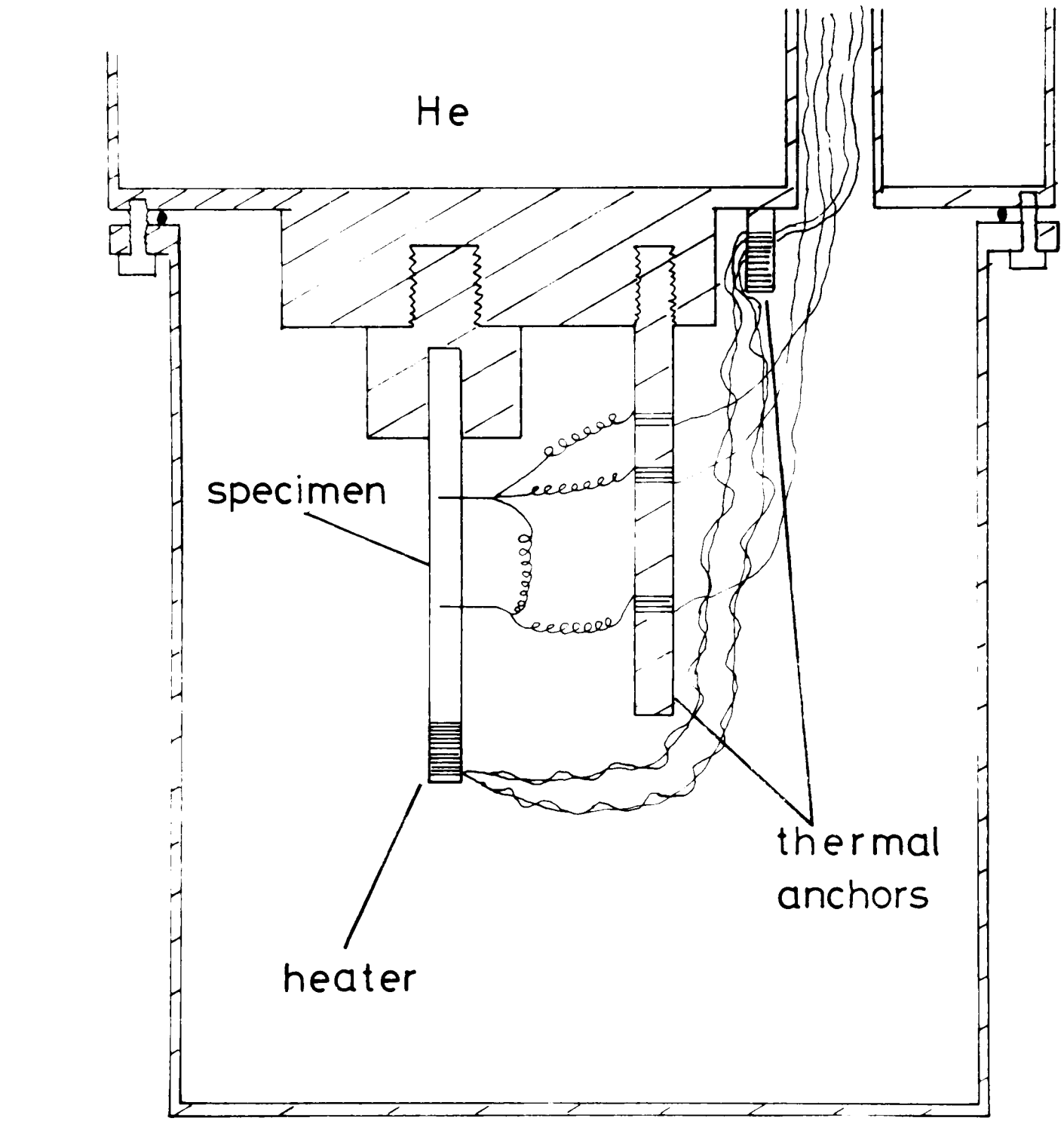


Fig 4.3 Schematic Diagram of Specimen Arrangement in Cryostat I.

The specimen holder was screwed into a copper block beneath the constant temperature bath.

(b) Specimens for measurements above 76 K

Preliminary measurements on an unfilled epoxy specimen of the type described in the previous section indicated results that were an order of magnitude higher than expected for general epoxies (e.g. Lee and Neville (1967)). This was attributed to radiation losses from the sample.

To investigate this loss of heat by radiation a number of experiments were performed. The details of these appear in table 4.1. The radiation protection was afforded by aluminised mylar tape which was wrapped around the specimen.

TABLE 4.1

	Sample description (d = diameter L = Length)	Radiation protection	K at 300 K $mW\ cm^{-1}\ K^{-1}$
a)	rod d = 5 mm L = 16 mm	No	14.1
b)	rod d = 5 mm L = 16 mm	Yes	5.0
c)	as (b) but heater in copper block	Yes	3.8
d)	rod d = 6 mm L = 13 mm	No	7.0
e)	Miniature Lees disc d = 5 mm L = 2 mm	Yes	2.2
f)	Conventional Lees disc L = 5 mm d = 100 mm	-	1.9

The rod specimen with radiation protection gave results lower than the unprotected specimen but at room temperature was still about a factor of 2 higher than that measured by a conventional Lees disc arrangement.

Ideally the room temperature measurements should be performed using the conventional Lees Disc method but with the filled epoxies it was not feasible to cast such large specimens because the quantity of filling material available was usually quite small.

It is possible to estimate the loss of heat radiated by measurements on two samples of the same length but different diameters but this was not thought worthwhile because of the very large proportion of heat loss and the difficulty of matching the filler concentrations of the two filled specimens.

It was therefore decided to use a miniature Lees disc type sample of diameter about 5 mm for all measurements at 78 K, 194 K and room temperature. The error in the conductivity due to radiation losses at room temperature is probably less than 10% for the unfilled resin, and even less for all the filled resins measured in this work as their conductivities are greater than that of the unfilled resin for temperatures above the liquid hydrogen range. At the lower temperatures the heat loss by radiation will of course bemuch less.

The details of the miniature Lees disc type specimen are given in fig. 4.4. A disc of about 2 mm thickness was machined from the 5 mm diameter sample rods and araldited between the copper post, of the same diameter of the sample, in the heat sink (a) and the heater block (b) also of the same diameter.

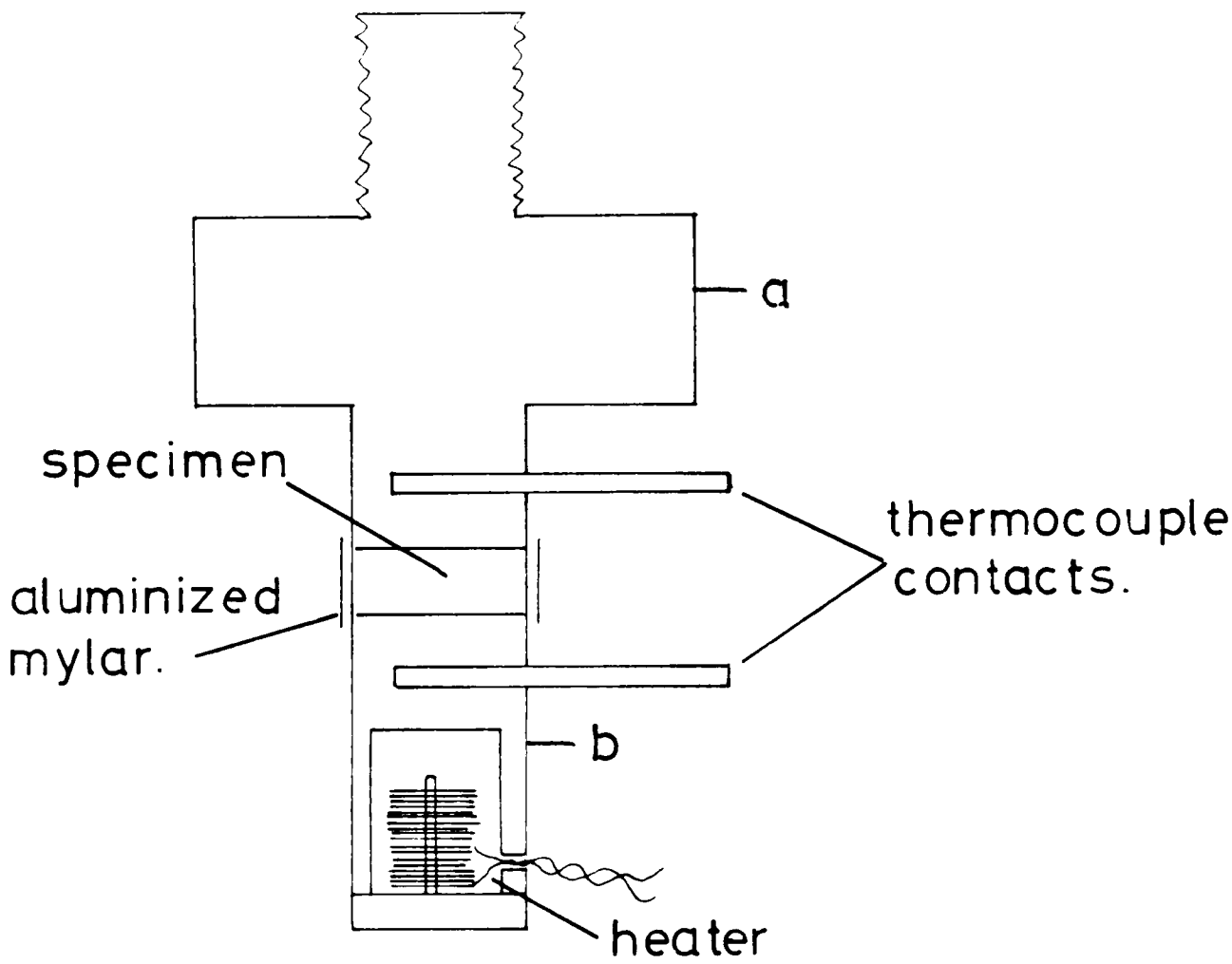


Fig 4.4 Schematic Diagram of Specimen for Cryostat II.

The heater consisted of about 400 ohms of 47 swg constantan wire wound on a former araldited inside the heater block.

The thermometer contacts were constructed usin copper pins 1 mm in diameter and 7 mm long. Electrical insulation was effected by baking a very thin coat of araldite on to the ends of the copper pins and then aralditing them into holes drilled in the heater block and heat sink. The copper-constantan thermocouple junctions were directly soldered onto the thermometer contacts.

To cut down radiation losses, aluminised mylar tape was wrapped around the epoxy disc and the copper was brightly polished.

4.4 Specimens for measuring the thermal contact resistance

A "sandwich" arrangement similar to that described by Anderson and Rauch (1970) was used to measure the thermal contact resistance between the epoxy and bulk samples of the filler material. Two bulk samples of the required material were cemented together with the epoxy, Araldite MY 740 and cured at the temperatures stated in section 3.5. The epoxy thickness was measured microscopically and was typically about 20 microns. The area of contact was typically about 0.10 cm^2. The heater and thermometer contacts were similar to that described above for the low temperature samples.

The total thermal resistance (W) of the epoxy-material sandwich

will be the sum of two epoxy-filler material thermal contact resistances ($2\ R_k$), the bulk thermal resistance of the epoxy (L_m/AK_m), where L_m is the thickness of the epoxy, A is the area of contact and K_m is the thermal conductivity of the epoxy, and the bulk thermal resistance of the material (L_f/AK_f) where L_f is the length of the material between the thermometer contacts and K_f is the thermal conductivity of the filler-material. The thermal contact resistance will, therefore, be given by

$$W = 2R_k + \frac{L_m}{AK_m} + \frac{L_f}{AK_f} \qquad 4.1$$

With values of A, K_m, L_f and K_f, the thermal contact resistance can be deduced from the experimental values of W.

4.5 Thermometry

a) Choice of the Cold-iron vs Chromel thermocouple

Thermocouples are the obvious instrument for measuring temperature differences and are therefore ideal for thermal conductivity measurements. They measure temperature differences directly and because of their small heat capacity they rapidly follow any temperature changes.

In general, however, the sensitivity of thermocouples decreases with decreasin temperature, becoming prohibitively low at liquid helium temperatures.

The effect of small amounts of transition element impurity in gold was investigated by Borelius et al (1932) and they found that gold-cobalt and gold-iron alloys had anomalously high thermopowers in the liquid helium temperature range.

The thermopower of gold-cobalt continues to rise with increasing temperature, whereas the gold-iron has a large thermopower only at low temperatures and drops away above about 20 K. Borelius recommended the use of gold + 2,1% cobalt versus silver normal (silver + 0,37 at % gold) as an all purpose thermocouple from helium temperatures up to room temperature. The sensitivities of copper versus constantan, gold-iron (0.03 at %) versus chromel, gold-iron versus silver normal and gold-cobalt (about 2%) versus silver normal are shown in fig. 4.5.

The gold-cobalt thermocouples have certain disadvantages. Their sensitivity is still rather low at helium temperatures (about 3 μV at 2 K) and the reproducibility of their calibration is fairly poor (Powell etal. 1961).

Gold-iron thermocouples have been found to maintain their calibration after aging and repeated thermal cycling. Berman et al. (1964) found that the calibration of their gold-iron thermocouples varied by less than 0.5% over periods of time up to two years. The low thermopower of the gold-iron above 40 K need not be a problem if the 2nd thermoelement is correctly chosen. From the work of

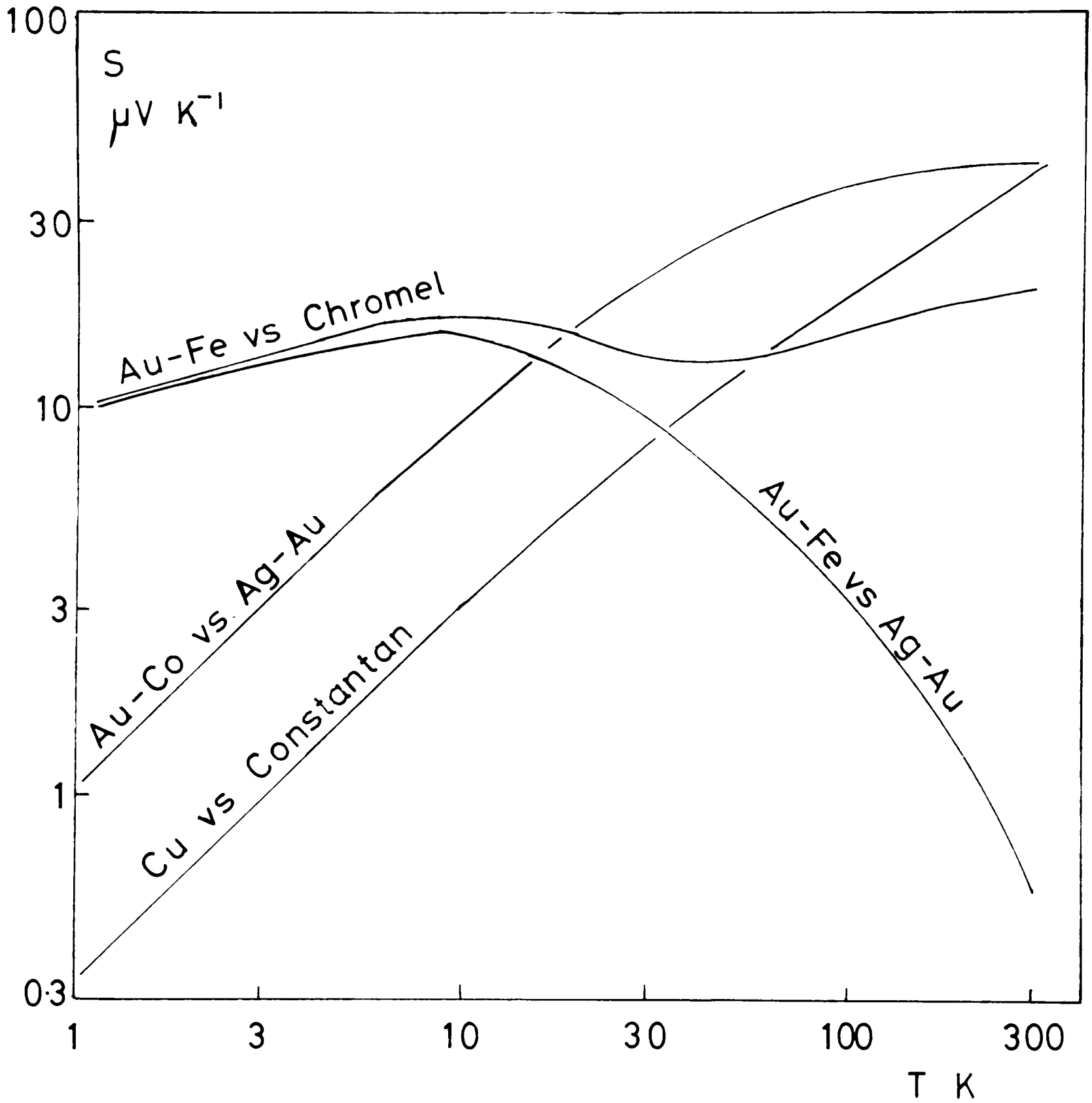


Fig 4.5 Sensitivity (S) of several Thermocouples.

Pearson et al. (1962) and Berman et al. (1964) an alloy with between 0.02 and 0.03 at % iron, seems to be the most satisfactory. Thermocouple wire of gold + 0.03 at % iron is commercially available from Johnson Matthey and Co. Ltd., London, and this has been used throughout this work for thermal conductivity measurements from 1.5 K to 20° K.

The choice of the 2nd thermoelement depends on the work the thermocouple is intended for. Berman et al (1964) found that chromel - P partnered with gold + 0.03 at % F_e was ideal as an all purpose thermocouple that can be used from 1 K up to room temperature. Chromel-P has:

(1) A high positive thermopower which greatly enhances the thermopower of the thermocouple above 40 K when that of the gold iron is decreasing.

(2) A low thermal conductivity to minimise heat leaks down the leads.

(3) Low inhomogeneity voltages.

The chromel-P thermocouple wire used in this present work was obtained from Johnson Matthey, London.

b) Calibration

The sensitivity of the gold + 0.03 at % Fe versus chromel thermocouple as measured by Berman et al (1964) is presented in fig. 4.6. The sensitivity is maintained above 10 μ V K^{-1} throughout the range 1 K to 300 K.

It has not been possible to calibrate the thermocouples used in this present work and so the calibration of fig. 4.6 has been

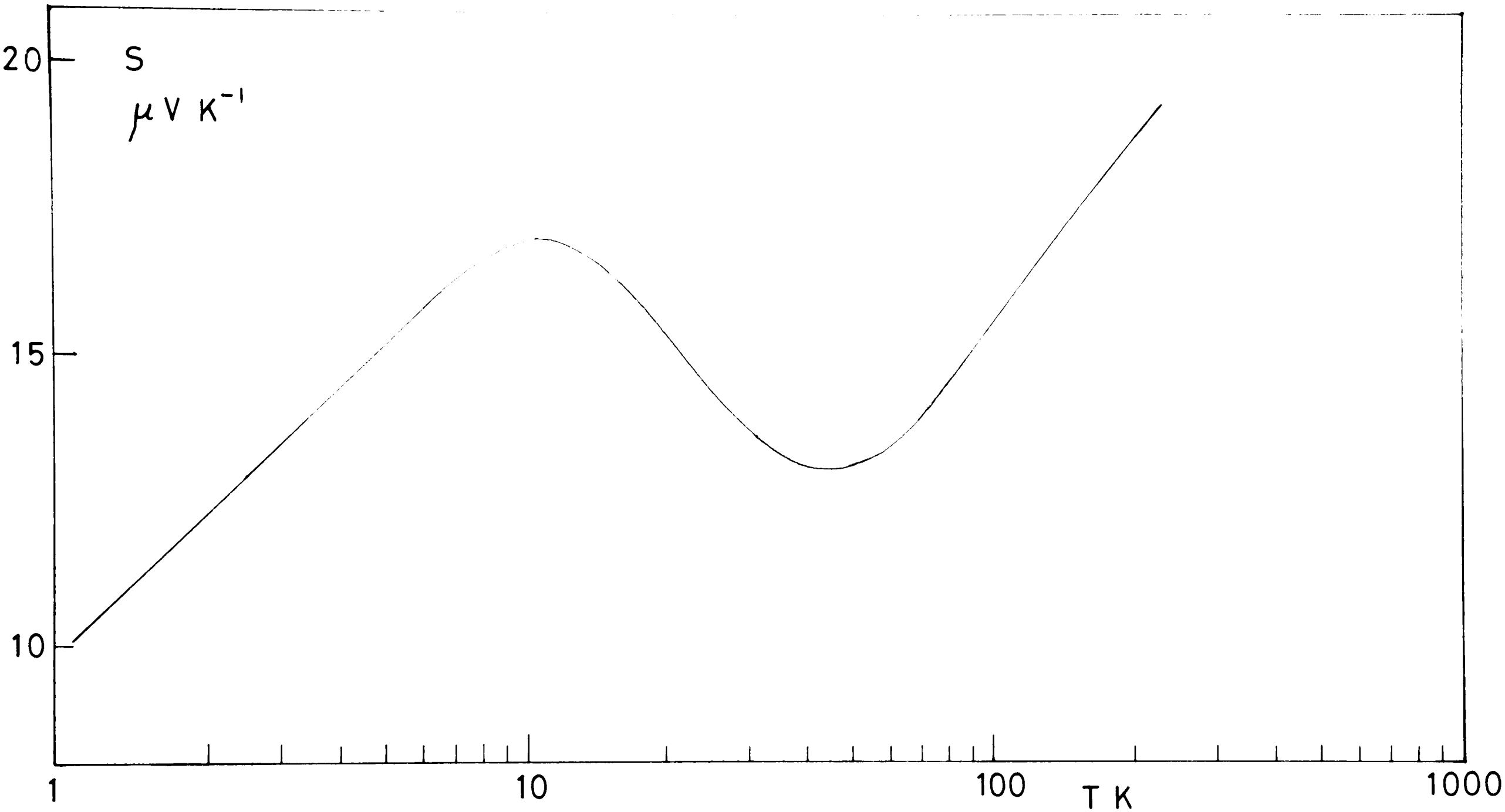


Fig 4.6 Gold+0·03% at. Fe. vs. Chromel Thermocouple Calibration. Sensitivity (S) vs. Temperature (T).

used throughout. The reproducibility of the gold-iron versus chromel is probably better than 0.5% but calibrations between different batches of the thermocouple wire may vary much more.

Introducing strains in the thermocouple wires will affect the sensitivity of the thermocouple. Berman et al (1963) investigated the effect of straining the gold iron wire but if care is taken in construction of the thermocouples and in changing samples this should not be a serious problem.

e) <u>The thermocouple circuitry and voltage measurement</u>

This section, though particular reference is given to the gold-iron thermocouples, applies to the thermocouple circuits of both cryostats I and II.

Basically the thermocouple voltage was measured directly by a Keithley model 148 nanovoltmeter the output of which was displayed on a Servoscribe chart recorder.

All the thermocouple leads from the cryostat consisted of screened cable comprising a central copper wire covered with insulation and a semi-conducting sheath, and shielded by an earthed copper braid. A Tinsley low thermal switch was used for switching between the two thermocouples. The screened cables were soldered to the switch using a low thermal cadmium-tin solder. This solder has a thermopower of $\pm$ 0.25 microvolt K^{-1} with copper and surrounding the connections with cotton wool to exclude draughts was sufficient to cut down stray thermals to an acceptable level. All the leads were taped closely together to diminish any induced voltage from

stray magnetic fields.

Constantan wire of 40 swg, enamelled and with a double silk covering was used down the cryostat and thermally anchored at 78 K. This wire was joined on to the screened copper cable using pressed copper contacts. These connections were immersed in a large oil bath to reduce stray thermals produced by joining together dissimilar metals. The constantan leads were taken directly out of the cryostat through a room temperature glass-to-metal seal consisting of fine bore tubes embedded in glass. The tubes were sealed with Araldite to make them vacuum tight.

In the specimen chamber about 20 cm of chromel thermocouple wire, diameter of .08 mm and diamel coated, was hard soldered on to the constantan wire. This was achieved by carefully cleaning off the enamel, twisting the ends of the wires together and quickly dipping the junction into molten hard solder. These junctions were thermally anchored at the temperature of the constant temperature bath by wrapping the junctions, and about 8 cm of wire on either side of them, around a copper post that was screwed and soldered into the bottom of the bath. The wires were cemented onto the rod using Durofix adhesive.

A length of about 50 cm of diamel coated gold-iron wire of diameter 0.08 mm was used in the thermocouples. The thermocouple junctions were made by hard soldering the gold wire to the chromel.

Two thermocouples were constructed in tandem. One measured the temperature difference along the specimen and its junctions were soldered directly onto the copper pins embedded in the specimen.

and the other measured the temperature difference between the top of the specimen and the constant temperature bath. Thermal contact between the thermocouple junction and the bath was achieved by winding the wires and junction around the copper post beneath the bath and cementing them with Durofix adhesive.

4.6 Experimental details

The thermal conductivity of the specimens was measured using the conventional steady state method.

Cryostat I was precooled with liquid nitrogen. Liquid helium or liquid hydrogen was syphoned into the inner can. Cryostat II was immersed in the appropriate liquid. When the specimen temperature had stabilised and the pressure in the specimen chamber was less than 10^{-5} torr a conductivity point was taken. The heater was energised and the change in the voltage readings of the thermocouple along the sample noted when the specimen had reattained thermal equilibrium. The voltage across the heater and across a 100 ohm standard resistor in series with the heater was measured using a digital voltmeter. The heater current was then switched off and the change in thermocouple voltage for the sample to attain temperature equilibrium was measured.

The temperature of the bath was varied by pumping on the liquid

using a rotary pump of displacement 334 litres minute^{-1}. The vapour pressure and therefore its temperature was stabilized by adjusting the pumping speed of the system by means of two throttling valves, a 1" Saunders valve and a needle value for fine adjustment. The vapour pressure of the liquid was measured using a mercury manometer for pressures down to 5 cm H_g and an oil filled manometer for lower pressures.

With liquid helium in cryostat I the lowest temperature obtainable was about 1.5 K, and using liquid hydrogen about 10 K. Values of the heater current were chosen to give a measured temperature difference of about 0.1 degrees at liquid helium temperatures and about 0.4 degrees at liquid hydrogen temperatures.

The conductivity was calculated from the formula

$$K = \frac{Q.F}{\Delta T} \qquad 4.2$$

where K is the thermal conductivity (W cm^{-1} K^{-1})

Q is the heater power (W)

F is the form factor of the specimen (cm^{-1})

ΔT is the measured temperature difference

The form factor is the distance between the thermometer contacts divided by the cross-sectional area of the specimen. Δ T was obtained from the calibration curve of the thermocouple knowing the average temperature of the sample between the thermocouple junctions. Q was obtained directly from the heater current and voltage readings.

4.7 Possible sources of error in the measurement

(a) Error in the form factor

Ideally the thermometer contacts should be as small as possible and they should not be too close together. They should also be at some distance from both the heater and the constant temperature bath to promote parallel heat flow. In practice this is difficult to achieve. For the low temperature rod samples the thermometer contacts were of thickness 0.8 mm and they were separated by a distance of about 6 mm. The specimens were fairly accurately cut and the uncertainty in the cross-sectional area was less than 0.5%.

Estimating the error in the distance between the thermocouples as one contact width gives an uncertainty of about ± 15%. The relative error between form factors for different samples will probably be less than this value as the holes for the thermometer contacts were drilled to a fair degree of accuracy, and the range of thermal conductivity values measured at a given temperature is not large.

For the high temperature "miniature" Lees disc samples, parallel heat flow is promoted by encasing the heater in a copper block of the same diameter as the sample slice. A possible error of about ± 5% is expected for these samples.

(b) Heat flow along thermometer leads

Some of the heat developed in the heater will find its way to the constant temperature bath via the thermometer leads.

For cryostat I about 10 cm of chromel wire of 0.08 mm diameter

was used between the thermal anchoring point and the specimen and this led to an error of 0.5% for the worst possible situation. For cryostat II, using about 15 cm of constantan wire of diameter 0.12 mm introduced at worst an error of less than 1%.

A length of about 50 cm of gold-iron wire of diameter 0.08 mm was used in the leg of the thermocouple which at 20 K will introduce a systematic error in the measured thermal conductivity at worst of about 1 %. This value decreases as the temperature is reduced. For the copper-constantan thermocouples a length of about 100 cm of 42 swg copper wire was used and at worst this will lead to an error of less than 1%.

At temperatures at which measurements were taken (> 1.5 K) the effect of the thermal contact resistance between the sample and the thermometer contact will be negligible compared with the thermal resistance of the specimen.

(c) Errors in measured specimen heater power

The heater power was determined by measuring the voltage across the heater and across a standard 100 ohm resistor in series. The possible random error in these measurements was less than $\pm$ 1%.

The heater consisted of about 200 cm of 47 swg. constantan of which about 2 cm was free. The current leads to the heater were 40 swg constantan and it is estimated that the heat developed in these was about 2% of that in the heater itself.

Thus there could be a systematic error of about $\pm$ 2% in all the measured values of heater power.

(d) Error in calibration of the thermocouples

As the thermocouples were not calibrated for each experiment it is difficult to estimate the error introduced but the relative error between different experiments will probably be less than ± 5%.

(e) Error in the thermocouple voltage measurement

At helium temperatures a spread of about 2% was found for thermocouple voltage readings for a given heater power. At hydrogen temperatures, where the time for the sample to obtain equilibrium when the heater was energised is measured in minutes compared with a few seconds at helium temperatures, the spread was typically about 5%. At higher temperatures a spread of about 5% was also obtained.

4.8 Summary of the accuracy of the experiment

The sources of error are most conveniently discussed in the following classification:

(a) Errors in the determination of the absolute magnitude of the thermal conductivity

These were errors which remain constant or nearly so over the whole temperature range. The main contribution was that from the measurement of the form factor together with the heat loss down the leads. This amounts to about ± 17% for the low temperature sample and about ± 9% for the high temperature samples.

(b) Relative errors in the thermal conductivity measured at different temperatures

Systematic errors arose from the thermocouple calibration and from the loss of heat from the sides of the specimen at high temperatures due to thermal radiation. The latter is probably less than 10% at room temperature and will decrease rapidly as the temperature is reduced.

Random errors in the thermal conductivity vary from about $\pm$ 6% at 20 K and above to about $\pm$ 3% at 2 K, and were those associated with heater power and thermometry measurements.

The values of the mean temperature of the specimen are accurate to about $\pm$ 0.05 K at helium temperatures. At liquid hydrogen temperatures the error will be larger as the ortho-para composition of the hydrogen is unknown, but will be less than $\pm$ 0.2 K.

The error in measuring the filler concentration of the specimens will depend on the density and volume concentration of the filler. For a quartz specimen at about 30% volume content the error in the filler concentration will be about $\pm$ 2%. At a lower concentration of about 5% an uncertainty of 5 $\pm$ 1% is to be expected.

CHAPTER 5

EXPERIMENTS ON THE UNFILLED EPOXY

5.1 Experimental results and discussion

The first experiments were performed on a specimen of the unfilled epoxy, Araldite MY 740. The specimen was prepared as described in section 3.5.

The thermal conductivity results from 2 K to room temperature are shown in fig. 5.1. The curve has the characteristic shape of amorphous glasses and polymers and the thermal conductivity increases monotonically with temperature and at around 10 K has the characteristic plateau.

From 1.6 K to about 2.3 K the relationship is approximately linear with temperature. This can be ascribed to the Klemens "intrinsic structure scattering" with a frequency dependent mean free path varying as ω^{-2}. At high temperatures, the slope decreases and becomes nearly temperature independent near 4 K. Above 10 K the thermal conductivity begins to rise again, becoming proportional to the specific heat.

Below 5 K the data could be fitted to within 3% by both equation 2.13 of Klemens and equation 2.19 of Dreyfus, as shown in fig. 5.2. The values of the parameters used for the fitting are shown in table 5.1, determined to about 10%

TABLE 5.1

	$A/a\ cm^{-1}$	T_o	Θ_R
Klemens	22.0×10^8	7.0 K	-
Dreyfus	7.0×10^8	-	10.0 K

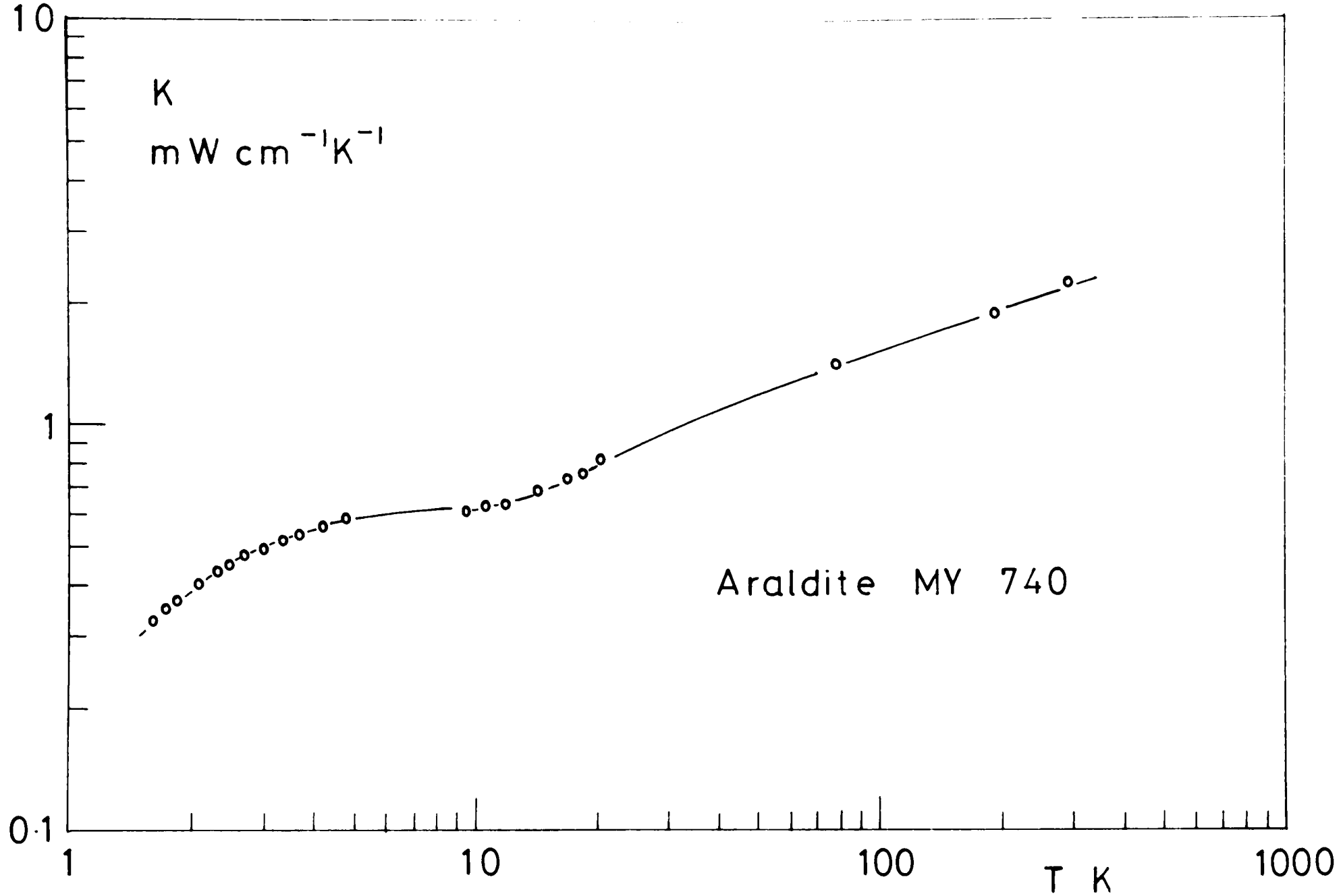


Fig 5.1 Thermal Conductivity (K) vs. Temperature (T).

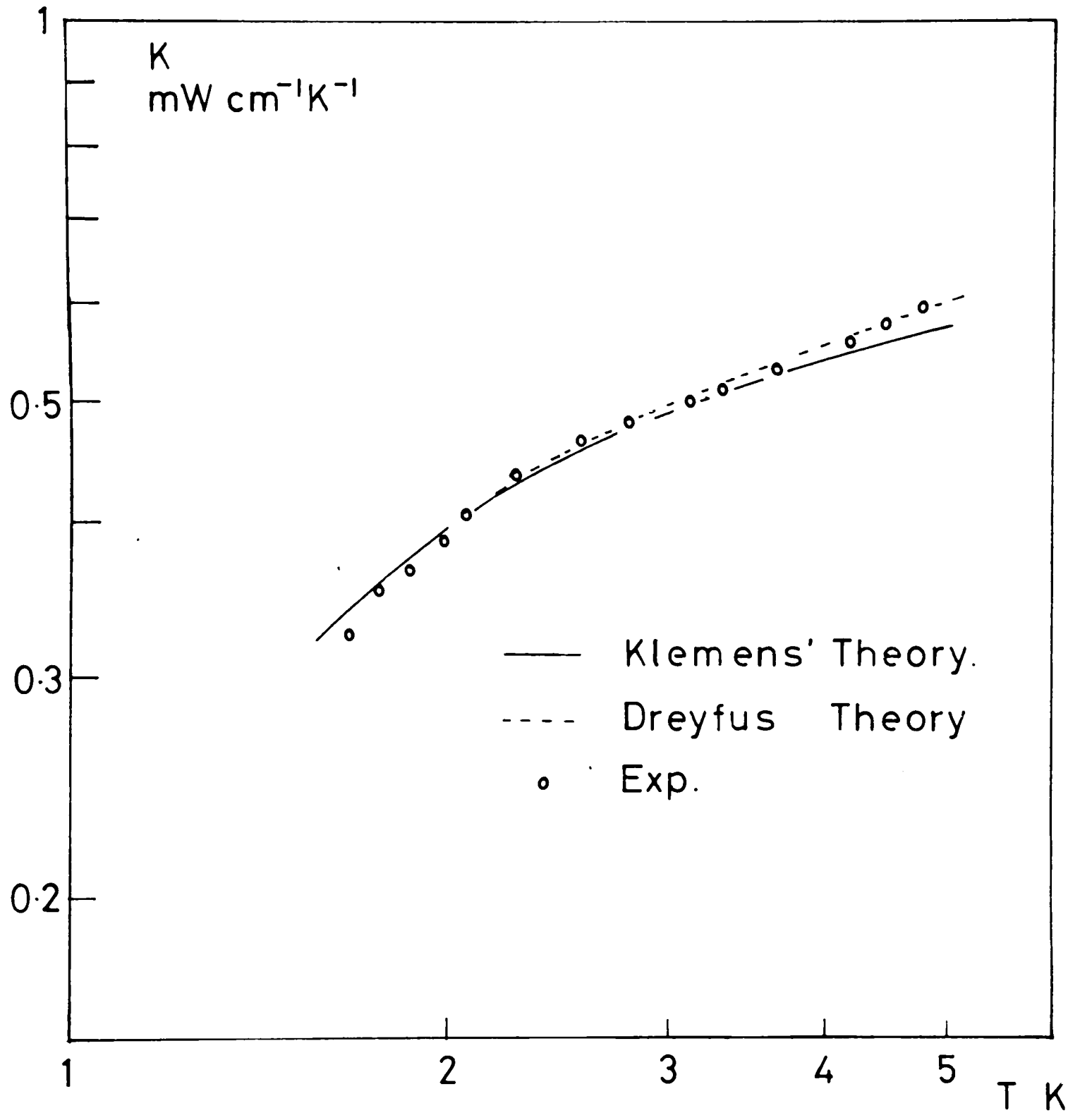


Fig 5.2 Thermal Conductivity (K) vs. Temperature (T).

Comparison between Experiment and Theory.

A/a is the constant of proportionality in the Klemens "structure scattering" mean free path (equation 2.11), T_0 is a parameter of temperature charaterising the process in which longitudinal waves are converted into transverse waves in the Klemens theory, and Θ_R is a characteristic temperature associated with the localized modes in the Dreyfus theory.

The large difference between the two values of A/a (about a factor of 3) in table 5.1 is accounted for in that in the Dreyfus approach A/a is an average over the three polarization branches of the phonon spectrums, whereas in the Klemens approach only the longitudinal modes are considered important.

Athougies et al. (1972) have reported an excess heat capacity in Epiband 121 and Epiband 100 - A at low temperatures which they suggest are due to non-acoustic modes in the phonon spectrum. These two epoxies are similar to the epoxy used in this work. The non-acoustic contribution must be subtracted from the calorimetric measurement of the heat capacity before use in the Klemens expression for the thermal conductivity. In addition, the Dreyfus approach requires a detailed analysis of the heat capacity to obtain the characteristic temperatures that are necessary for evaluating the Dreyfus equation.

A detailed knowledge of the high temperature specific heat of epoxies is not available. However, the similarity between the values of the parameters for fitting the low temperature thermal conductivity of the epoxy in this work and polymethyl methacrylate (PMMA) in Reese (1966[b]) and Choy et al. (1969) suggest that the

chemical and physical characteristics of the two materials are not unlike. The calculations of Choy et al. for PMMA using the Dreyfus approach are compared with the epoxy, Araldite MY 740 results in fig. 5.3 Although no great importance can be attached to this comparison, it suggests that the epoxy results above 10 K could be explained using the Dreyfus model.

Choy et al. on PMMA and Anderson et al. (1963) on epoxies found a temperature dependence greater than T in the thermal conductivity at low temperatures, indicating the presence of another scattering mechanism which they ascribed to be scattering by internal boundaries (section 2.4). Although this was not found in the epoxy results, measurements were not taken at the temperatures (about 1 K) where this effect was observed.

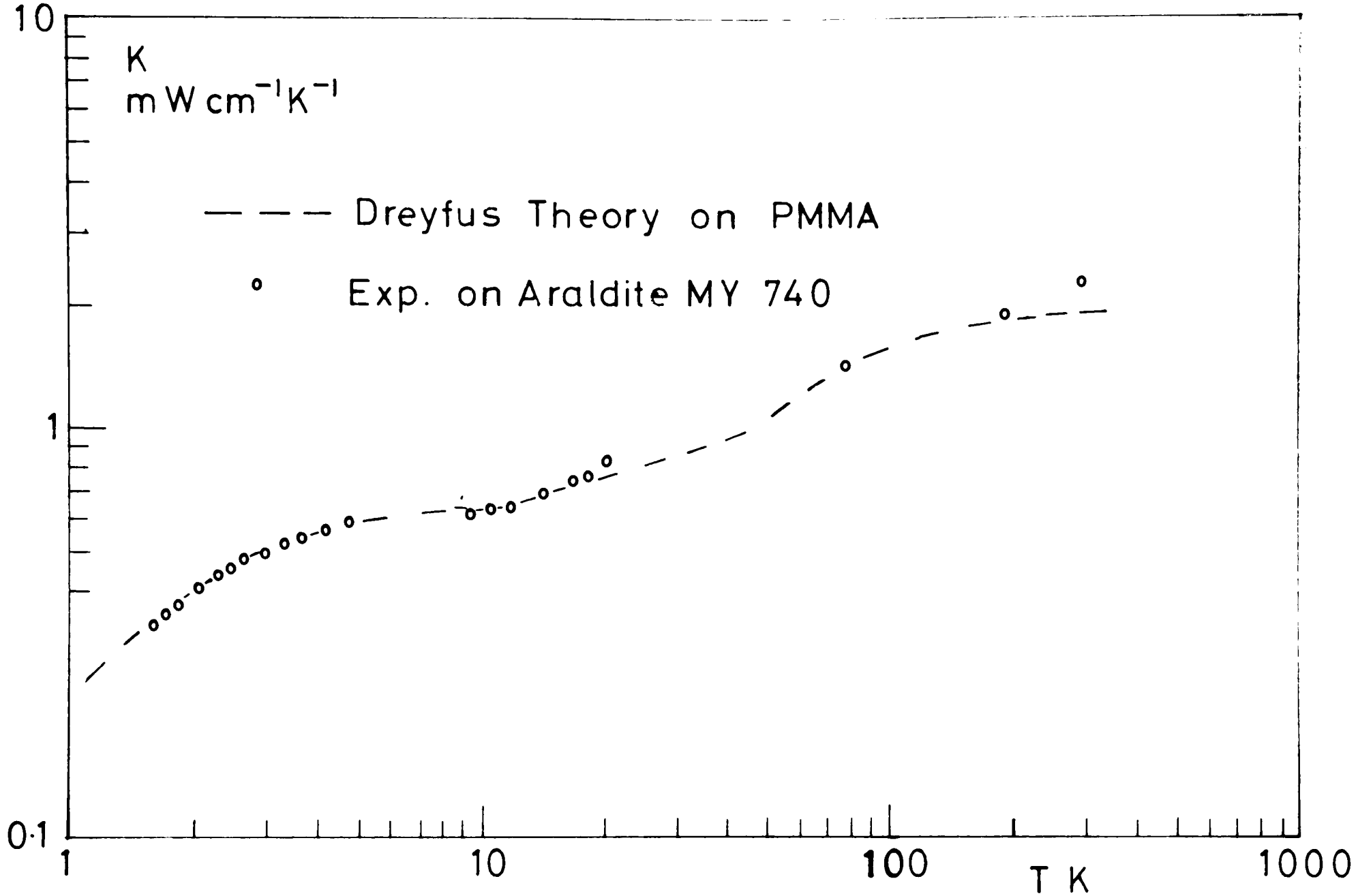


Fig 5.3 Thermal Conductivity (K) vs Temperature (T). Comparison between Experiment on MY 740 and Dreyfus Theory on PMMA.

CHAPTER 6

EXPERIMENTS WITH FILLED EPOXIES

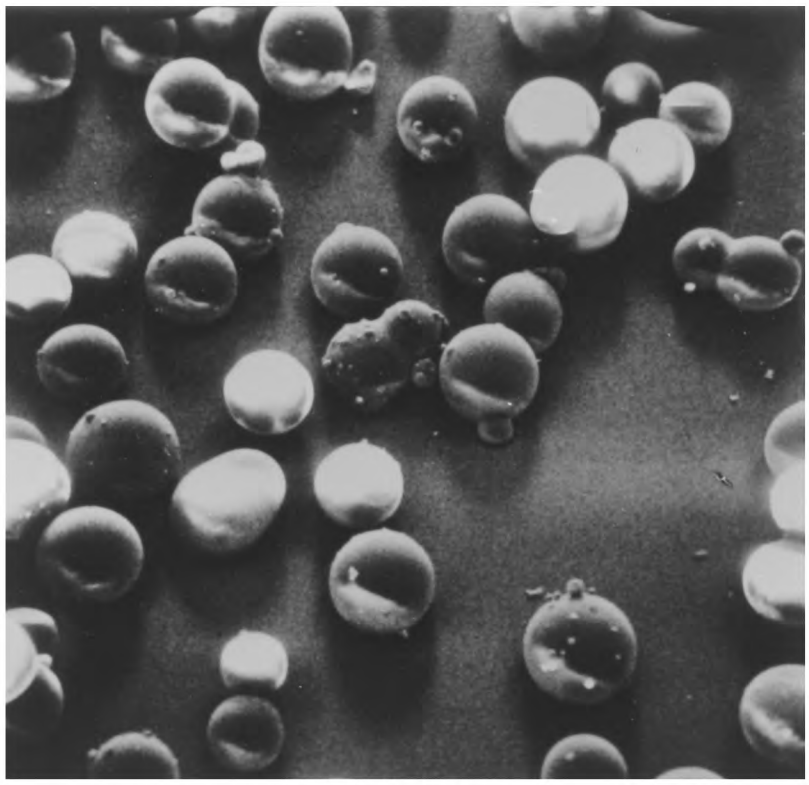
GLASS FILLED EPOXIES

6.1 Specimens Solid glass beads are used as a general purpose low cost filler for thermoplastic and thermosetting resins. Ballotini 2024, obtained from Plastichem Ltd., Esher, England, was used in the specimens. It consists of spherical solid beads of soda glass and can be obtained from the manufacturers in various ranges of particle sizes. The glass beads are coated with a coupling agent CP02 to improve the adhesive properties of the glass-epoxy interface.

Scanning electron micrographs were taken of the Ballotini 2024 and two of these are shown in plate 1. The remarkable sphericity of the glass beads can be clearly seen. The analysis of particle size is greatly simplified because of this fact and a volume weighted bead diameter of 132 microns was obtained from measurements from the micrographs. This value was used in all calculations in which a particle size was required. The particle size range stated by the manufacturers for this grade of Ballotini is 105 to 210 microns.

Spherical glass beads produce a low viscosity mix of filler and uncured resin because of their low surface area for a given volume. This allows high filler concentrations to be used in the specimens. Also, the pourability of the glass-resin mix is enhanced by the "ball bearing" type action of the glass spheres.

Another benefit of the spherical shape of the beads is that the Maxwell-Rayleigh equations for predicting the effective conductivity of a two phase composite, assume spherically shaped filler



200μ

Ballotini 2024

Plate 1

particles. The thermal conductivity of the glass is never greatly different from that of the epoxy matrix from 2 K to room temperature, and it should be an ideal filler for comparison between the measured values of the composite thermal conductivity and those predicted by theory.

The specimens were prepared as described in section 3.5 and had glass concentrations of 8.7%, 27.8% and 44.0% by volume, for measurements at liquid hydrogen temperatures and below, and 8.7%, 31.7%, 38.6%, 49.2% and 53% by volume for measurements at 78 K and above.

6.2 Results The thermal conductivity of the glass filled epoxies are shown in figs. 6.1 to 6.4. The results are presented both against temperature for a given glass concentration, and against glass concentration for a given temperature. The full temperature curves from 1.5 K to room temperature are obtained by reading off the thermal conductivity values in fig. 6.3 for the glass concentrations of the low temperature samples.

The general shape of the thermal conductivity vs temperature curves of the filled samples is similar to that of the unfilled

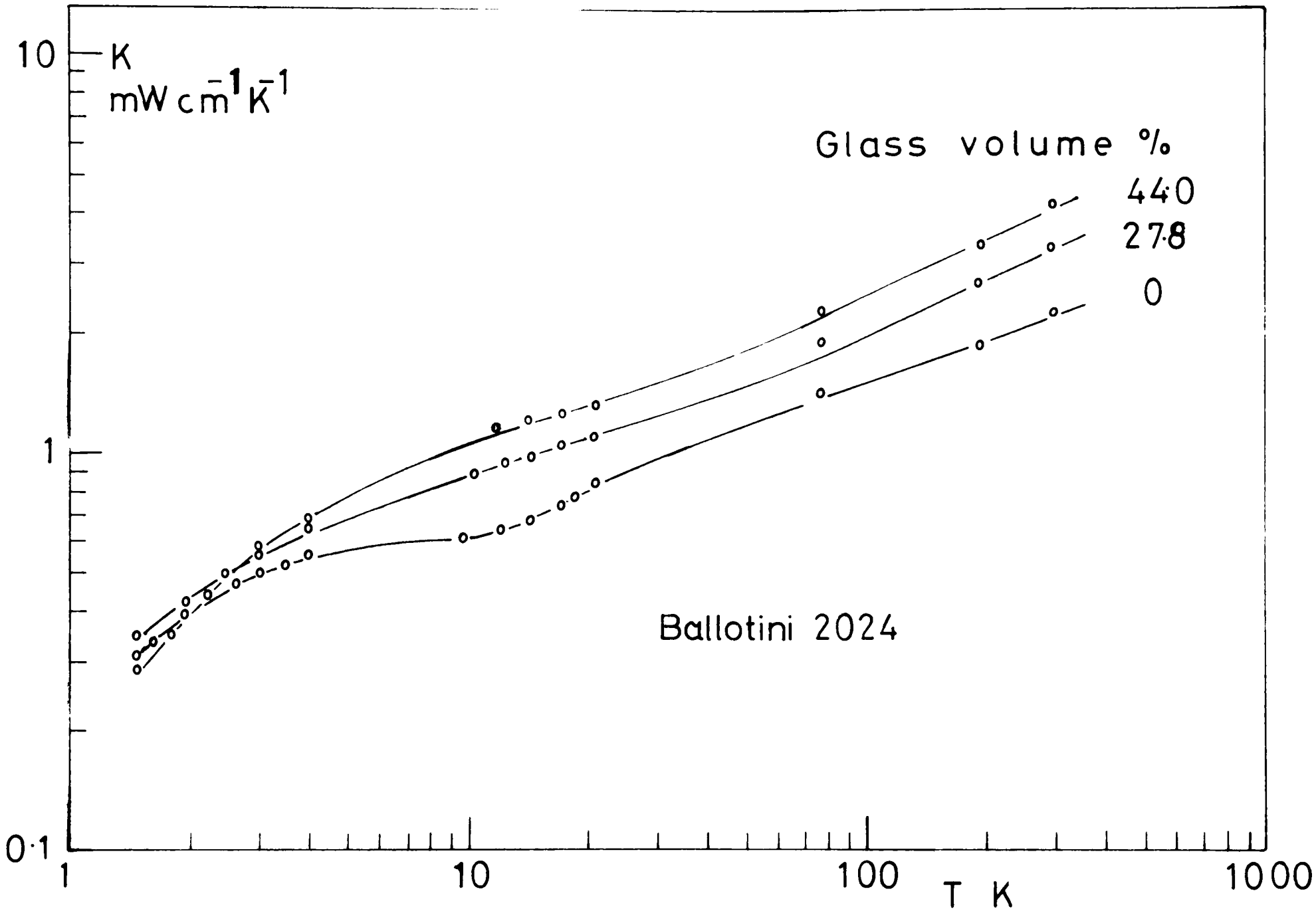


Fig 6.1 Thermal Conductivity (K) vs Temperature (T).

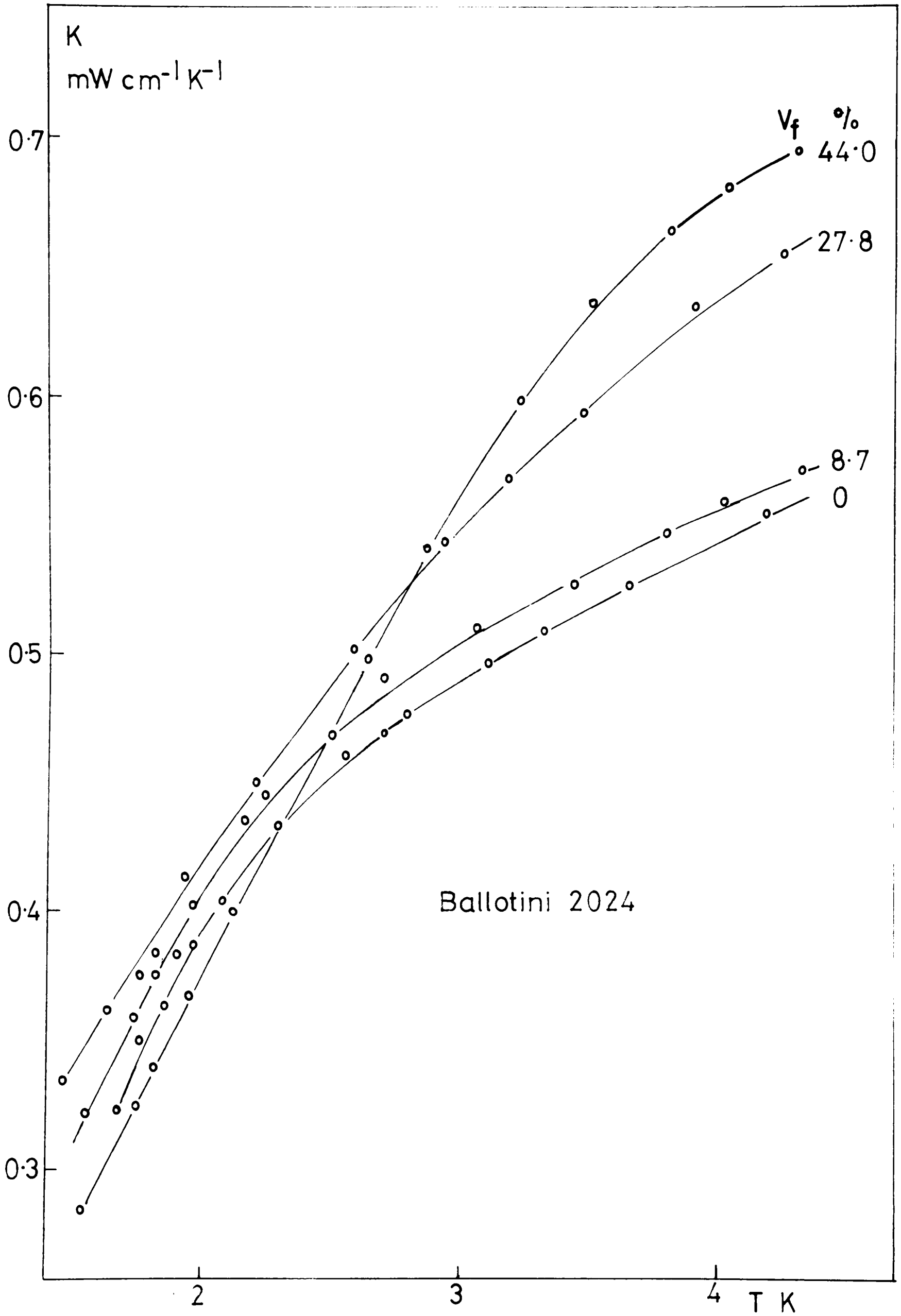


Fig 6.2 Thermal Conductivity (K) vs. Temperature (T).

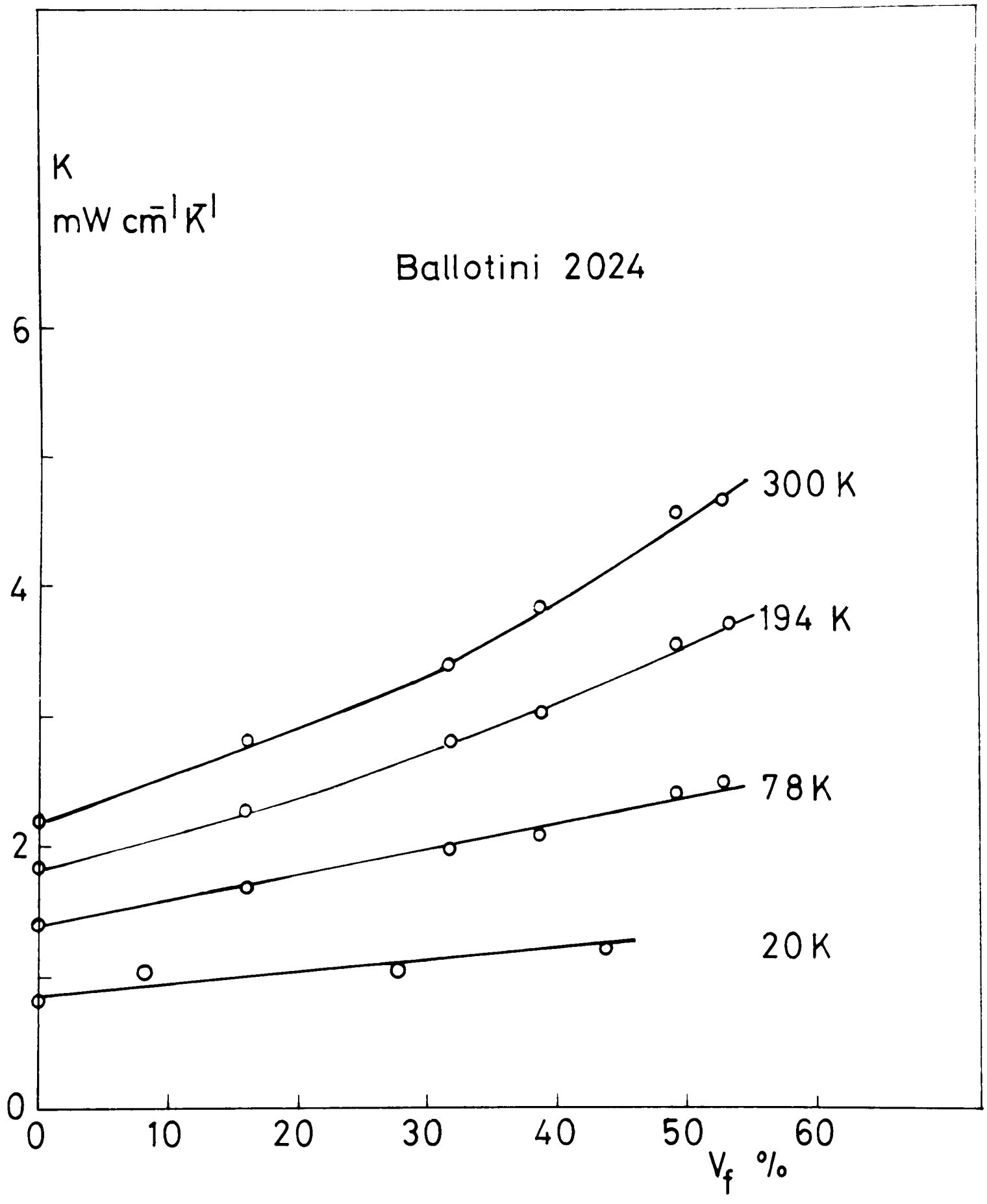


Fig 6.3 Thermal Conductivity (K) vs. Glass Concentration, Volume % (V_f).

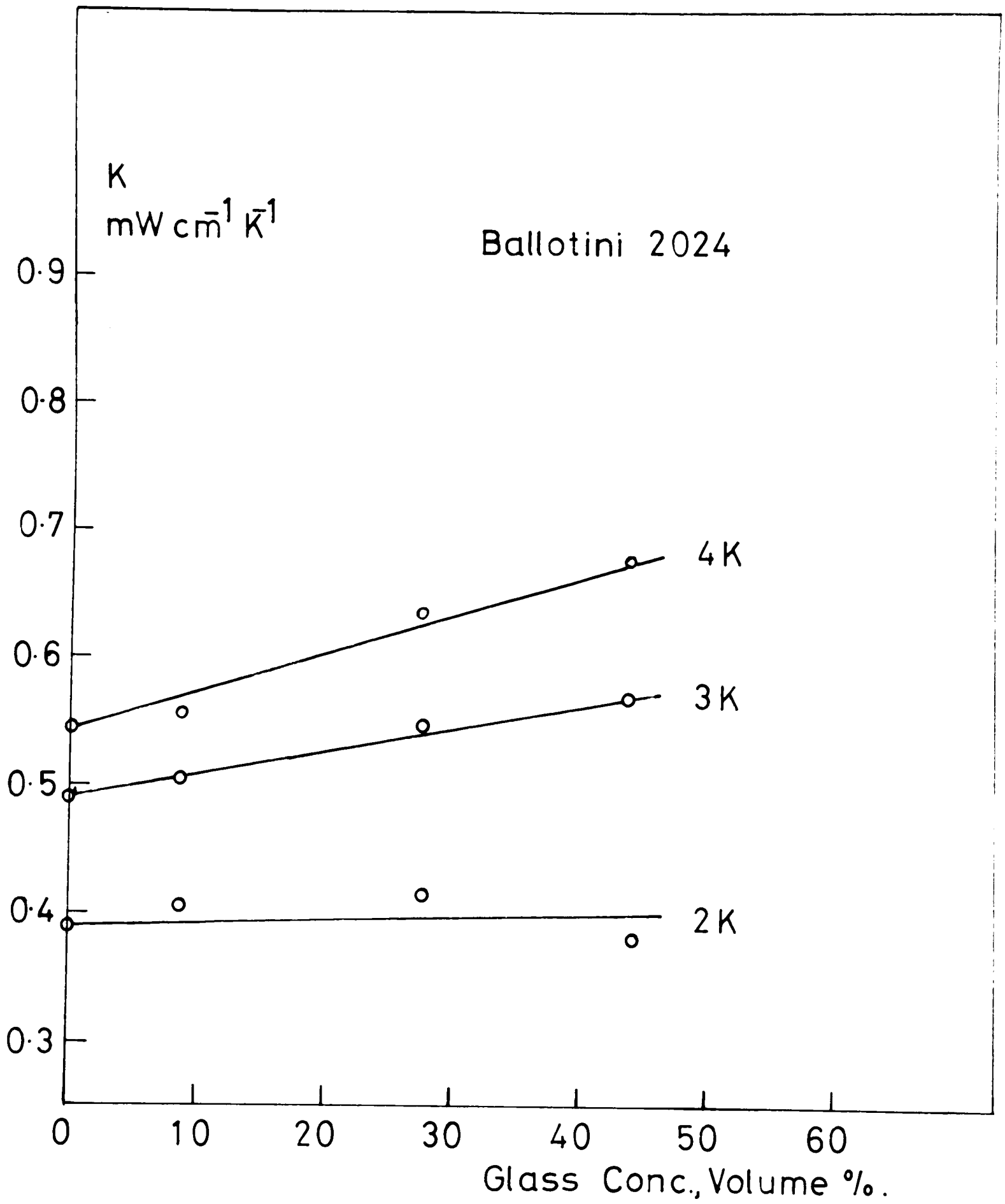


Fig 6.4 Thermal Conductivity (K) vs. Glass Concentration, Volume %.

epoxy and the thermal conductivity of the epoxy is included in the graphs for purposes of comparison.

The thermal conductivity of the filled specimens is greater than that of the unfilled epoxy for all temperatures and all glass concentrations at which measurements were taken, except for the heavily loaded sample below 2 K. Above 2 K the thermal conductivity always increases with increasing filler concentration, signifying that the particle thermal conductivity is higher than that of the epoxy matrix at these temperatures.

The thermal conductivity of a soda glass specimen was measured from 1.6 K to room temperature and the results are shown in fig. 6.5. Below 5 K the results compare favourably with those of Berman, Foster and Rosenberg (1955) on a similar glass.

The thermal contact resistance of the glass-epoxy interface was measured using a sample similar to that described in section 4.4. This contact resistance, however, was negligible compared with the thermal resistance of the glass comprising the "sandwich", and no meaningful results could be obtained.

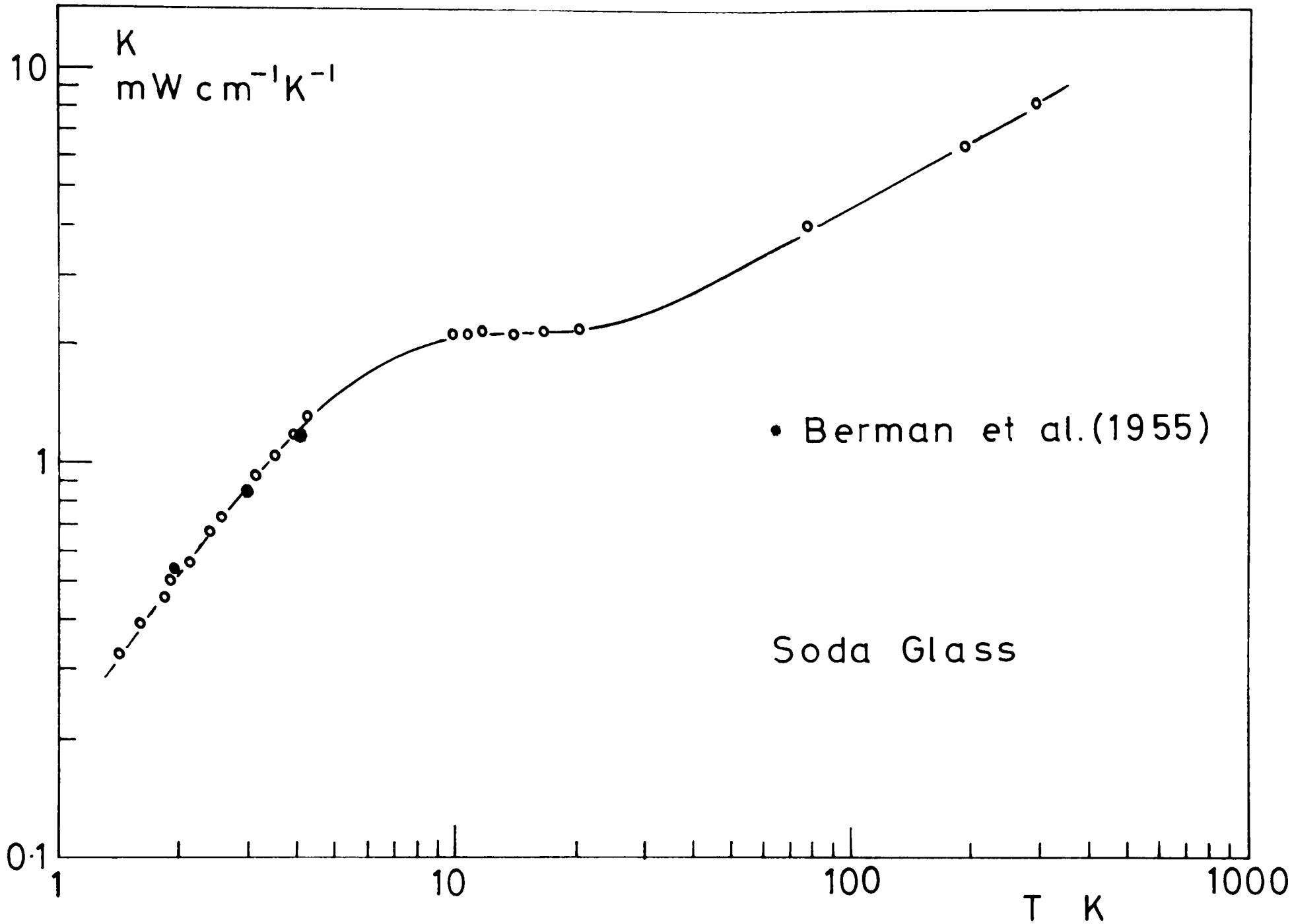


Fig 6.5 Thermal Conductivity (K) vs. Temperature (T).

6.3 Comparison between theory and experiment At 1.5 K the average phonon mean free path in a glass is typically 0.4 microns and thus the thermal conductivity of the Ballotini glass beads will be independent of bead size, for all temperatures at which measurements were taken, the size range of the beads being 105 to 210 microns. Similarly the average mean free path in an epoxy is typically 0.2 microns at 1.5K, and is negligible compared with the average distances between the glass beads for concentrations used in these measurements. Therefore in the calculations of the thermal conductivity of the glass-epoxy composites we can use the bulk conductivities of soda glass and the epoxy without modification due to size effects.

In figs. 6.6 and 6.7 the results of the glass filled epoxies are compared with the Rayleigh model of a two-phase composite at various temperatures.

At liquid hydrogen temperatures and above the agreement is to within 5% even for filler concentrations of about 50% by volume. At liquid helium temperatures, however, the agreement is less satisfactory, the predicted thermal conductivities being about 15% higher than the measured values. Following Anderson & Bauch (1970) this is probably caused by a small thermal contact resistance at the glass-epoxy interface which would lower the effective thermal conductivity of the particles and hence that of the composite.

Although measurement of this contact resistance was not possible,

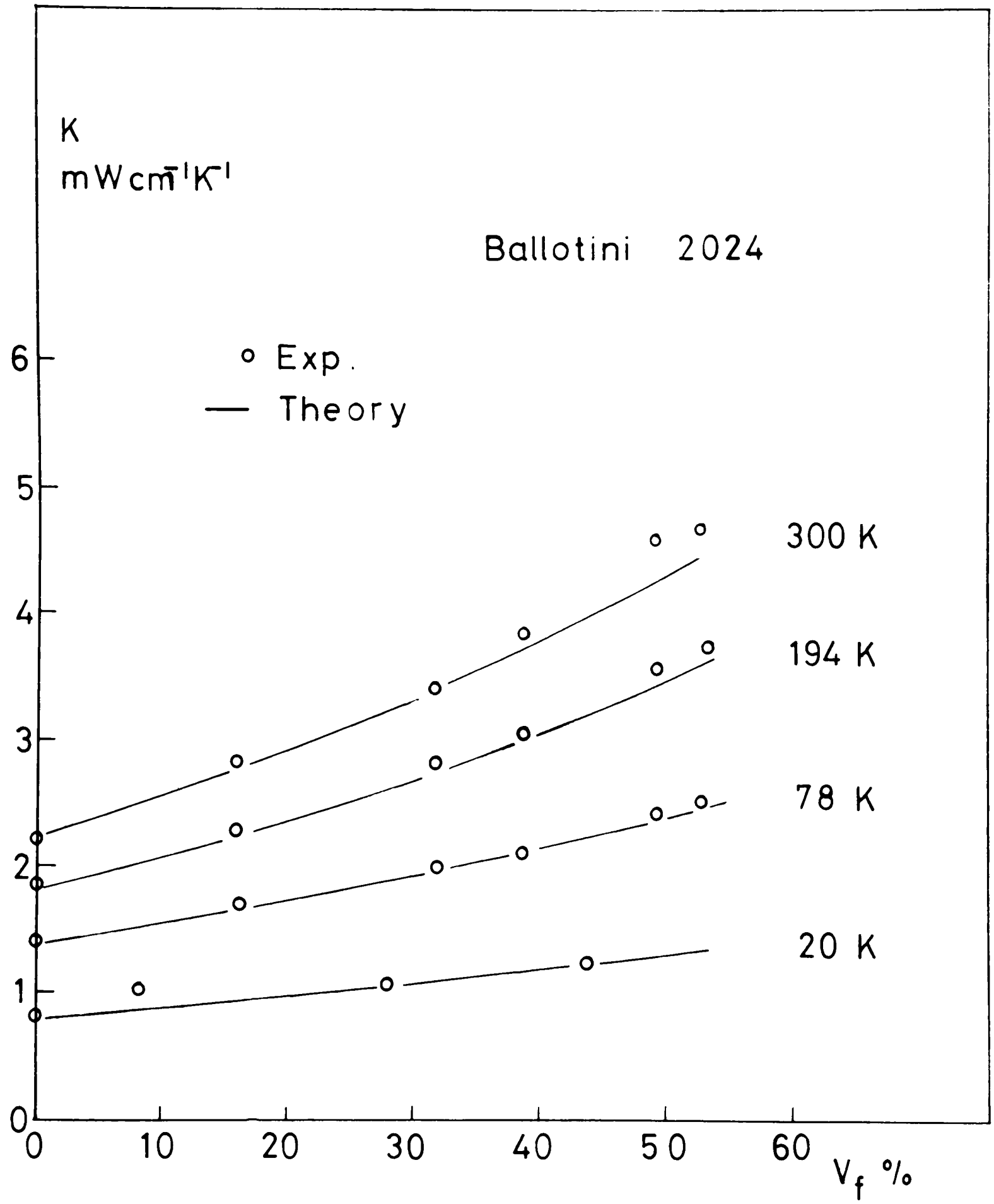


Fig 6.6 Thermal Conductivity (K) vs Glass Concentration, Volume % (V_f).
Comparison between Experiment and Rayleigh Equation.

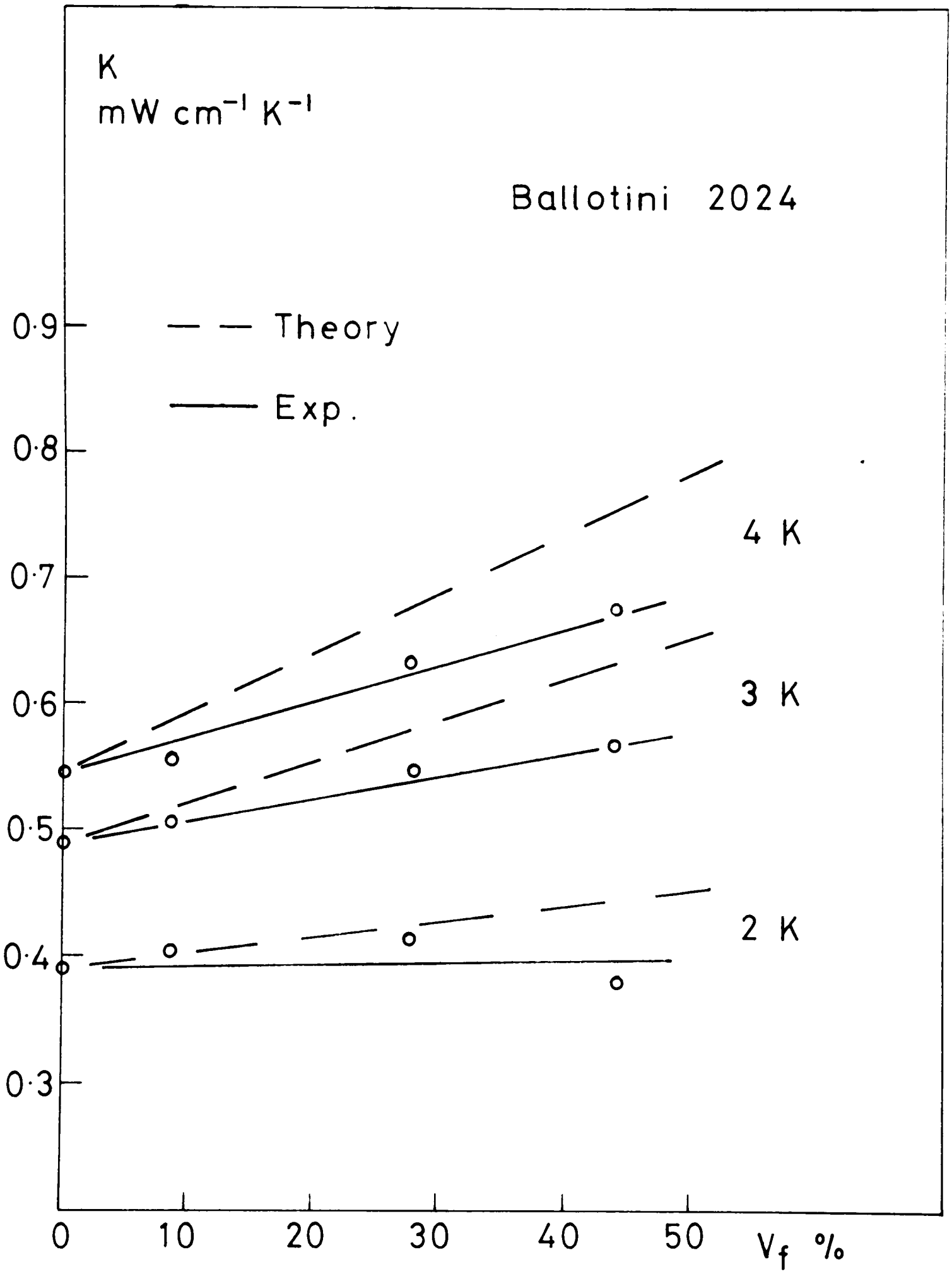


Fig 6.7 Thermal Conductivity (K) vs Glass Concentration, Volume % (V_f).
Comparison between Experiment and Theory.

we can estimate it using Little's theory (section 2.5). Using values of $v_l = 3.22 \times 10^5$ cm second $^{-1}$, $v_t = 1.64 \times 10^5$ cm sec $^{-1}$, for the epoxy measured by Athougies et al on a similar epoxy (1972), and $v_l = 5.64 \times 10^5$, $v_t = 3.28 \times 10^5$ cm sec $^{-1}$ for the glass, (American Institute of Standards on Pyrex) we obtain at low temperatures,

$$R_k = \frac{40}{AT^3} \text{ K W}^{-1} \qquad 6.1$$

where R_k is the thermal contact resistance averaged over the two directions of heat flow and A is the area of contact.

If it is possible to modify the thermal conductivity of the particles to include the thermal contact resistance at the glass-epoxy interface we can use this effective particle thermal conductivity in the Rayleigh equation. The thermal resistance of a sphere is a difficult concept to deal with when the sphere is not embedded in a matrix. We can approximate the problem by considering the particle to be a cube whose face area is equal to the projected area of 132 micron diameter sphere. If we assume that the isotherms are planes perpendicular to the direction of heat flow, then the effective particle conductivity will be given by

$$\frac{1}{K_{fe}} = \frac{2R_k}{Z} + \frac{1}{K_f} \qquad 6.2$$

where K_{fe} is the effective particle thermal conductivity, K_f is the filler thermal conductivity and Z is the cube length, remembering

that there are two thermal contact resistances associated with each particle.

Calculations along these lines yield effective particle conductivities of 1.06, 0.67, 0.36 mW cm $^{-1}$ K $^{-1}$ for temperatures of 4 K, 3K and 2 K respectively.

These values should be compared with those required to achieve the best fit for the experimental results. By experiment effective particle thermal conductivities of 0.90, 0.68 and 0.40 mW cm $^{-1}$ K $^{-1}$ are required for temperatures of 4 K, 3 K, 2 K respectively. The agreement between these two sets of values is good considering the uncertainty in the computed value of the thermal contact resistance and the model employed, but the main point is that the existence of a small thermal contact resistance at the glass-epoxy interface will lower the effective thermal conductivity of the glass composites.

In fig. 6.8 the experimental results of a 27.8% glass volume composite from 2 K to room temperature are compared with the predictions of the Rayleigh formula. Below 4 K the computed effective particle thermal conductivity is used. The agreement is excellent. With a knowledge of the bulk thermal conductivities of the epoxy and the soda glass the Rayleigh formula can be used to predict the thermal conductivity of the glass filled epoxies at liquid hydrogen temperatures and above. At liquid helium temperatures the presence of a thermal contact resistance at the glass-epoxy interface will result in the predicted values being

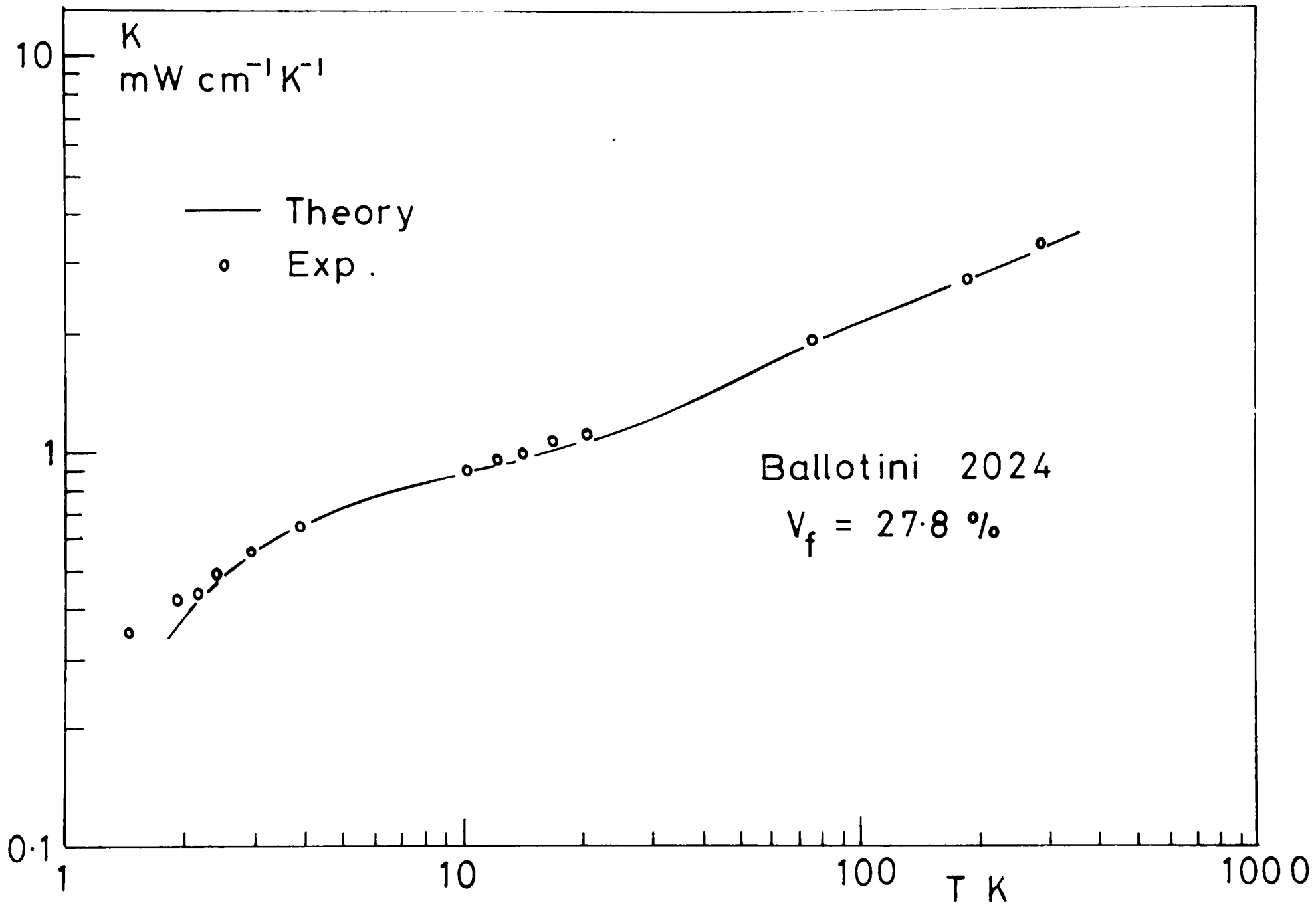


Fig 6.8 Thermal Conductivity (K) vs. Temperature (T).
Comparison between Theory and Experiment.

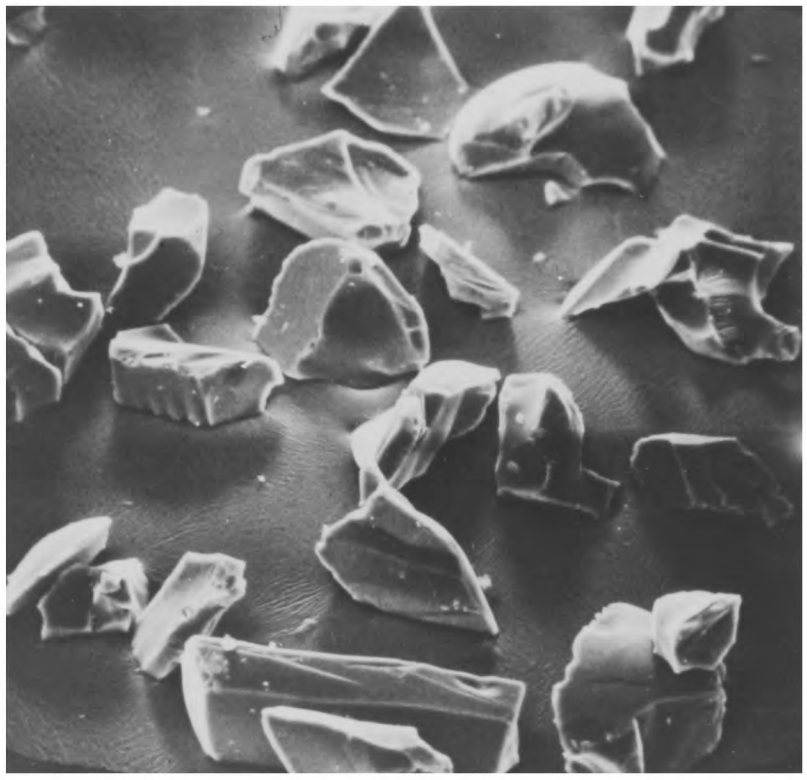
higher than the measured ones. With a knowledge of the size of the particles and a value for the thermal contact resistance it is possible to use the Rayleigh formula at helium temperatures by using an effective particle conductivity which includes the effect of the thermal contact resistance.

QUARTZ FILLED EPOXIES

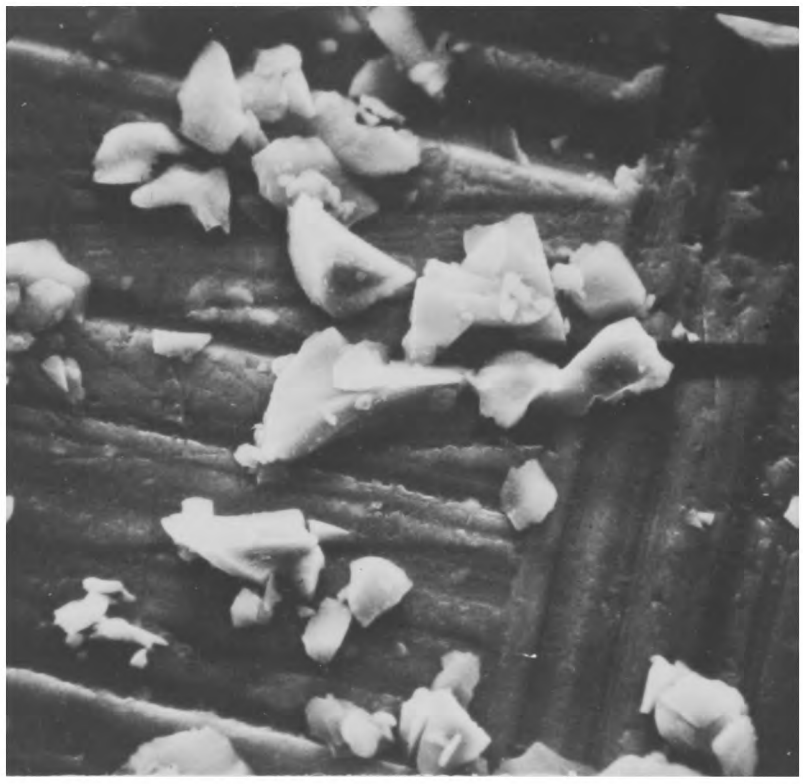
6.4 Samples Crystalline Quartz powders are used in thermo-setting epoxy resins to increase the room temperature thermal conductivity and abrasive resistance of the epoxy. The quartz-epoxy composites were filled with powdered crystalline quartz of commercial purity, obtained from Thermal Syndicate Ltd., Wallsend, Northumberland. The Quartz was obtained from the manufacturers in a size range of - 75 microns, having passed through a 75 micron aperture sieve.

The quartz powder was sieved using screens of aperture sizes 60, 40, 20 and 10 microns and two size ranges of particles were used; those retained on the 60 and 10 micron sieves.

Scanning electron micrographs of the two size ranges of the quartz powders were taken and two of these are shown in plate 2. The particles are of a random and irregular shape. Following the procedure of section 3.6 a volume weighted average cube length for the two size ranges was deduced from measurements from the micrographs. For the smaller size powder the weighted length was 11 microns, and for the larger size it was 95 microns. Sieving selects only the second largest particle dimension and as the large particles are important in determining the volume weighted average size of the particles this can account for the apparent discrepancy between the sieve sizes and the measured weighted length. The 10 micron sieve is at the limit of aperture size for sieving. The efficiency of this



100μ Quartz 95 micron



20μ Quartz 11 micron

Plate 2

sieve will not be very great and the fairly large proportion of fine particles retained on the sieve will lower the weighted average size of the particles.

The specimens were prepared as described in section 3.5 using a matrix of Araldite MY 740. The quartz was dried before mixing but no coupling agent was used. Quartz powder concentrations of up to about 50% by volume were used in the samples.

6.5 Experimental results

The thermal conductivities of the quartz filled samples from 2 K to room temperature are shown in fig. 6.9 to 6.11. The results are also presented against quartz volume concentration for various temperatures in figs. 6.11 to 6.17.

The thermal conductivity of the quartz-epoxy composites always decreases with decreasing temperature and above helium temperatures the general shape of the curves is similar to that of the unfilled epoxy.

Above 10 K there is no particle size dependence in the thermal conductivity. For a given quartz concentration similar thermal conductivity values are obtained for the two particle sizes. This is clearly shown in the conductivity versus concentration plots. The conductivity always increases with filler content, the dependence

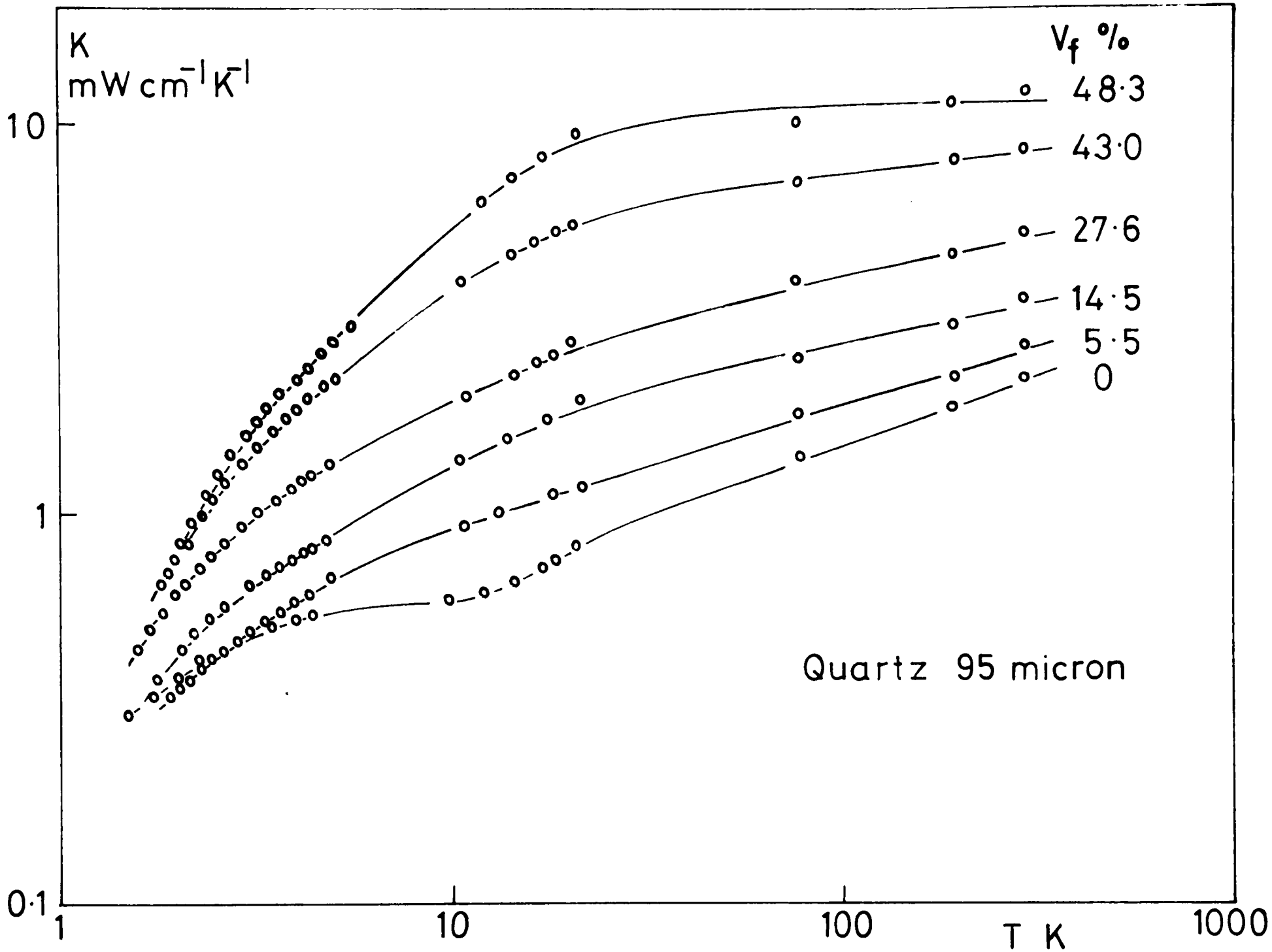


Fig 6.9 Thermal Conductivity (K) vs. Temperature (T)

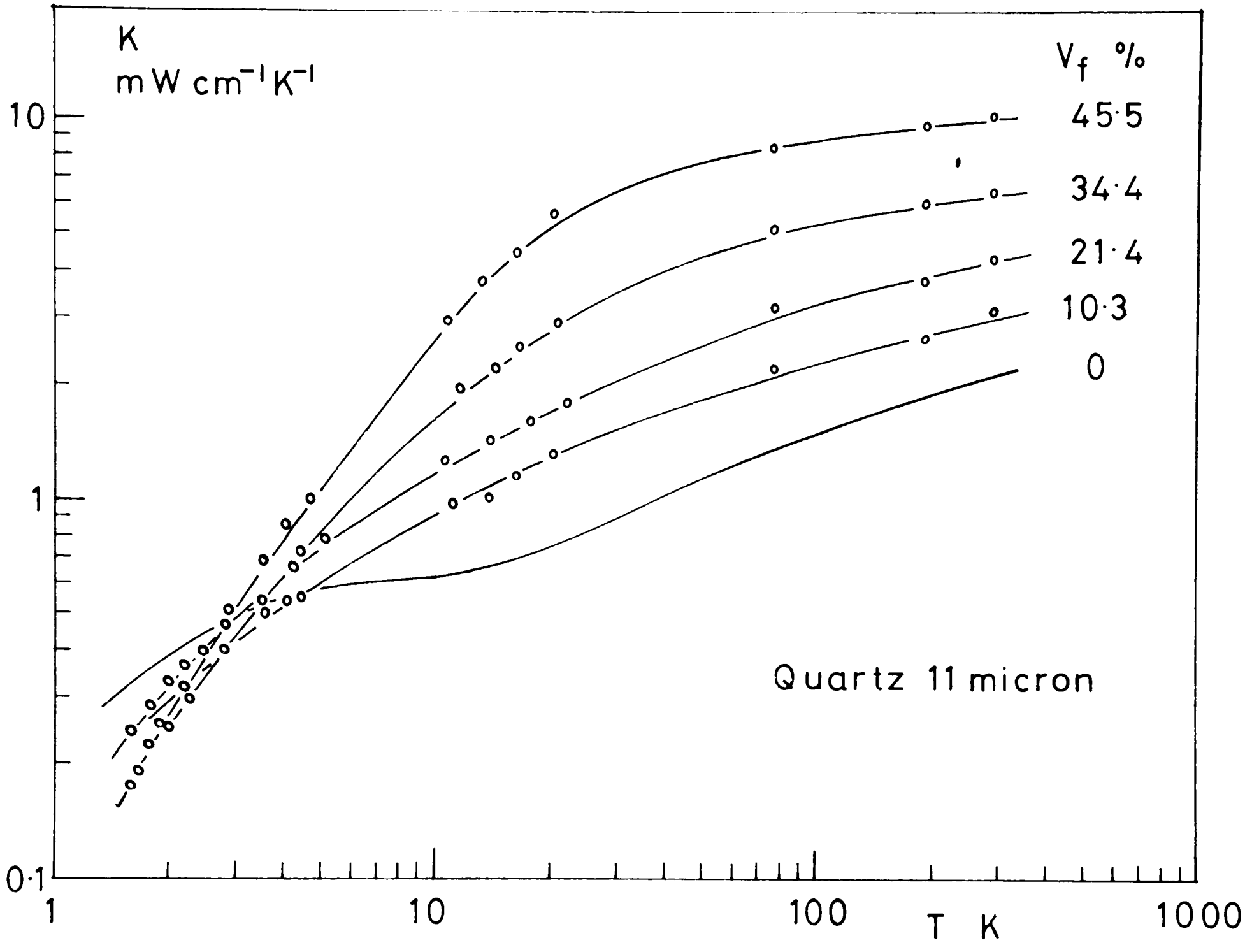


Fig 6.10 Thermal Conductivity (K) vs. Temperature (T).

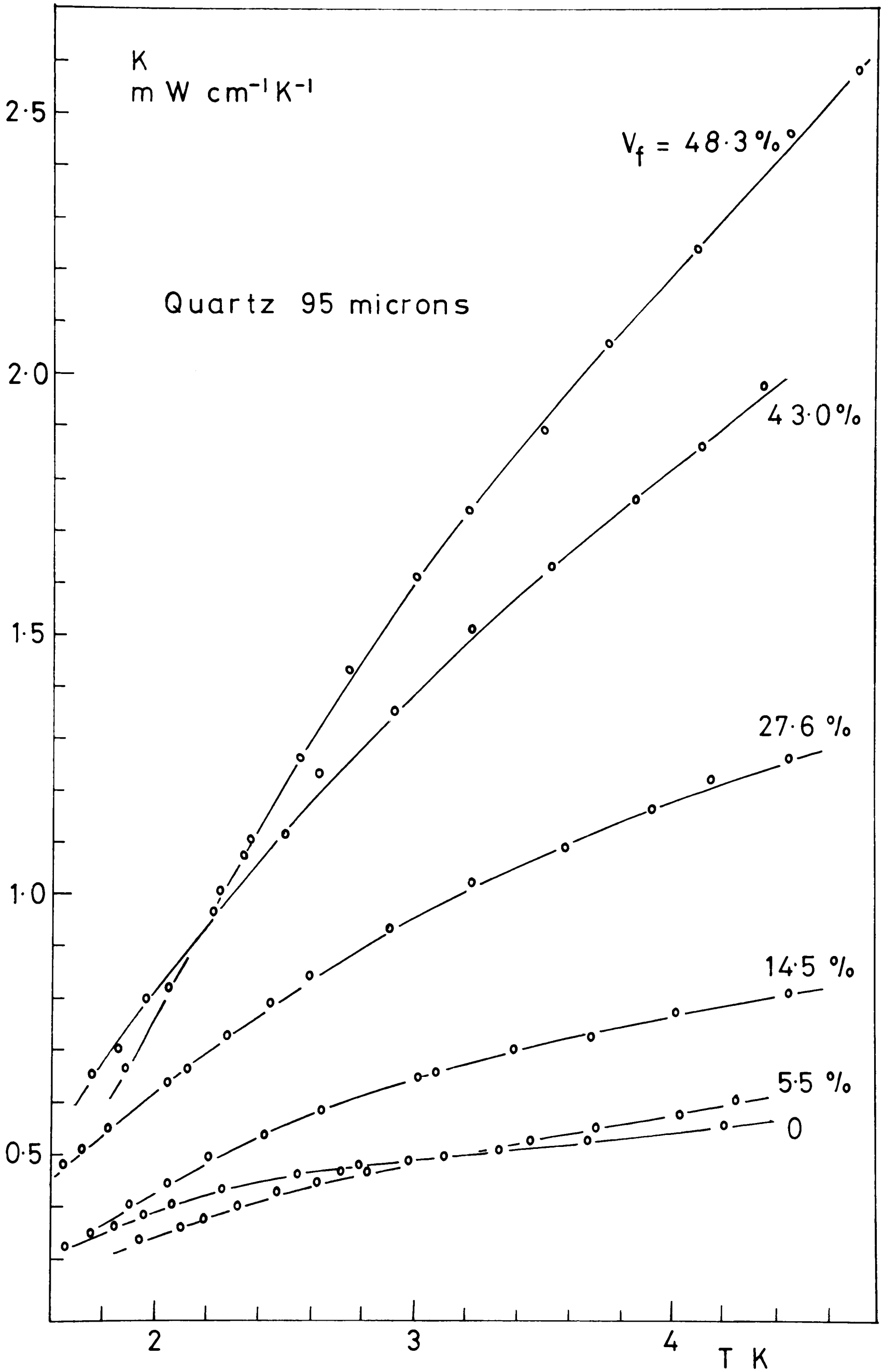


Fig 6.11 Thermal Conductivity (K) vs. Temperature (T).

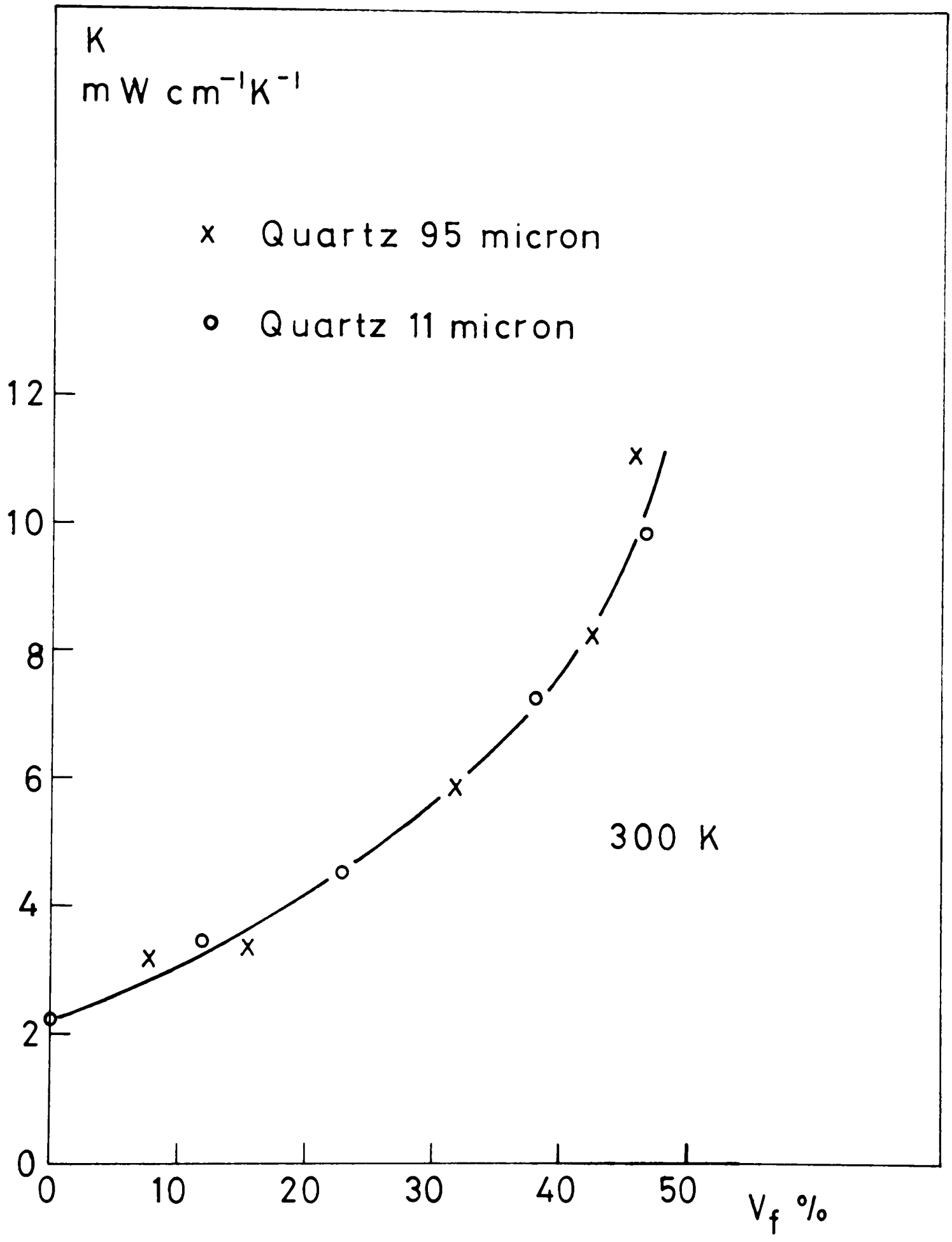


Fig 6.12 Thermal Conductivity (K) vs. Quartz Concentration, Volume % (V_f).

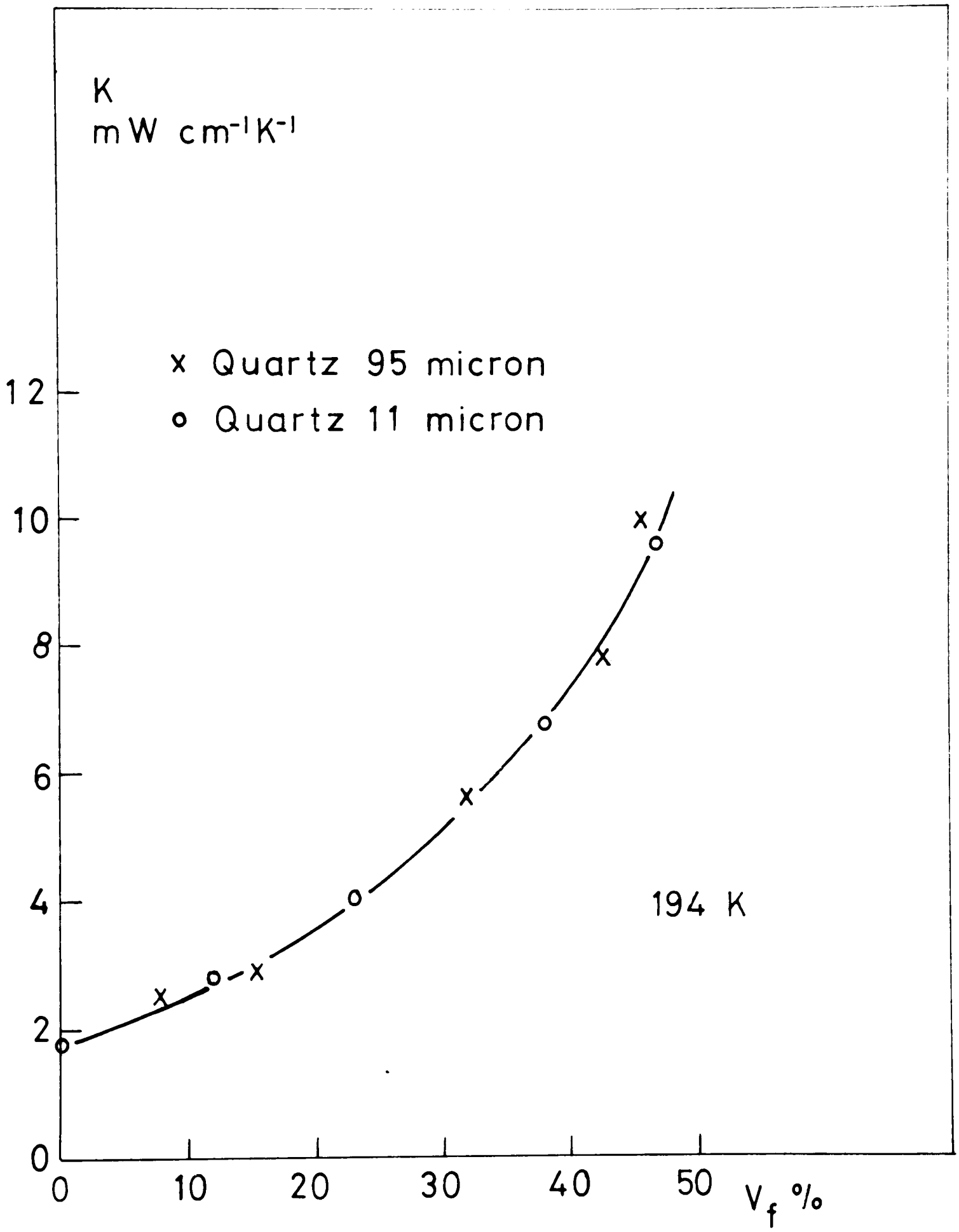


Fig 6.13 Thermal Conductivity (K) vs. Quartz Concentration, Volume % (V_f).

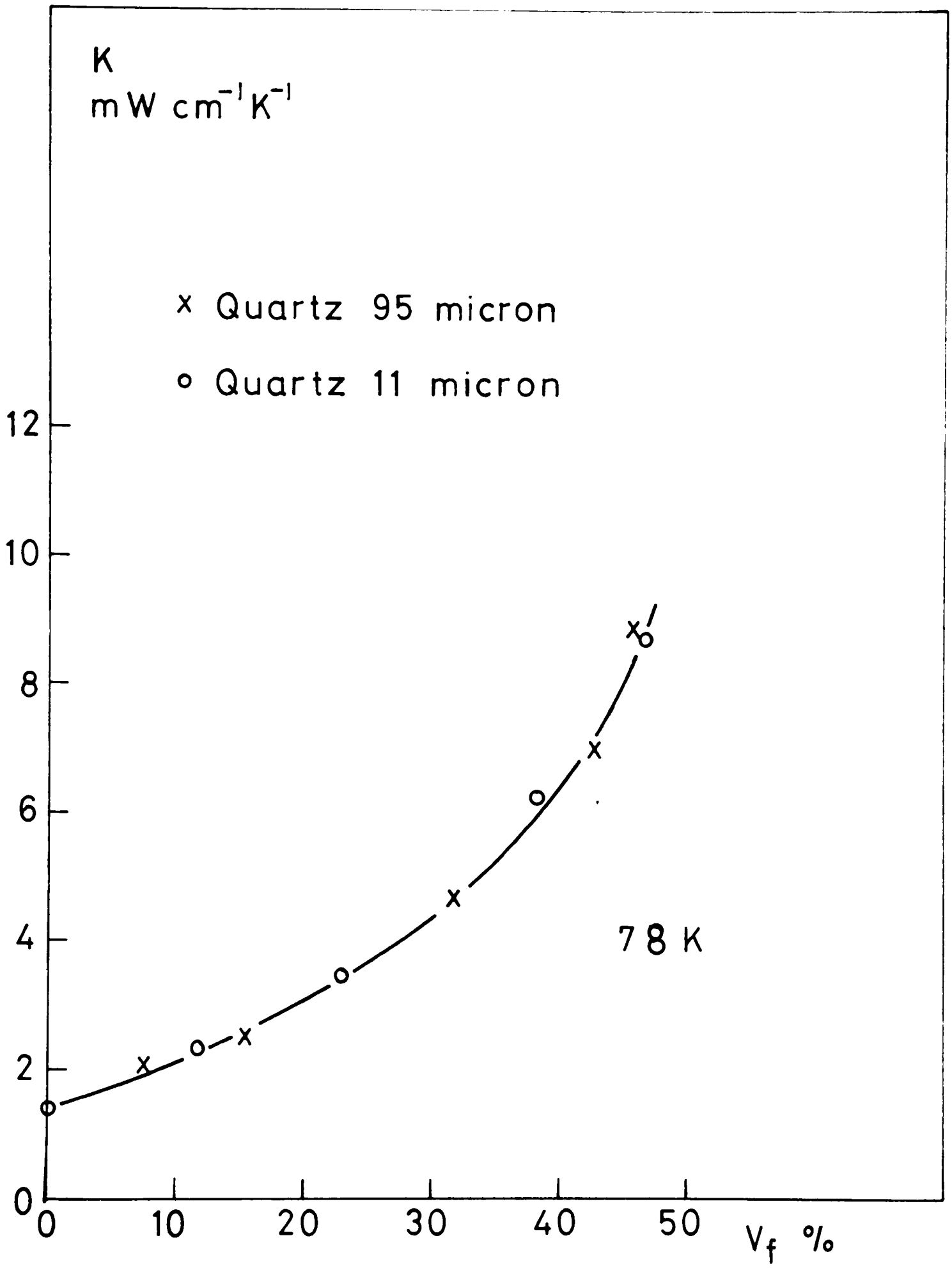


Fig 6.14 Thermal Conductivity (K) vs. Quartz Concentration, Volume % (V_f).

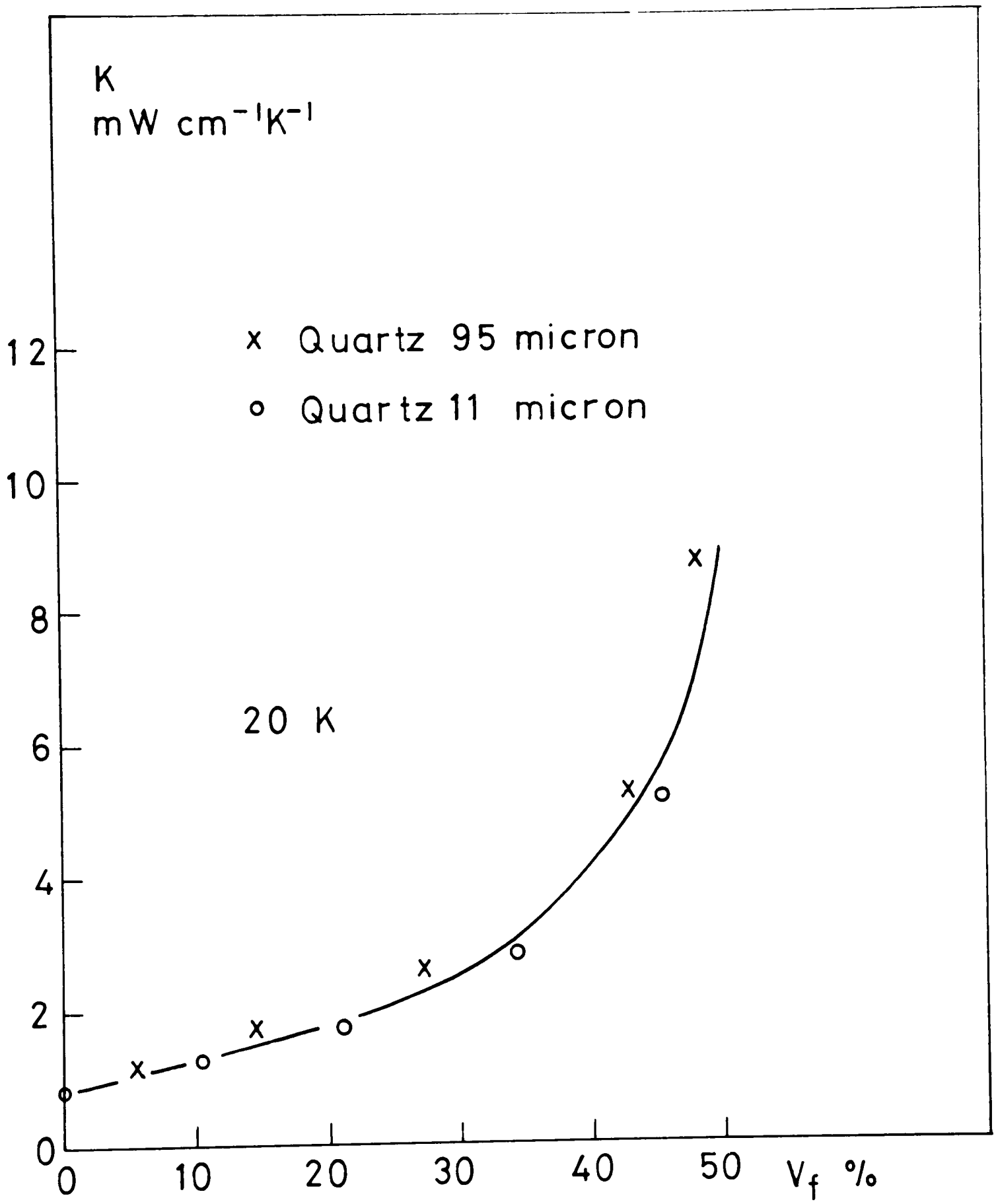


Fig 6.15 Thermal Conductivity (K) vs. Quartz Concentration, Volume % (V_f).

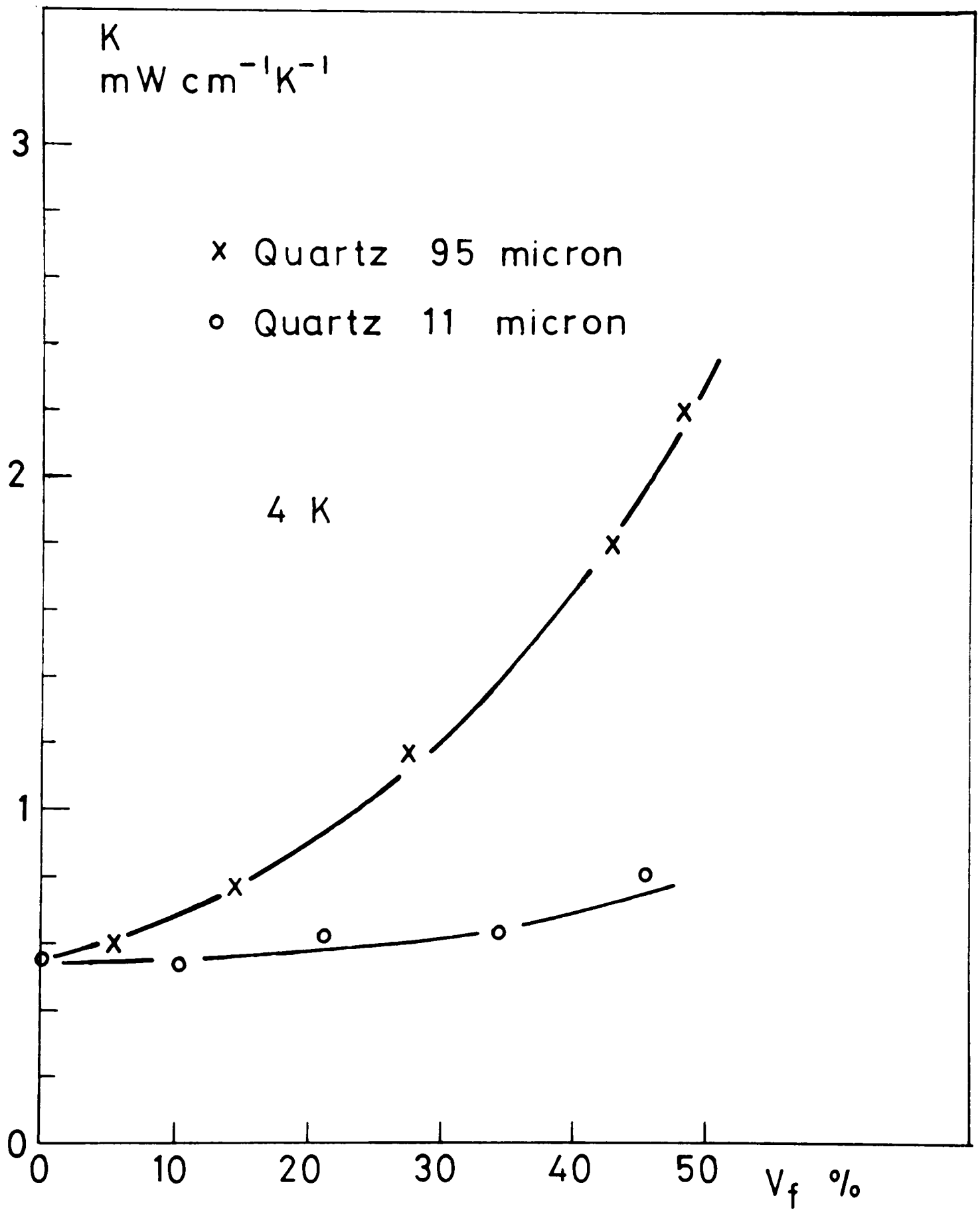


Fig 6.16 Thermal Conductivity (K) vs. Quartz Concentration, Volume % (V_f).

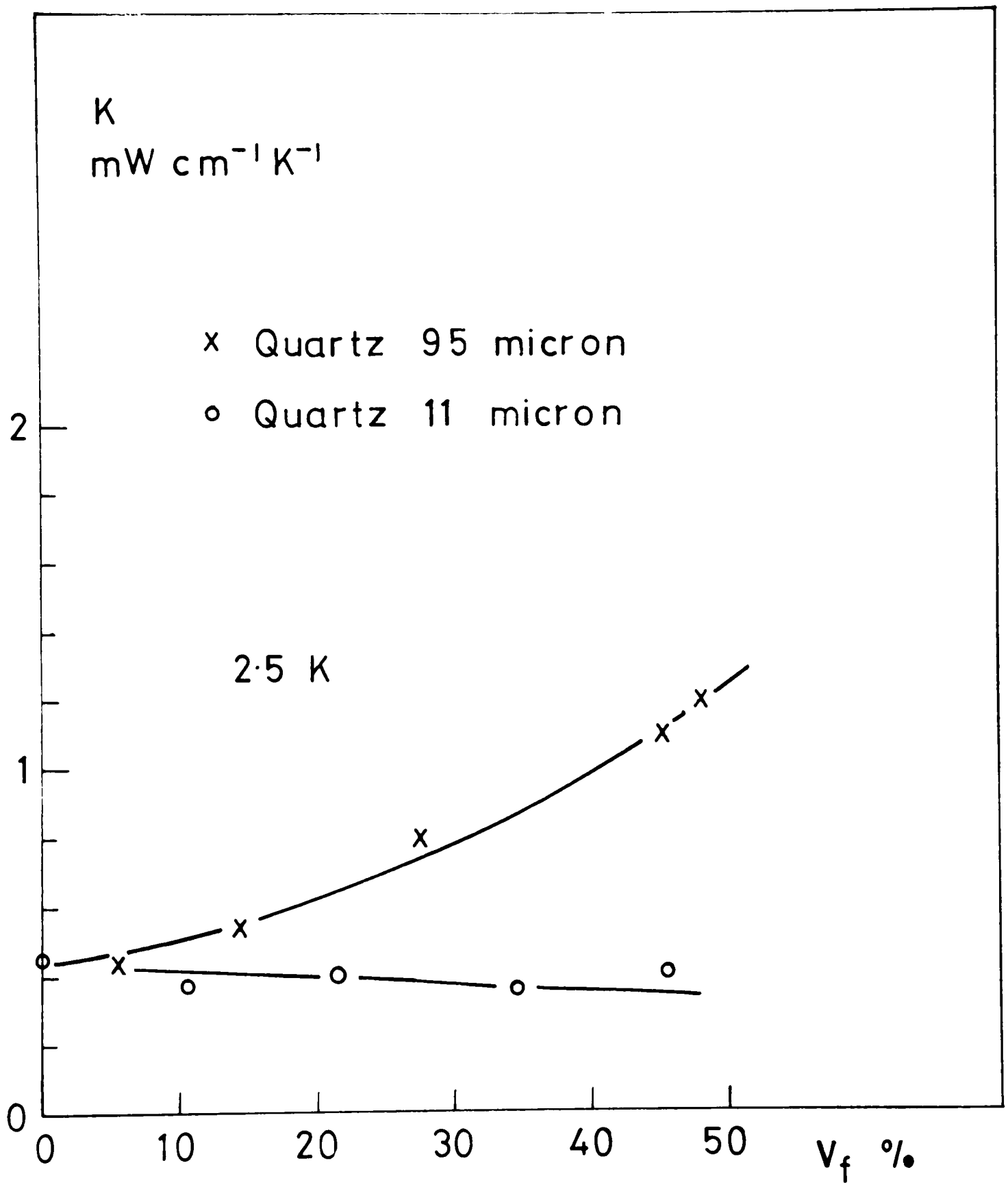


Fig 6.17 Thermal Conductivity (K) vs. Quartz Concentration, Volume % (V_f).

being approximately linear for concentrations up to about 30% by volume, increasing more rapidly for higher concentrations.

At helium temperatures the particle size strongly affects the measured thermal conductivity, the 11 micron composites having a lower conductivity than the 95 micron composites. At 4 K they differ by about a faster of about 2 for a volume concentration of 30% quartz. The thermal conductivity of the 95 micron composites are higher than the unfilled epoxy for all concentrations of filler at all temperatures at which measurements were taken, whereas the conductivities of the 11 micron composites are smaller than the resin for temperatures below about 3 K. Below 3 K, for the 11 micron composites, the thermal conductivity decreases with increasing filler concentration. Above 3 K the reverse is true.

The particle size dependent conductivity at helium temperatures can be accounted for by a combination of two effects. The smaller size quartz particles will have a lower thermal conductivity due to the frequency independent boundary scattering described in section 2.3. In addition to this, at the quartz-epoxy interface there will be a thermal contact resistance at low temperatures due to the accoustic mismatch described in section 2.5. This contact resistance will be high between the amorphous epoxy and the crystalline quartz. For a given filler concentration there will be a greater surface area for smaller particles and hence a greater scattering of phonons and the effect of the contact resistance will, therefore, be greater for smaller particles.

The thermal contact resistance between bulk specimens of X - cut quartz and the epoxy was measured using a sample similar to that described in section 4.4. The results are shown in fig. 6.18. The rapid increase in the thermal contact resistance at helium temperatures is clearly shown and a temperature dependence of $T^{2.5}$ is obtained at these temperatures.

The thermal conductivity of the X - cut quartz crystal, a rod of 3 mm diameter, was measured at the same time and the results are shown in fig. 6.19. Included in the figure are the expected thermal conductivities along the X - direction, of a 93 and 11 micron crystal, scaled down from the 3 mm sample results in the low temperature region of frequency independent boundary scattering. At temperatures near the maximum, the contributions from the boundary scattering and other effects are assumed to be reciprocally additive. Accurate values of the quartz thermal conductivity are not necessary in this region as the quartz thermal conductivity is so much higher than that of the epoxy matrix. Indeed, as the purity of the commercial quartz is not known, it is impossible to predict the values of this thermal conductivity near the maximum.

The thermal conductivity of crystalline quartz is highly anisotropic. The values along the Z - axis are about twice that measured along the other two axes. Table 6.1 in the next section shows the variation of the anisotropy with temperature. The values are taken from a paper by Slack (1961). The anisotropy of the quartz thermal conductivity must be taken into account when values

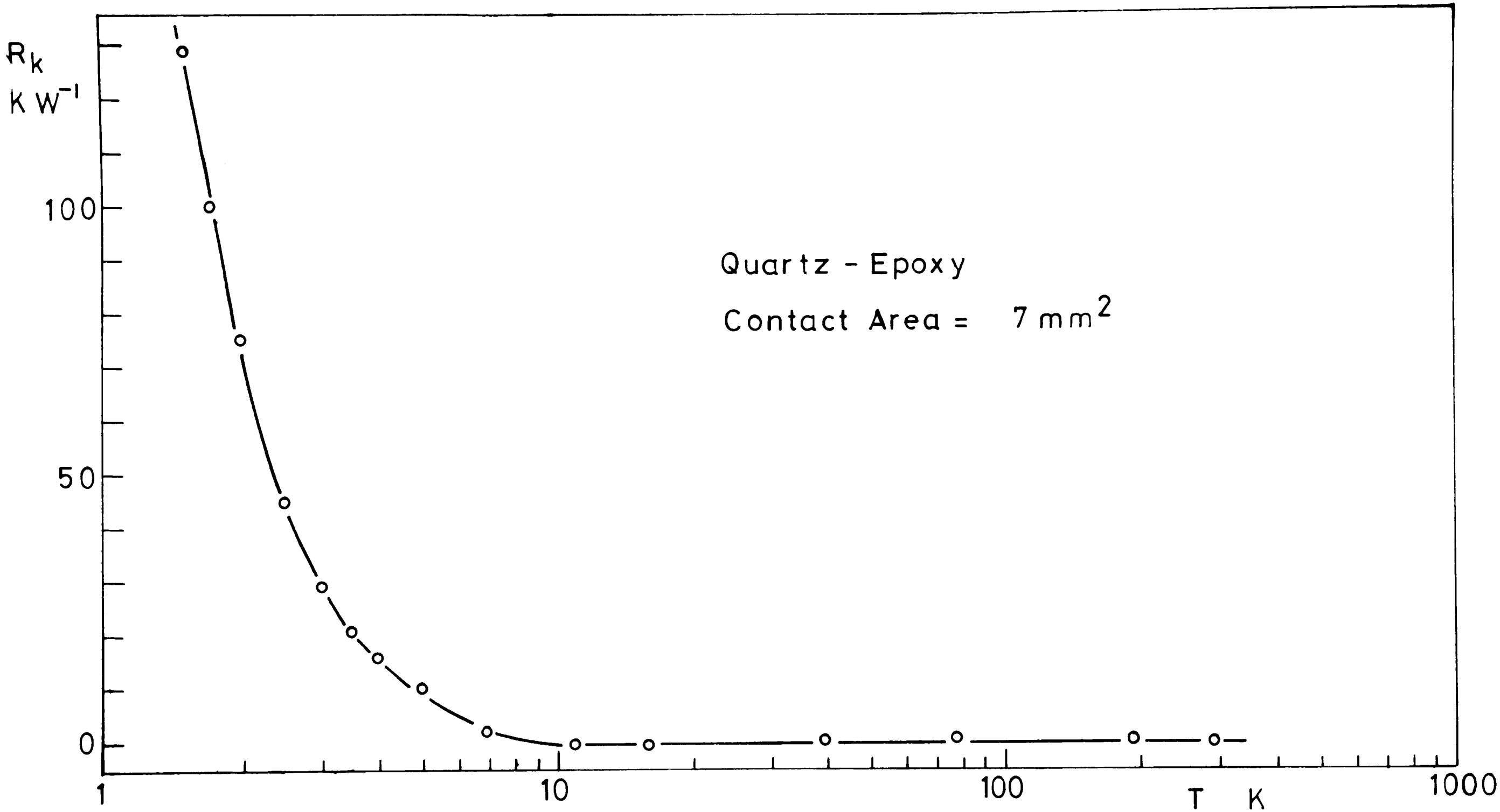


Fig 6.18 Thermal Contact Resistance (R_k) vs Temperature (T).

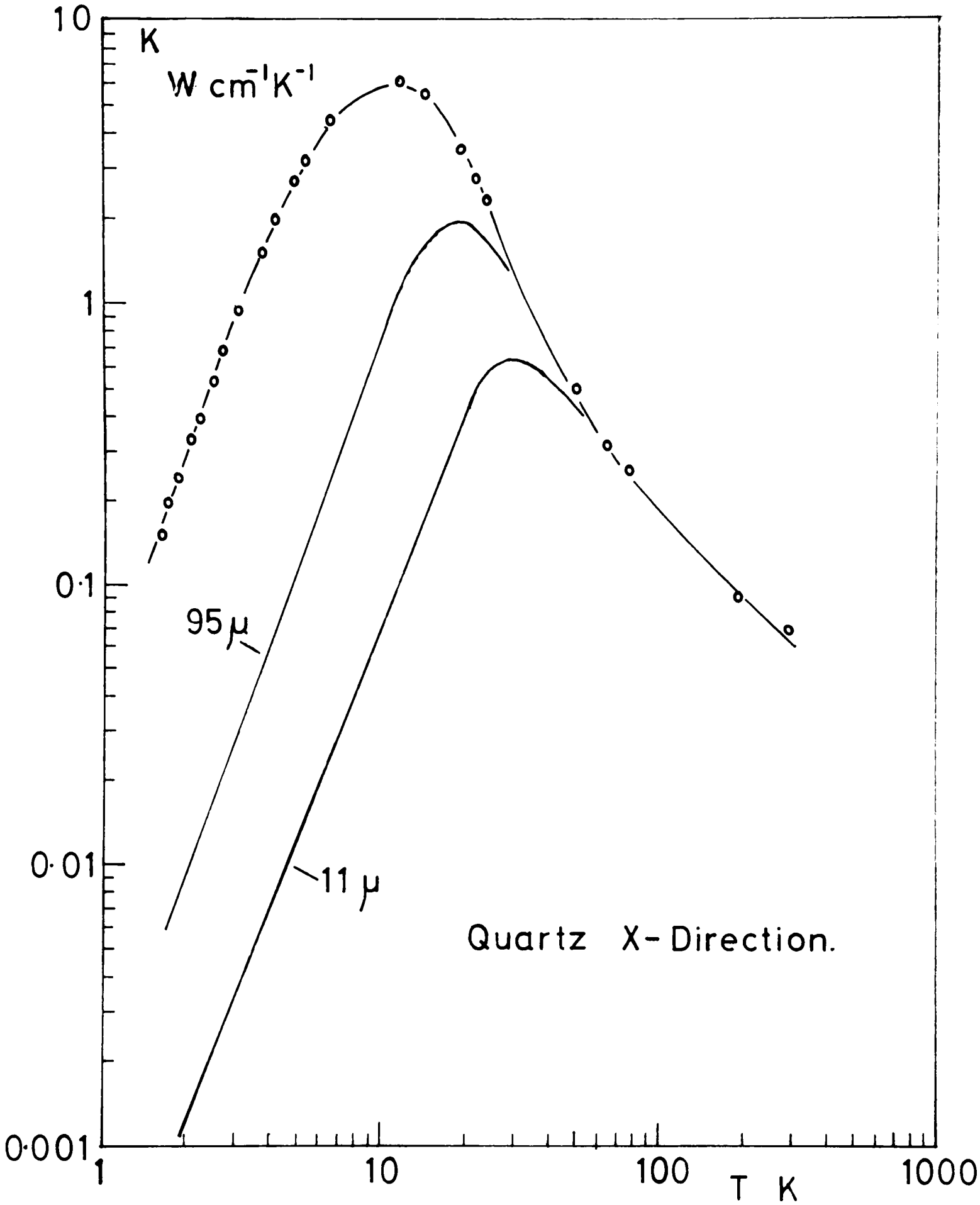


Fig 6.19 Thermal Conductivity (K) vs. Temperature (T).

of the thermal conductivity of the quartz filler are used in calculation.

With values of the thermal conductivity of the epoxy, thermal conductivity of the quartz, thermal contact resistance between the quartz and the epoxy, and the particle size of the quartz it is now possible to compare the experimental results of the thermal conductivity of the composites with those predicted by the various equations.

6.6 Comparison of the high temperature results with theory

The quartz-filled composite thermal conductivity at temperatures of 10 K and above, where there is no pronounced size dependence, appears to be dependent only on the thermal conductivities of the matrix and the filler and the volume concentration of the filler. The thermal conductivity as predicted by the Meredith and Tobias formula for a two-phase composite (section 2.6) has been compared with the experimental values and as an example the comparison at 78 K is shown in fig. 6.20. Table 6.1 indicates the values of the filler thermal conductivity (K_f) and the matrix thermal conductivity (K_m) used in the calculations.

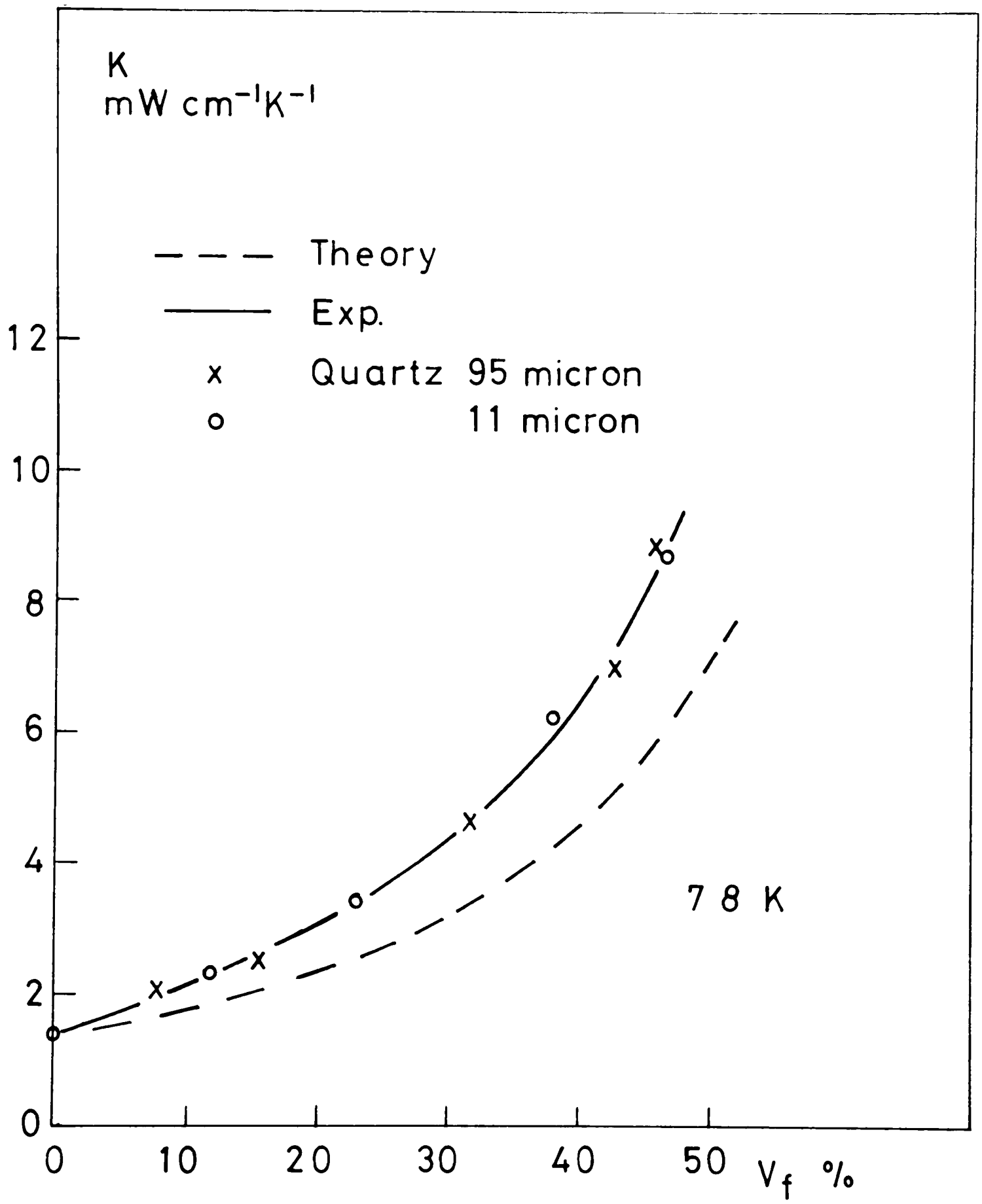


Fig 6.20 Thermal Conductivity (T) vs. Quartz Concentration (V_f).

Comparison between Experiment and Meredith and Tobias Equation.

TABLE 61

T K	Aniso-tropy	K_m mW (cm K)$^{-1}$	K_f (95 micron) mW (cm K)$^{-1}$	K_f (11 micron) mW (cm K)$^{-1}$
300	1.8	.2	80	80
194	1.95	1.85	125	125
78	2.0	1.4	350	350
20	2.0	0.80	2500	530

The Meredith & Tobias formula underestimates the measured thermal conductivity for all the temperatures at which calculations were effected. As the ratio of the thermal conductivity of the particle to that of the resin increases, the agreement worsens, the disparity being about 25% at 78 K and 20 K for a filler concentration of 30%.

The quarts powder used in the samples in this work are of a random and irregular shape and so there is a possibility of a shape effect (section 2.6) being important. The shape effects becoms more important as the ratio K_f / K_m increases as seems to be exhibited in the quarts composite results. The thermal conductivity of a two-phase material which includes particle shape is given by ~~given~~ equation 2.31 of Hamilton and Crosser.

Unfortunately because of the random, irregular shape of the quartz particles it was not possible to estimate the sphericity of the particles, hence the shape factor "n" which appears in the Hamilton and Crosser equation, from the scanning micro-graphs. Instead we can reverse the calculation and find "n" for a given composite thermal conductivity at a certain temperature and quarts concentration. Using the value of "n" we can then deduce the composite conductivities for the other temperatures and concentrations of quartz.

The value of "n" was found for a volume concentration of 30% quarts at 300 K and a value n = 4.3 was obtained. This corresponds to a sphericity of 0.70. As similar thermal conductivities were obtained for the two size ranges of quarts powder used, the same

value of n must apply to both. This is not unreasonable as both consist of random irregular particles and the sphericity depends only on particle shape not average size.

In fig. 6.21 to 6.24 the experimental results are compared to the predictions of the Hamilton and Crosser equation with n = 4.5 at temperatures of 300 K, 194 K, 78 K, 20 K and 10 K. At 300 K and 194 K the agreement is good. At 78 K and hydrogen temperatures the agreement is good up to about 35% volume quarts concentration, but at higher concentrations the predicted values of the thermal conductivity are lower than the measured values, being about 20% lower at 45% volume concentration. At these temperatures the quarts thermal conductivity is about 3 orders of magnitude higher than that of the epoxy matrix. The Hamilton and Crosser equation is derived assuming the particles are so far apart that there will be no interactions between particles. This will not be true when the filler concentration is high and the ratio $\frac{K_f}{K_m}$ is high.

What seems to be required is the Meredith and Tobias formula with a shape effect included in the analysis. This is not feasible because of the difficulty in solving Lapaces equation for arbitrary boundary conditions and geometry.

At temperatures above 10 K satisfactory agreement between theory and experiment can be obtained for concentrations up to about 35% by volume with the predictions of the Hamilton and Crosser

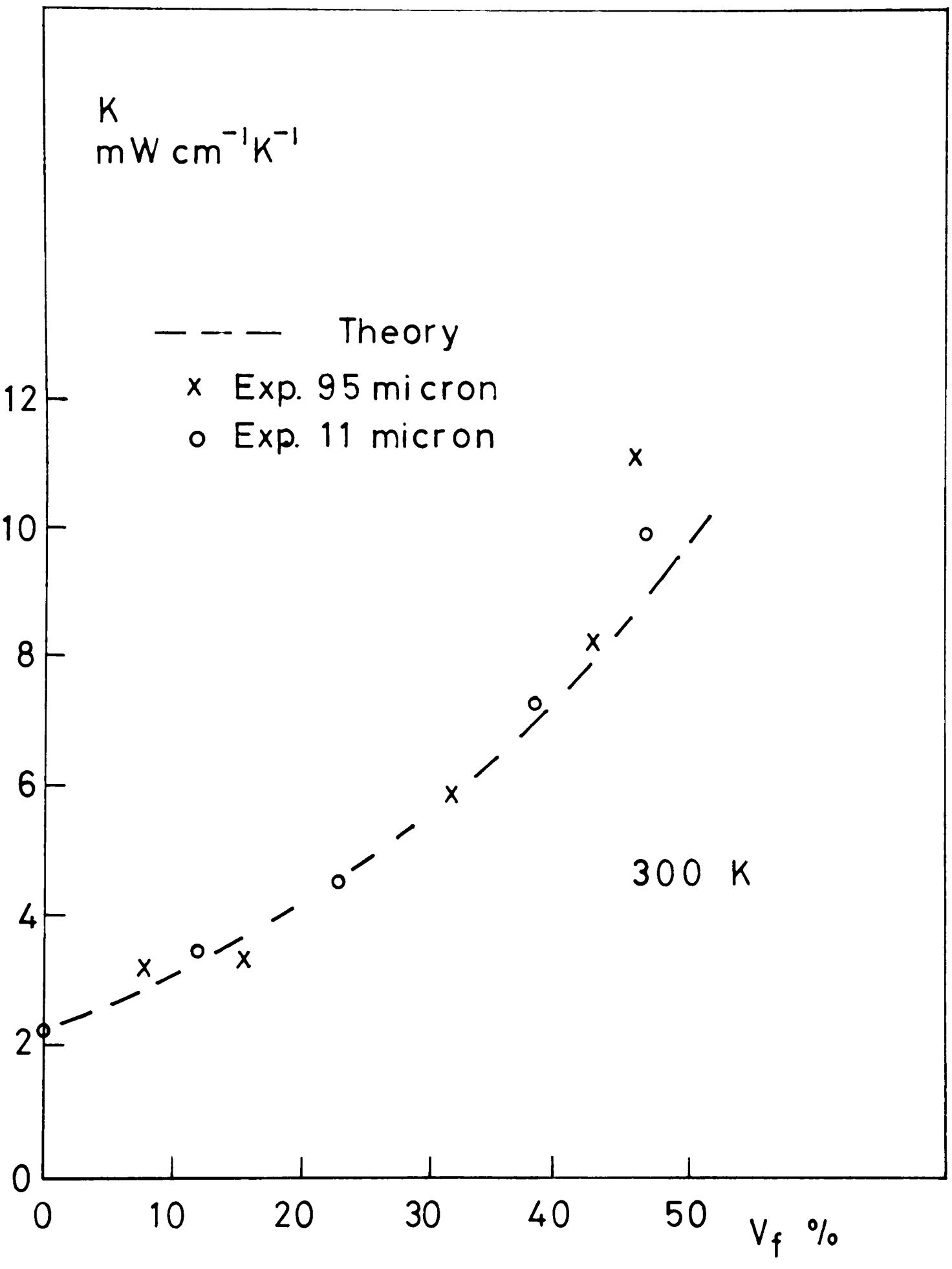


Fig 6.21 Thermal Conductivity (K) vs. Quartz Concentration, Volume % (V_f).
Comparison between Experiment and the Hamilton and Crosser Equation.

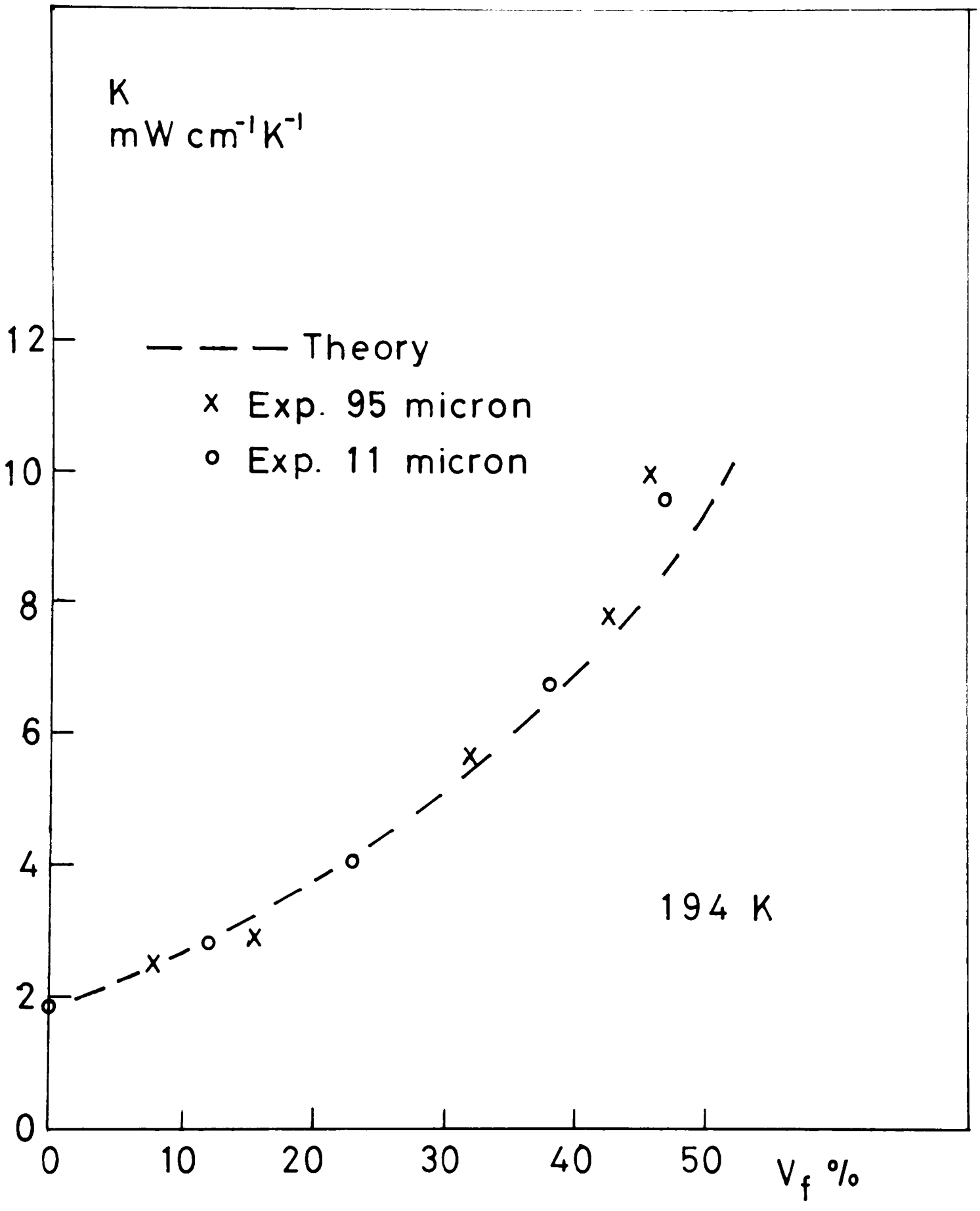


Fig 6.22 Thermal Conductivity (K) vs. Quartz Concentration, Volume % (V_f). Comparison between Experiment and the Hamilton and Crosser Equation.

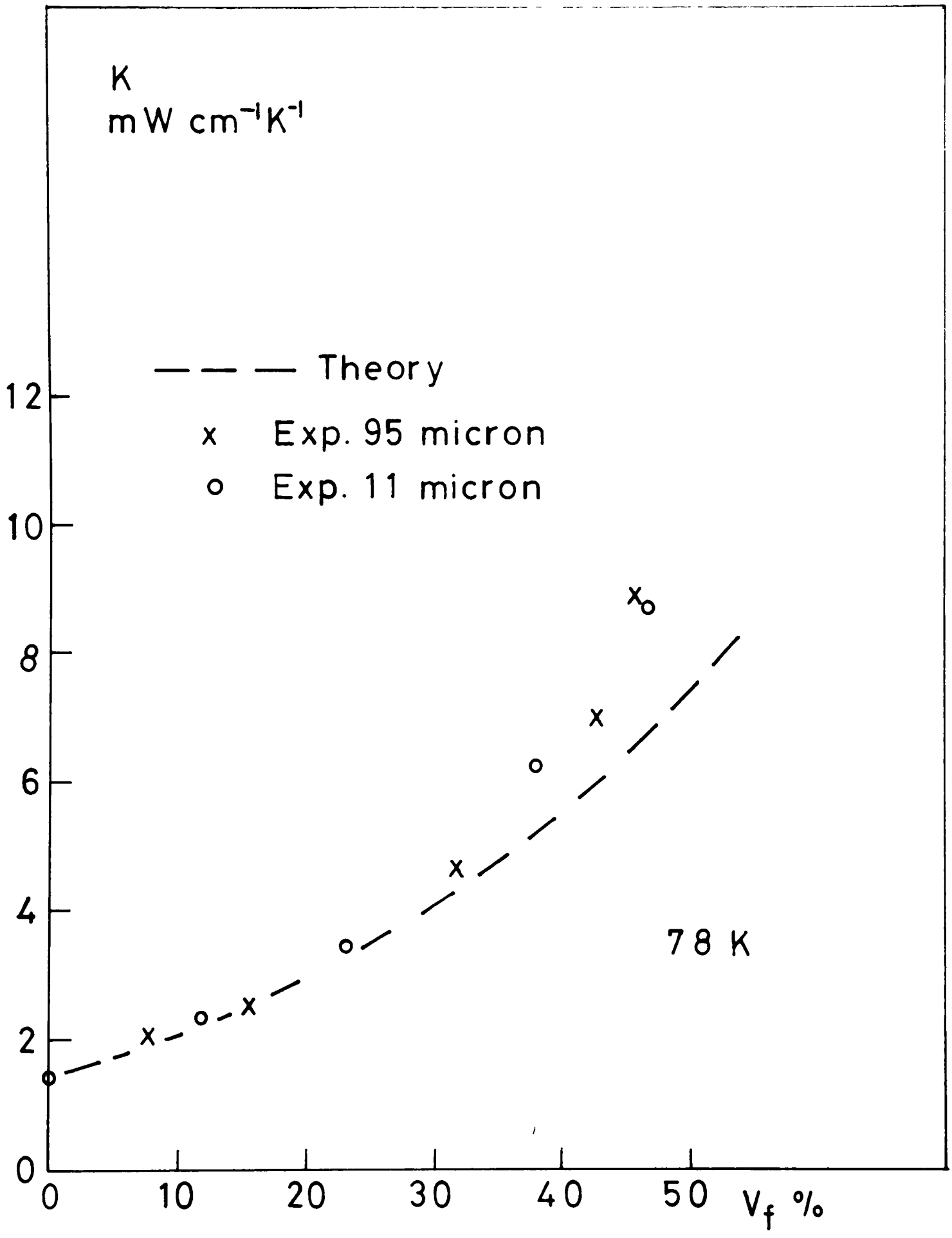


Fig 6.23 Thermal Conductivity (K) vs. Quartz Concentration, Volume % (V_f). Comparison between Experiment and the Hamilton and Crosser Equation.

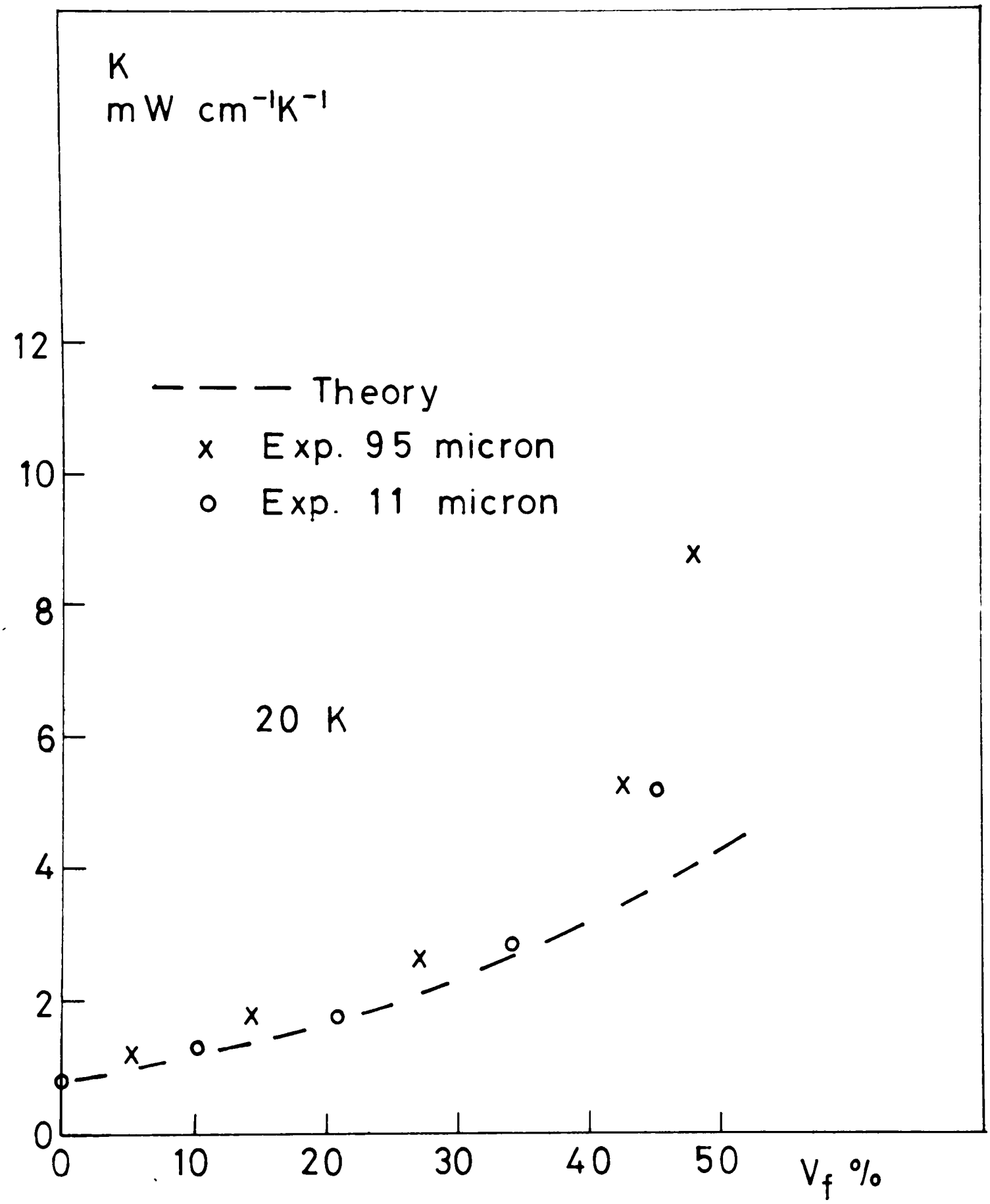


Fig 6.24 Thermal Conductivity (K) vs. Quartz Concentration, Volume % (V_f). Comparison between Experiment and the Hamilton and Crosser Equation.

equation, using a reasonable value for the sphericity of the particles. For higher concentrations the theory will underestimate the thermal conductivity values especially when $\frac{K_f}{K_m}$ is large.

6.7 Comparison of the low temperature results with theory

At helium temperatures the thermal conductivity of the quarts composites depends strongly on the size of the quarts powder. The 11 micron quartz composite has a lower thermal conductivity than that of the 95 micron composite for all concentrations.

The 11 micron quartz particle will have a lower thermal conductivity than the 95 micron particle in the frequency independent boundary scattering region at helium temperatures. However, putting these adjusted values into the Hamilton and Crosser equation with n = 4.3 give values which are much higher than those found by experiment. For a quartz volume concentration of 30% at 4 K the predicted thermal conductivities of the 11 micron composites is a factor of 2 higher than that measured. Clearly there is another factor that is important at these temperatures and we believe this to be the presence of a thermal contact resistance at the quarts-epoxy interface.

We can introduce the thermal contact resistance into the Hamilton and Crosser equation by deducing an effective particle thermal conductivity in a similar way to that described in section 6.3 on the glass-epoxy composite. We have approximated randomly shaped quarts particles to a cube average volume, with cube lengths of 11 microns and 95 microns for the two size ranges of particles. Assuming isotherms plane perpendicular to the direction of heat flow we can combine the thermal contact resistance with the thermal resistance of the particle to produce an effective particle thermal conductivity K_{fe}. The values obtained are shown in table 6.2 and the effect of the thermal contact resistance R_k is clearly demonstrated.

TABLE 6.2

TK	R_k K mW^{-1}	Size microns	K_f mW (cm K)$^{-1}$	K_{fe} mW (cm K)$^{-1}$	K_m mW (cm K)$^{-1}$
4	$\frac{10 \times 10^{-4}}{A}$	95	80	4.5	0.54
		11	8.8	0.52	
2.5	$\frac{29 \times 10^{-4}}{A}$	95	23	1.5	0.45
		11	2.5	0.18	

For the smaller particles the contact resistance will have a larger effect than for the larger particles. The smaller particles have a larger surface area for a given concentration of filler and hence there will be a greater scattering of phonons.

Figs. 6.25 and 6.26 show the result of using the values of the effective particle thermal conductivity in the Hamilton and Crosser formula. The agreement is good up to about 30% filler concentration. At higher concentrations the predicted results are lower than the experimental results. It is possible that at high concentrations of filler there will be some particle contact and so the thermal contact resistance will be short-circuited increasing the measured thermal conductivity over that predicted.

At helium temperatures the thermal conductivity of the 95 micron quartz composites are always higher than that of the epoxy matrix. For the 11 micron quartz composite samples this is not so. The temperature dependence of the curves at helium temperatures is higher than that of the epoxy matrix, as the effective thermal conductivity of the particles rapidly decreases due to the effect of the thermal contact resistance and at about 3 K the curves cross over each other. In this region the effective thermal conductivity of the particles will be similar to that of the epoxy. This is illustrated in table 6.2.

For quartz volume concentrations of up to about 35% the Hamilton and Crosser equation can satisfactorily predict the thermal

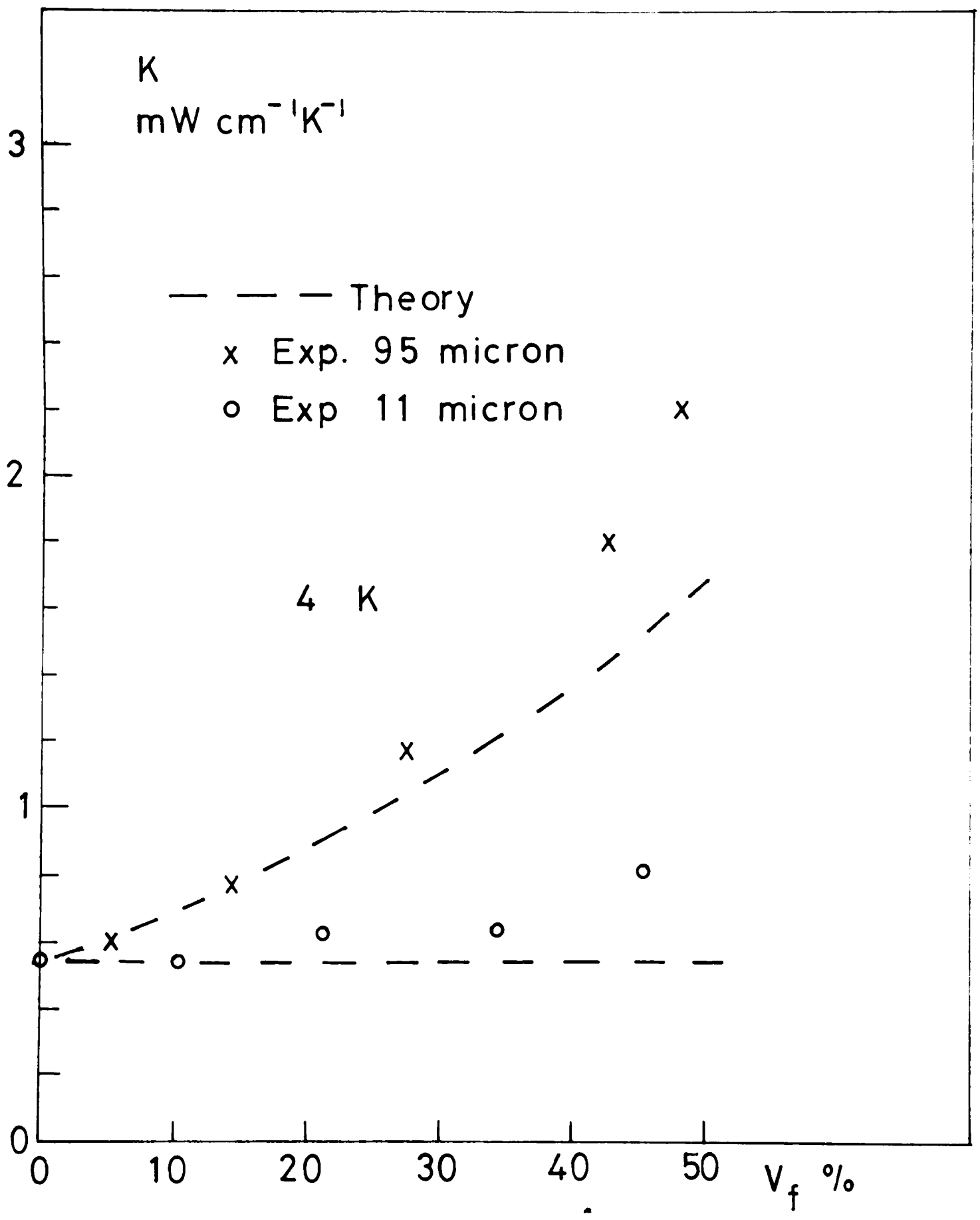


Fig 6.25 Thermal Conductivity (K) vs. Quartz Concentration, Volume % (V_f). Comparison between Experiment and the Hamilton and Crosser Equation.

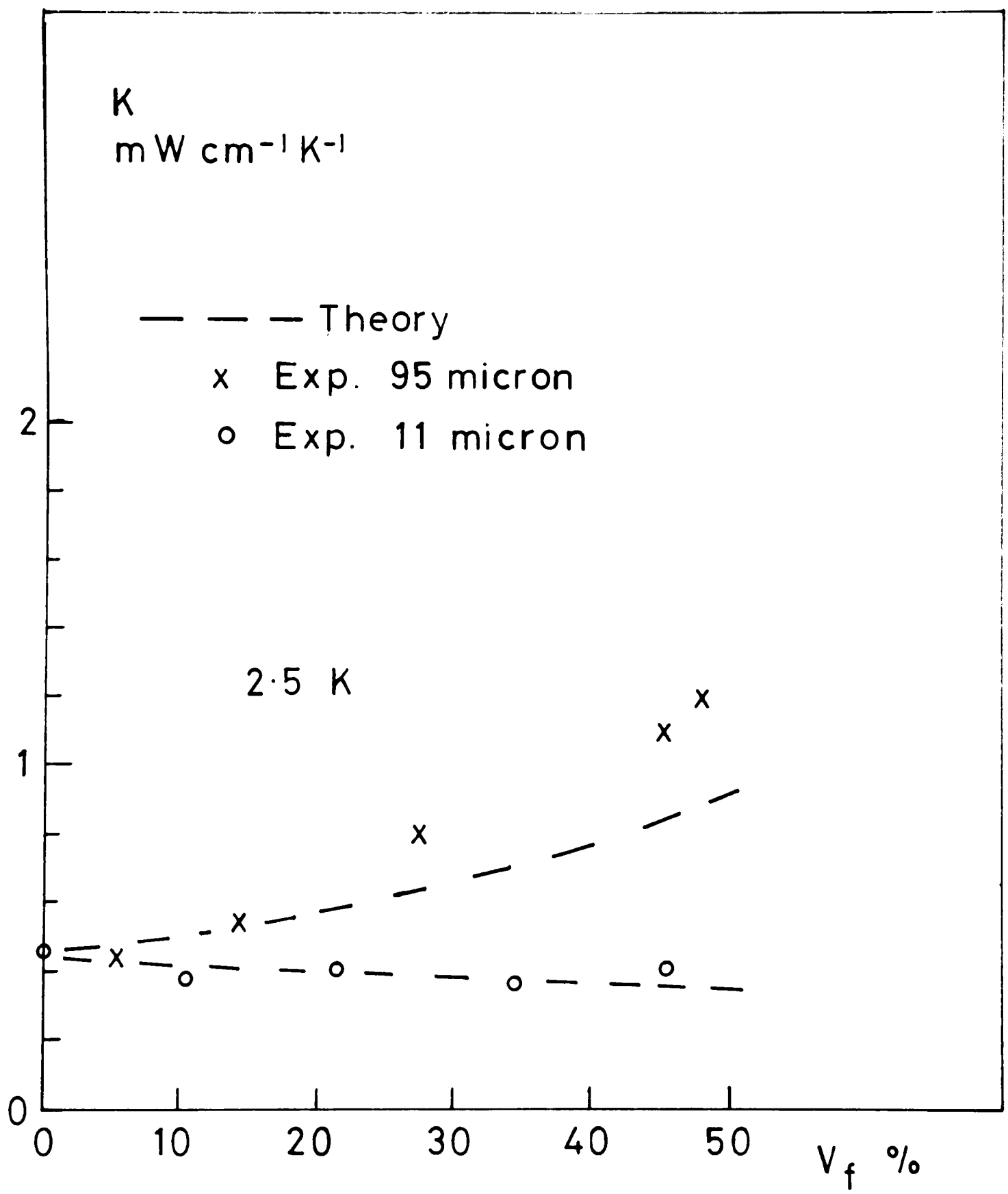


Fig 6.26 Thermal Conductivity (K) vs. Quartz Concentration, Volume % (V_f). Comparison between Experiment and the Hamilton and Crosser Equation.

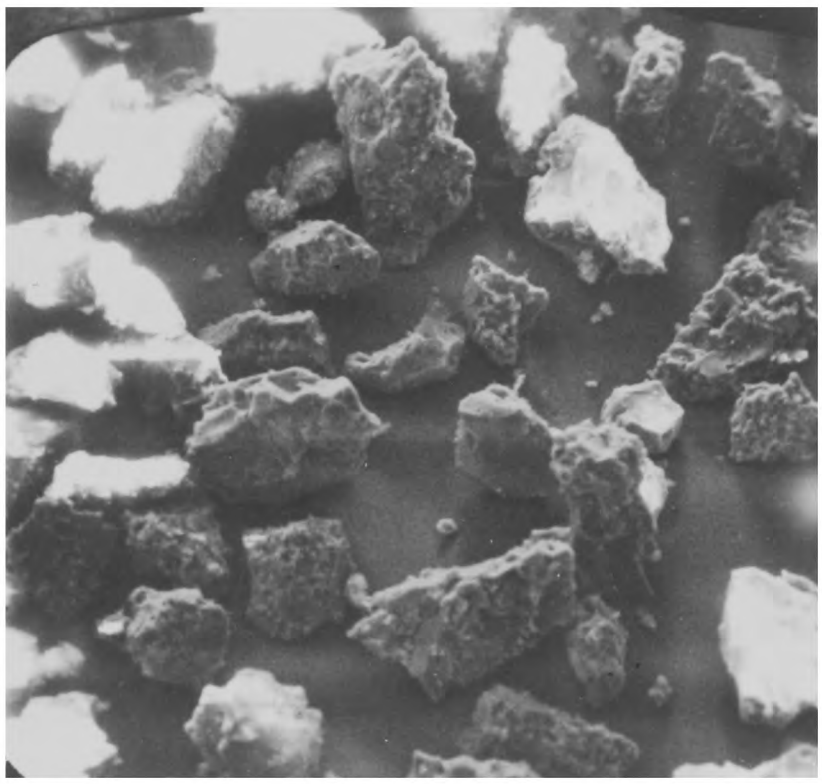
conductivity of the quartz composite for the whole of the temperature range at which measurements were taken. At helium temperatures it is necessary to use an effective particle thermal conductivity which incorporates the thermal contact resistance at the quartz-epoxy interface. For volume concentrations above 35% the Hamilton and Crosser equation predicts lower values than those measured especially when the filler thermal conductivity is much higher than that of the matrix.

ALUMINA FILLED EPOXIES

6.8 Specimens Alumina is a widely used filler in epoxy systems. Alumina fillers increase the room temperature thermal conductivity, decrease the coefficient of thermal expansion and improve the abrasive resistance of the system.

Powdered crystalline alumina ($Al_2 O_3$) obtained from Aloca Alumina Products, the British Aluminium Co. Ltd., London, was used in the specimens. Three size ranges of particles were used. The smaller particle sizes consisted of micronised furnace grade alumina MA 65 and MA 250. The former has a specific surface of $6,500 \pm 1,500$ cm^2 gm^{-1} and mean particle size of 6.9 micron. The latter has a specific surface of 25,000 cm^2 gm^{-1} and mean particle size of 1.8 micron. These figures are quoted from the manufacturer's data sheet. The large particle size was obtained by sieving Tabular Alumina T - 61 between screens of 60 and 90 micron apertures. This powder was obtained from the manufacturers as - 48 mesh, having passed through a sieve of aperture size 325 micron. Essentially, the alumina is an alpha alumina of high chemical purity (99.5 + %).

Scanning electron micrographs of the three grades of alumina were taken and two of these are shown in plate 3. The 60 to 90 micron tabular alumina consists of random irregular particles. A volume weighted average cube length of 63 micron was obtained from the micrographs following the procedure of section 3.6. This grade of alumina will be referred to as the 63 micron alumina. The MA 65 appears to consist of platelet-like particles of thickness



100 μ Alumina 63 micron



4 μ Alumina MA 65

Plate 3

about 1 micron and length about 7 micron. For the MA 250 powder satisfactory micrographs could not be obtained, although the particles appear to have the same platelet structure as the MA 65.

Specimens of filler concentrations up to about 35% by volume were used in the experiments. For the specimens containing the MA 65 and MA 250 powders this was the largest amount of filler that could be incorporated into the epoxy, compared with about 50% by volume of quartz. This is probably due to the plate structure of the particles which will disrupt the packing of the particles.

The Alumina was dried before use but no coupling agent was used. The specimens were prepared as described in section 3.5.

6.9 Experimental results The thermal conductivity of the alumina filled specimens against temperature and volume concentrations of filler for various temperatures are shown in fig. 6.27 to 6.32.

For the composites containing MA 65 and MA 250 fillers, there is a striking difference between the high temperature results where increasing filler content increases the thermal conductivity and at helium temperatures where increasing filler content substantially decreases the thermal conductivity. The composite of the smaller particles (MA 250) has a lower thermal conductivity than that of

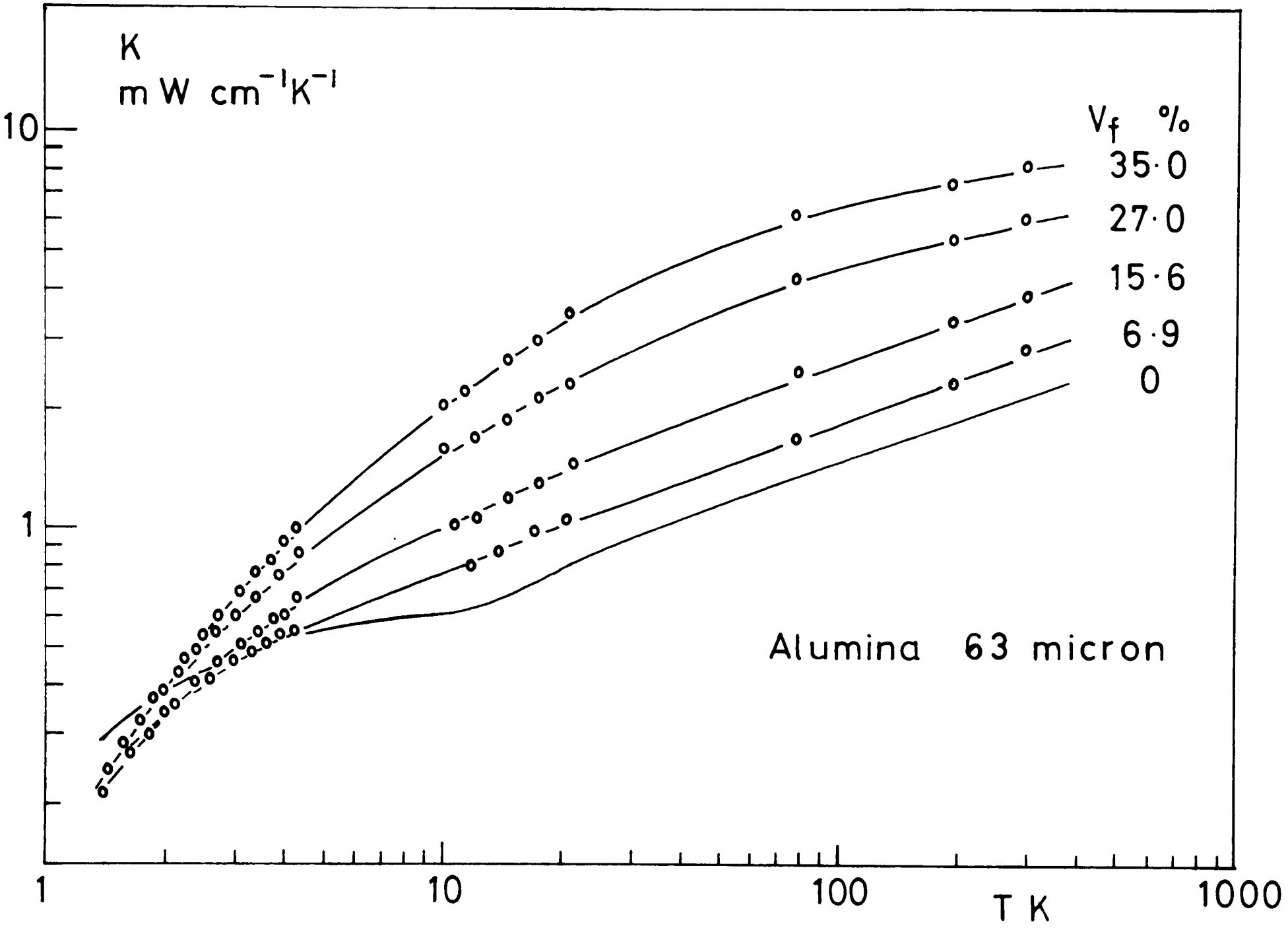


Fig 6.27 Thermal Conductivity (K) vs. Temperature (T).

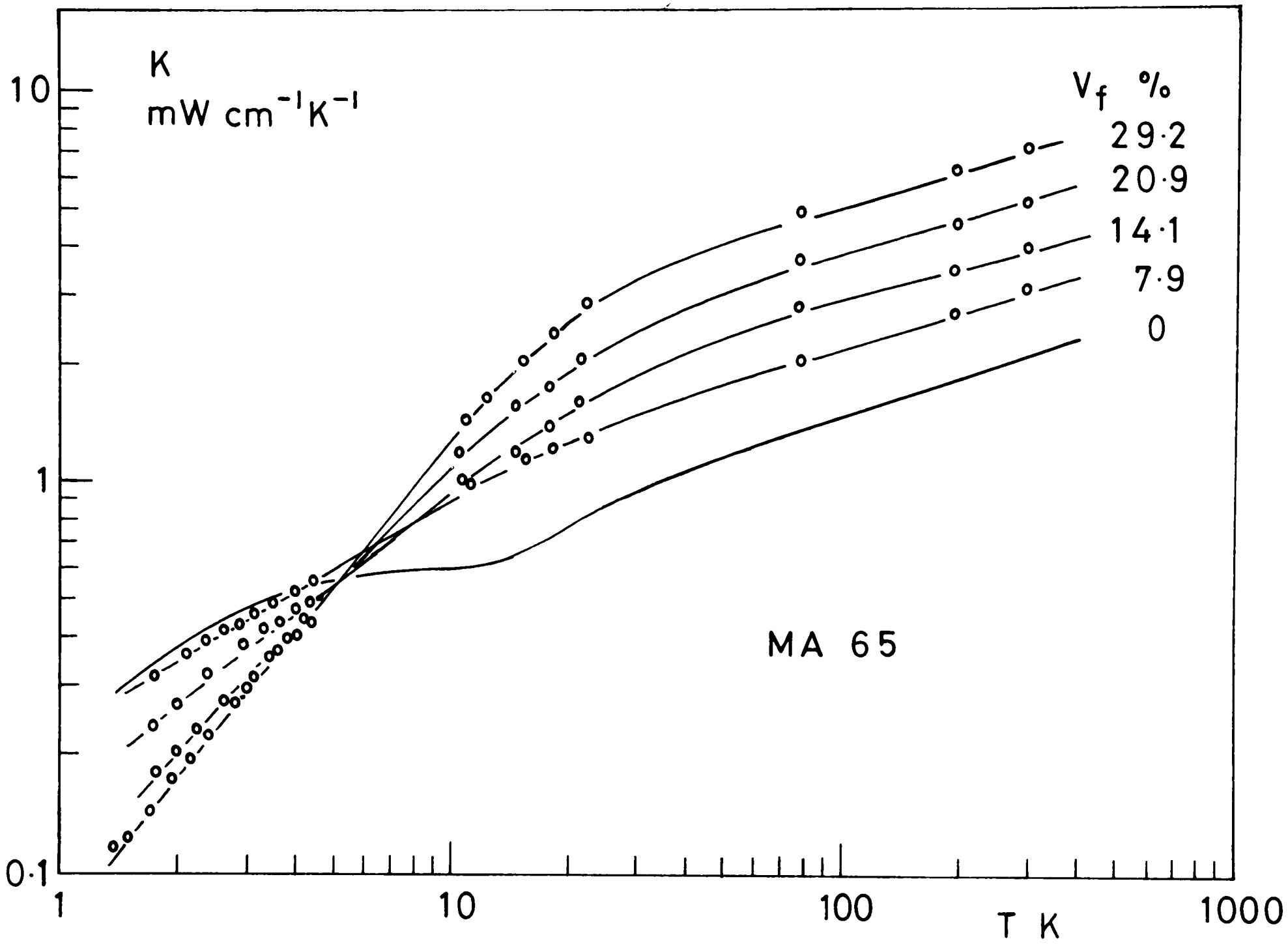


Fig 6.28 Thermal Conductivity (K) vs. Temperature (T).

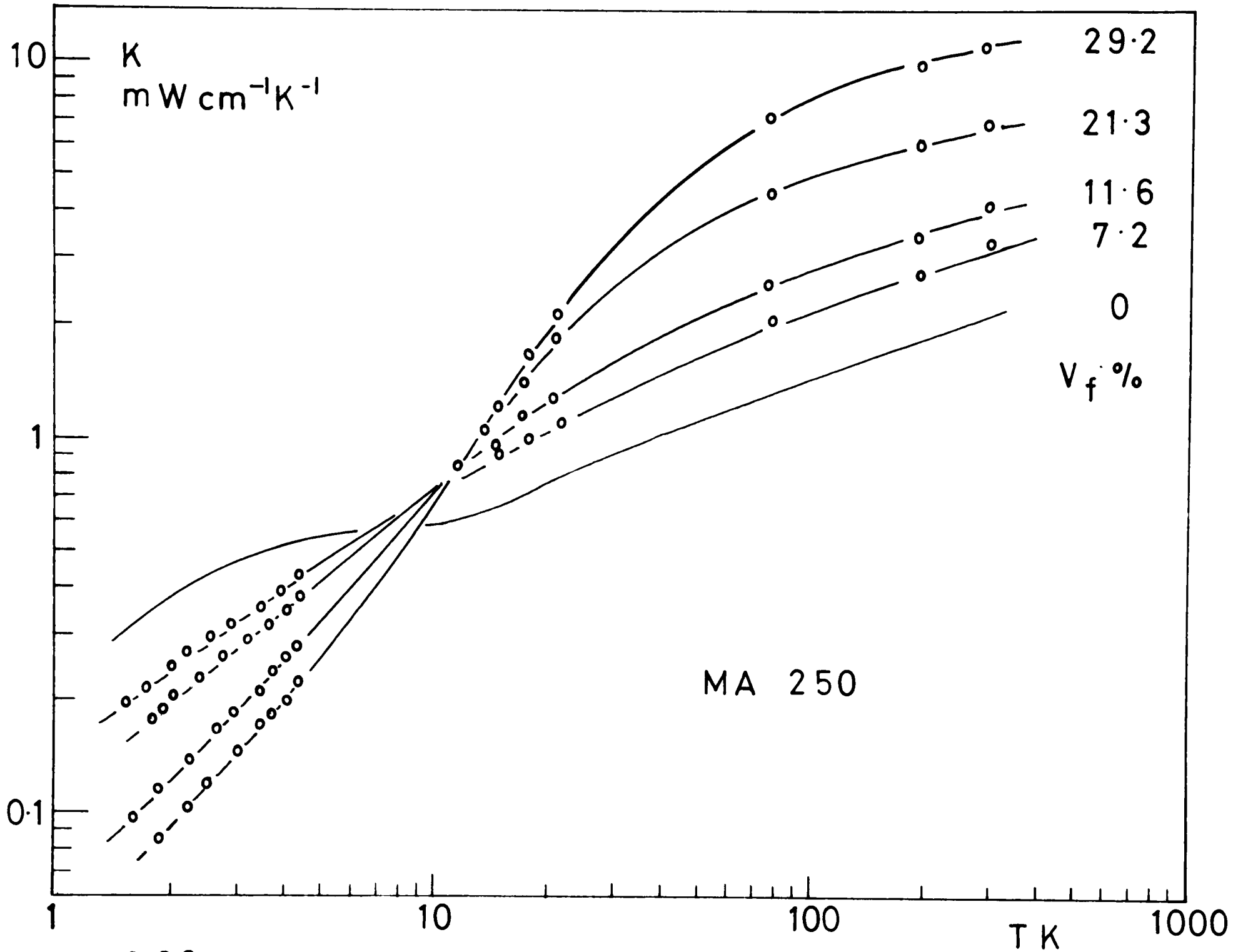


Fig 6.29 Thermal Conductivity (K) vs. Temperature (T).

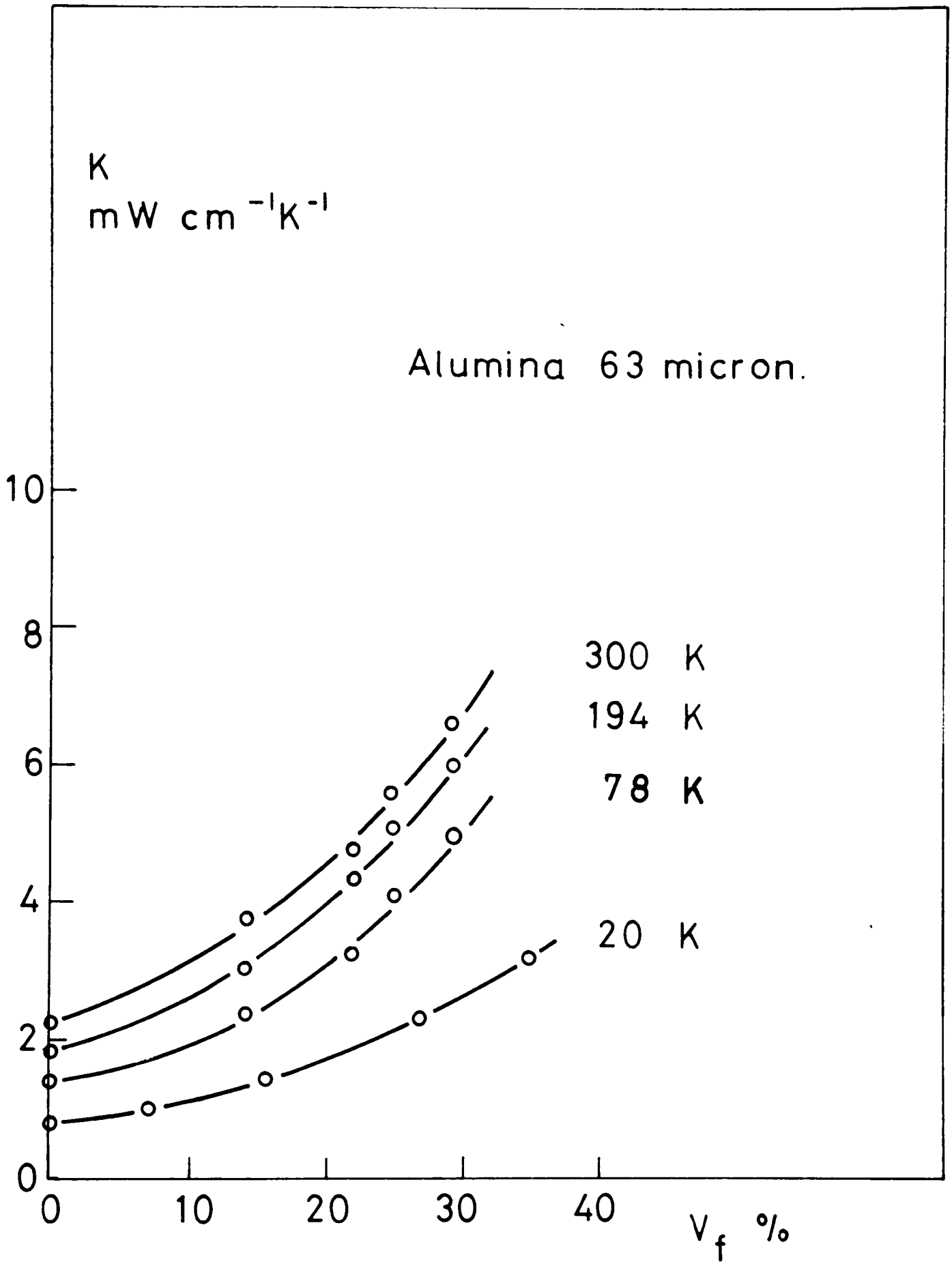


Fig 6.30 Thermal Conductivity (K) vs Alumina Concentration, Volume % (V_f).

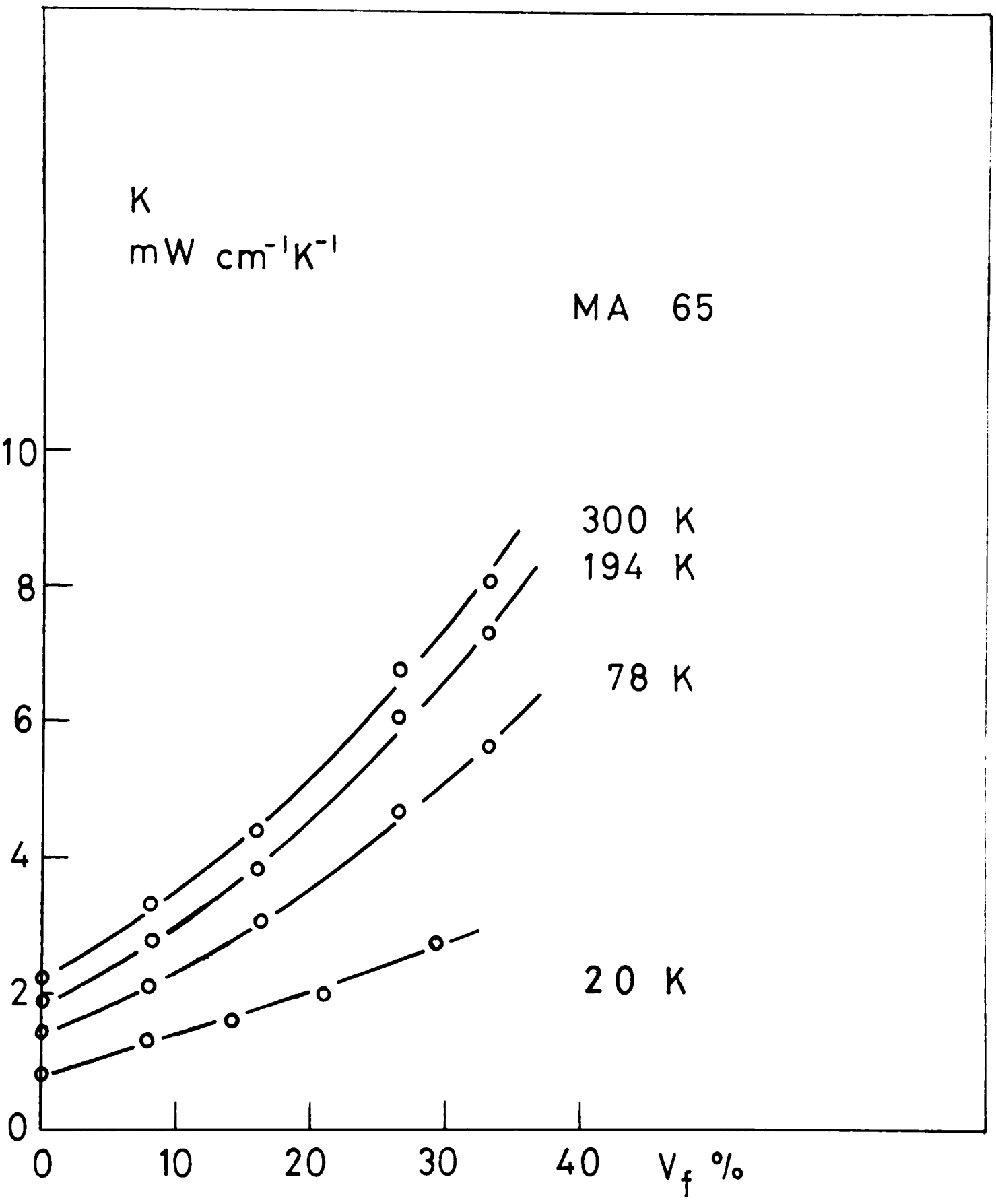


Fig 6.31 Thermal Conductivity (K) vs. Alumina Concentration, Volume % (V_f)

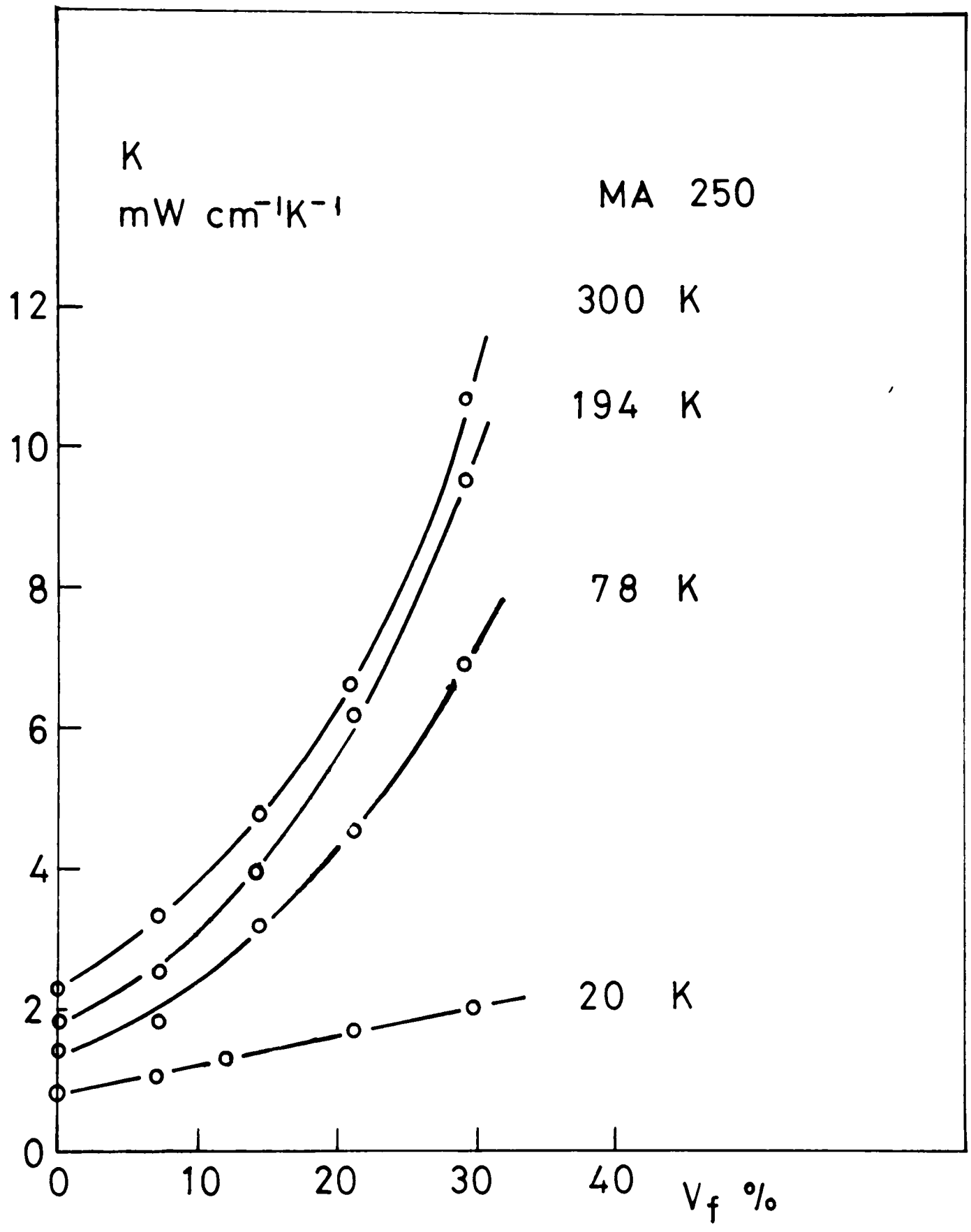


Fig 6.32 Thermal Conductivity (K) vs. Alumina Concentration, Volume % (V_f).

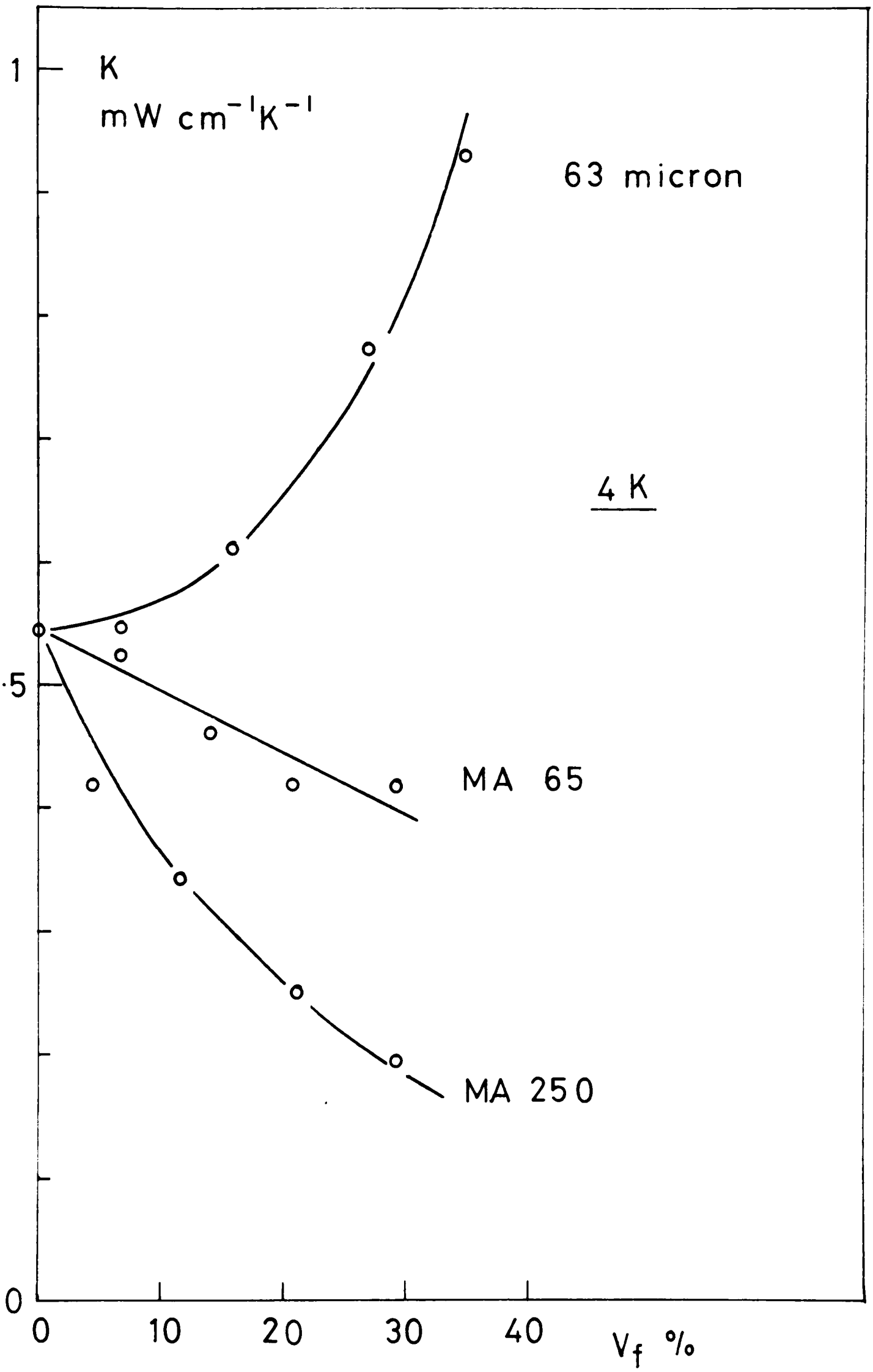


Fig 6.32a. Thermal Conductivity (K) vs Alumina Concentration, Volume % (V_f).

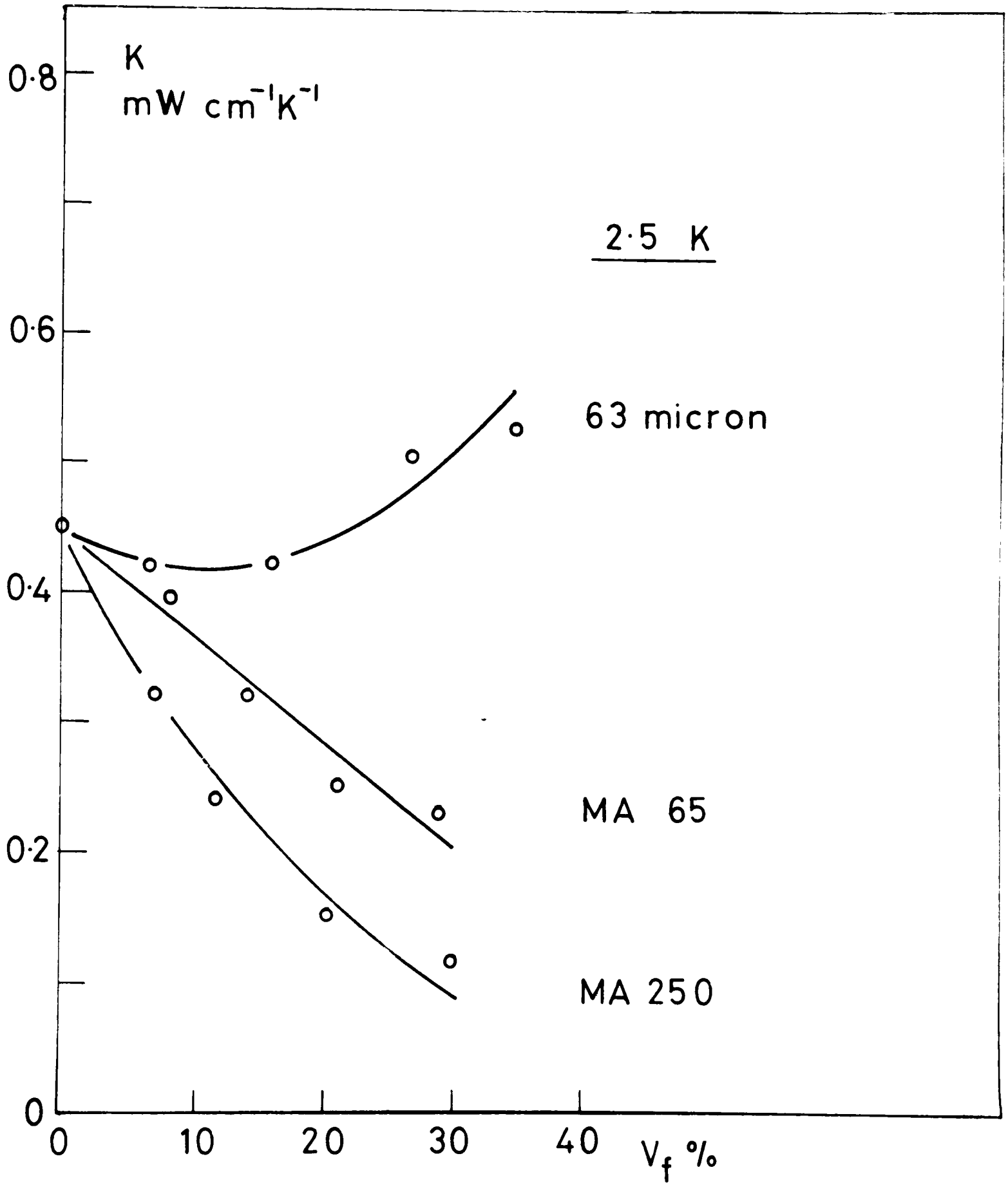


Fig 6.32b. Thermal Conductivity (K) vs. Alumina Concentration, Volume % (V_f).

the larger (MA 65) at helium temperature. For the MA 250 composites the conductivity versus temperature curves cross over each other at about 11 K and for the MA 65 composites at about 6 K. The cross-over point indicates the temperature at which the particles have an effective conductivity similar to that of the epoxy. The smaller the particle the higher this temperature will be, all other things being equal. The conductivity of the 65 micron alumina composites have values which increase with filler concentration at 4 K. This increase gets smaller as the temperature decreases and at about 2 K all concentrations have a conductivity similar to that of the unfilled epoxy.

At high temperatures the thermal conductivity always increases with increasing filler concentration but there appears to be a substantial shape effect. For example, at 194 K and at a filler concentration of 29% by volume the thermal conductivity of the MA 250 composite is 9.6 mW cm^{-1} K^{-1} and that of the 65 micron composite is 5.8 mW cm^{-1} K^{-1}.

The thermal contact resistance between bulk specimens of alumina and epoxy was measured and the results are shown in fig. 6.33. At helium temperature the temperature dependence is $T^{-2.7}$. The thermal contact resistance at the alumina-epoxy interface is higher than that at the quartz-epoxy interface because of the higher sound velocities and density of the alumina.

Thermal conductivity of a 1 mm square specimen of artificial sapphire is shown in fig. 6.34. (Hudson 1972). Sapphire has a

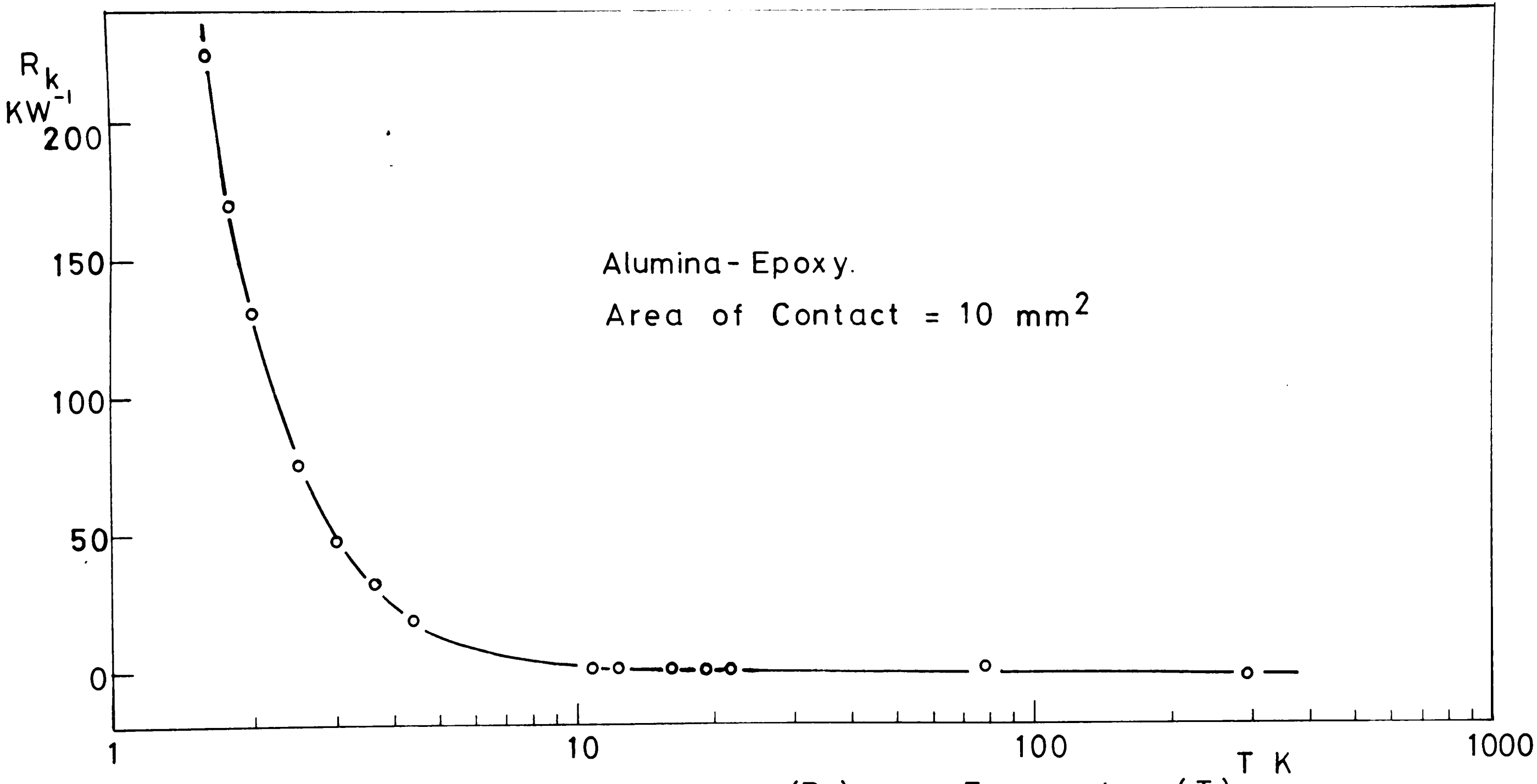


Fig 6.33 Thermal Contact Resistance (R_k) vs. Temperature (T).

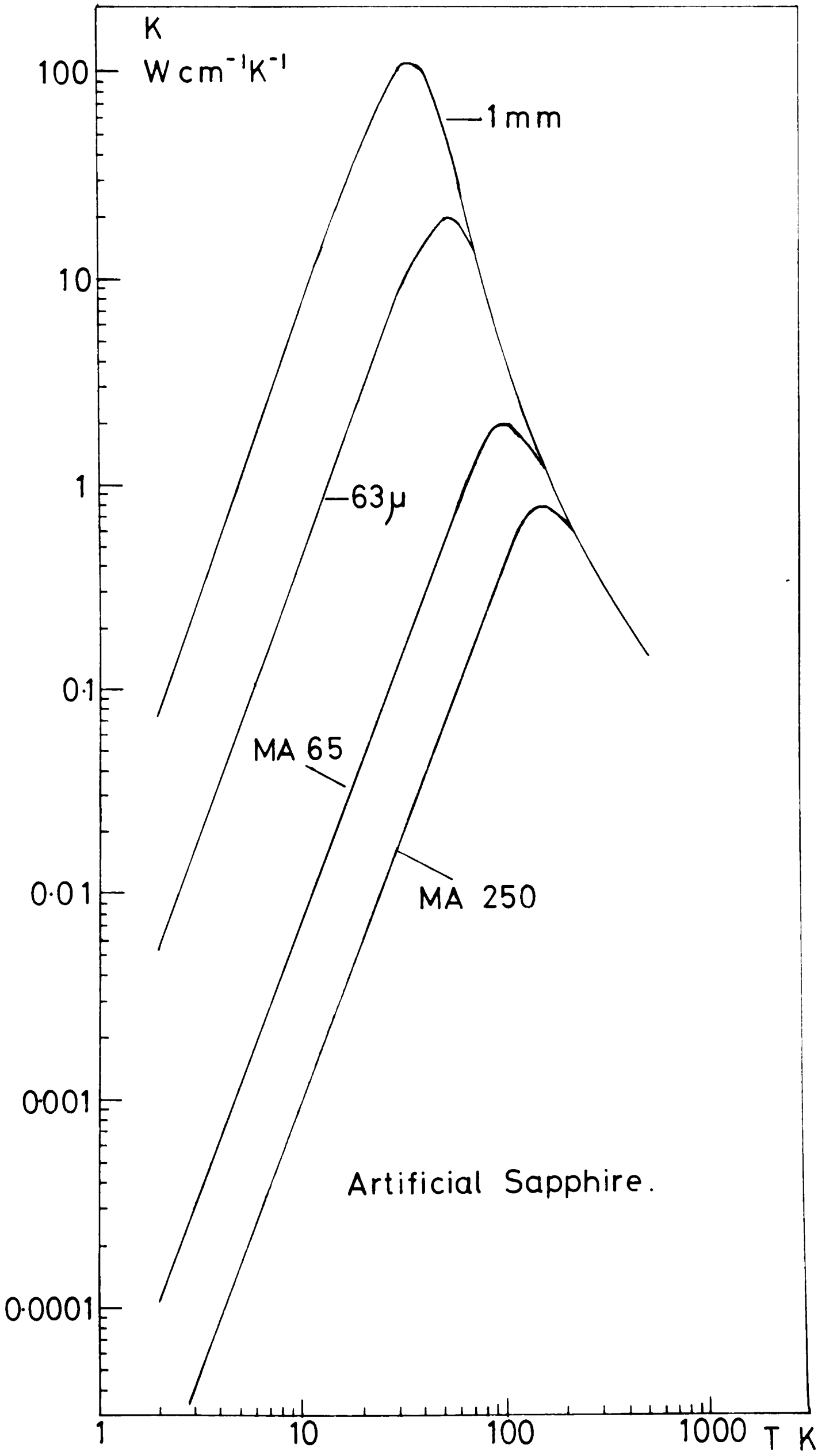


Fig 6.34 Thermal Conductivity (K) vs. Temperature (T).

small anisotropy in its thermal conductivity (< 5%) but in the calculations this is small enough to be ignored.

6.10 Comparison of high temperature results with Theory

There appears to be a considerable shape effect in the thermal conductivity of the alumina filled composites. The results obtained are higher than those predicted from the Meredith and Tobias formula. This is more pronounced for the MA 65 and MA 250 filled samples indicating that the shape of these particles is vastly different from spheres. From the scanning micrographs it appears that these particles are in the form of platelets and will, therefore, have a low sphericity.

From the results at 300 K and at a filler concentration of 20% by volume the value of the parameter "n" hence the sphericity Ψ was determined from the Hamilton and Crosser equation. The values of Ψ obtained are shown in table 6.3.

TABLE 6.3

	n	Ψ
MA 250	7.81	0.38
MA 65	5.5	0.55
63 μ	4.5	0.67

As expected from the micrographs, the 63 micron particles, which are of a random, irregular shape, have the highest sphericity. The sphericity of 0.55 for the MA 65 powder means the platelets will have a ratio of length of plate to thickness of plate of about 5.8:1, assuming the plates to have a square cross section. From the scanning electron micrograph this is not unreasonable. If the plates have an average length of 6.9 microns, which is the average size stated by the manufacturers, the average thickness will be about 1.2 micron. For the MA 250 powder the ratio of length of plate to thickness of plate will be about 12:1.

Because of the small size of particles used there will be a pronounced size effect due to the frequency independent boundary scattering at temperatures below about 150 K and the thermal conductivity of the alumina is scaled down accordingly, using the smallest dimensions of the particles as the scaling factor. For the MA 65 powder, this dimension was taken to be 1.2 micron, the thickness of the plates. For the MA 250, assuming the plates to be square in cross section with a length of 1.8 micron, as stated by the manufacturers, the dimension was taken to be 1.8/12 micron where the number 12 is the length to thickness ratio of the platelets, calculated from Ψ . The scaled thermal conductivities are shown in fig. 6.34 and these values were used in the analysis of the results.

Using the values of "n" from table 6.3, and the scaled thermal conductivities, the experimental results at 300 K, 194 K, 78 K and

20 K are compared with the predictions of the Hamilton and Crosser equation in fig. 6.35 to 6.38. The agreement is good. There is some deviation at 30% concentration especially for the HA 250 composites, the predicted values being lower than the experimental values, where because of the nature of the shape of the particles there is a high probability of particle contact for which there is no provision in the theoretical equation.

At 20 K the particle thermal conductivity is vastly different for the different particle sizes, being 6 mW cm^{-1} K^{-1} for the HA 250 and at the other extreme 2.8 W cm^{-1} K^{-1} for the 63 micron powder, but the agreement between experiment and Hamilton & Crosser is excellent.

6.11 Comparison between theory and experimental results at Helium temperatures. At helium temperatures the Hamilton and Crosser will seriously overestimate the thermal conductivity of the alumina composites, because of the thermal contact resistance at the alumina-epoxy interface.

For the 63 micron particles the procedure of secion 6.7 is followed and an effective particle thermal conductivity K_{fe} incorporating the thermal contact resistance of fig. 6.33 is deduced. The values obtained are shown in table 6.4.

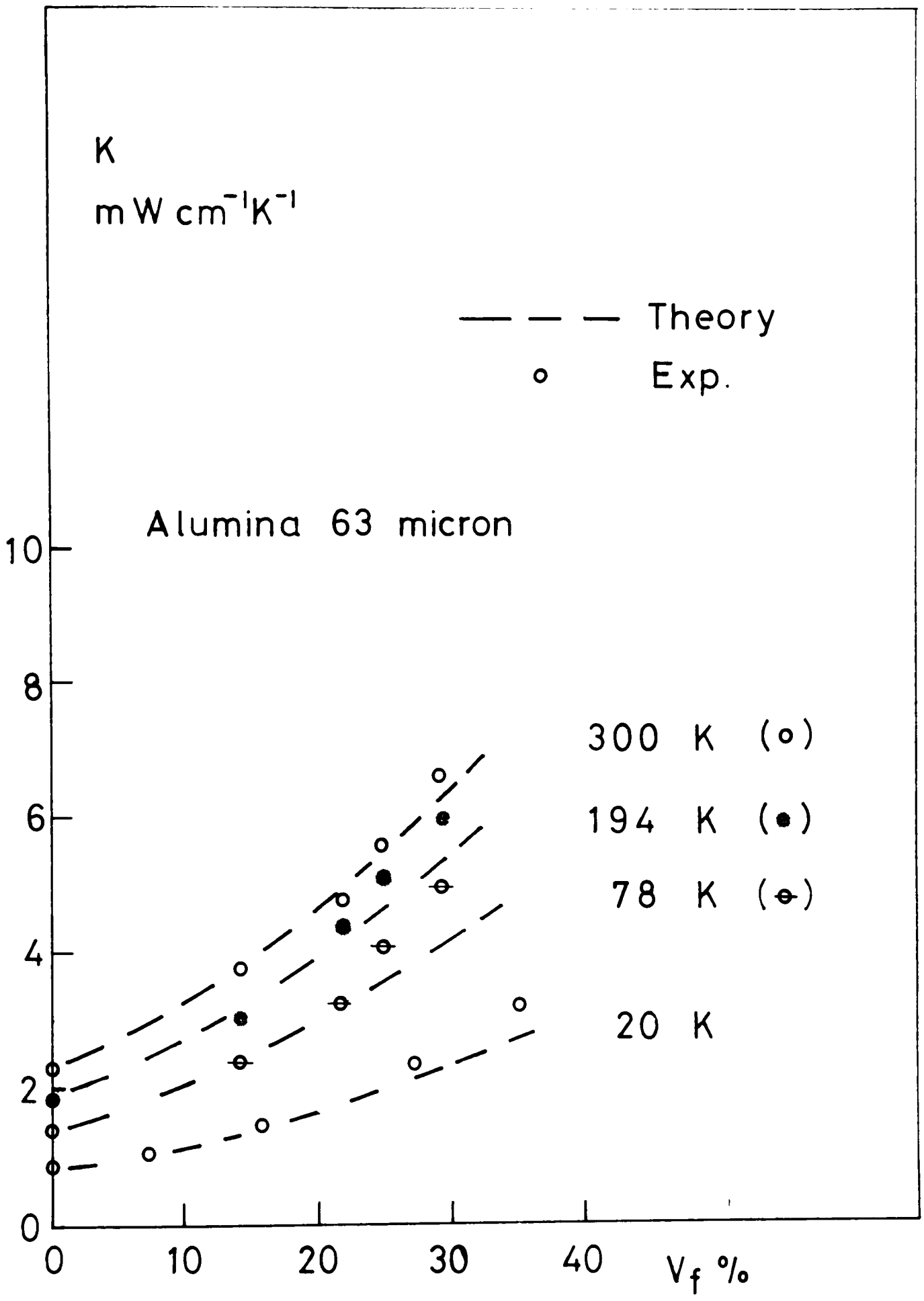


Fig 6.35 Thermal Conductivity (K) vs. Alumina Concentration, Volume % (V_f).

Comparison between Experiment and Hamilton and Crosser Equation.

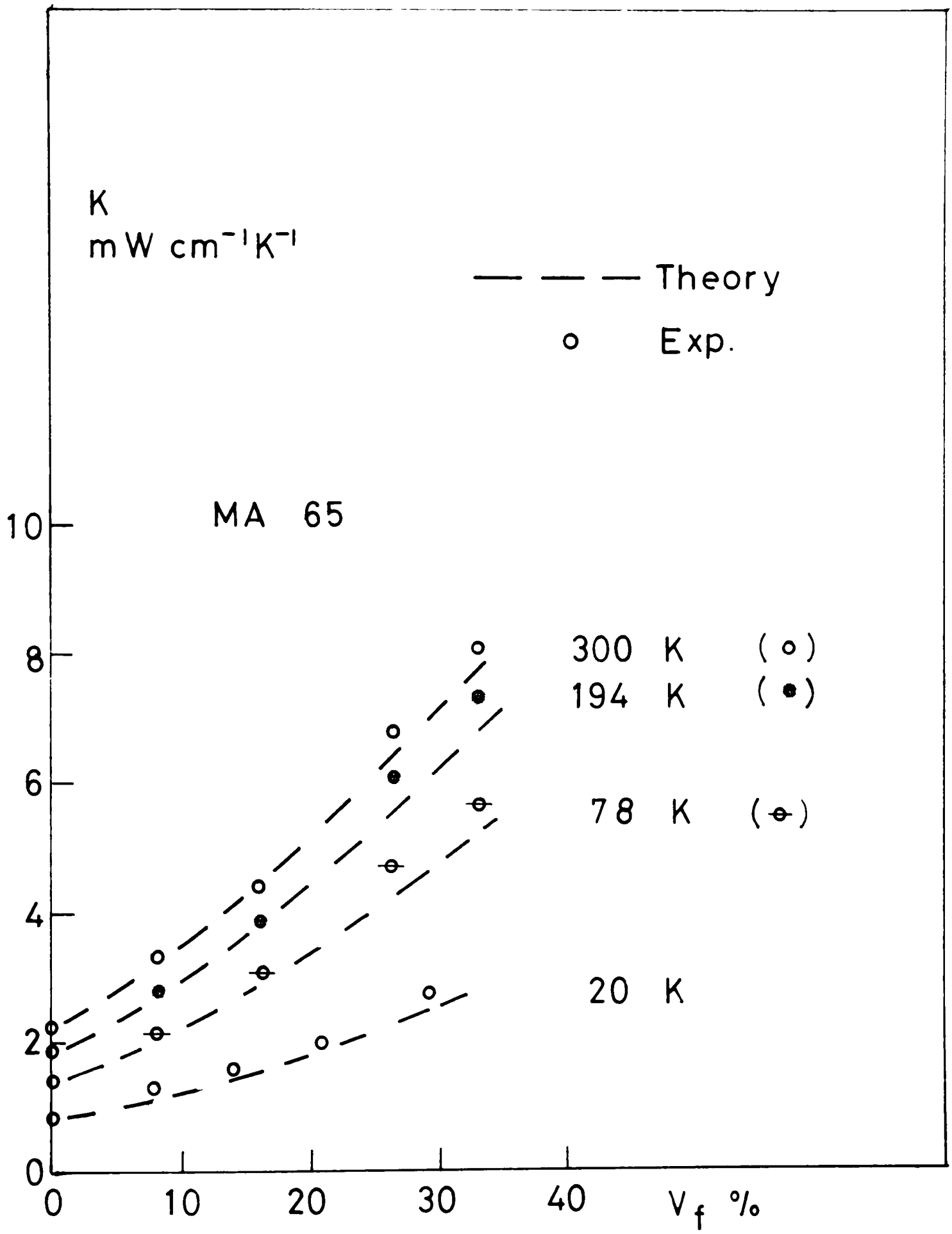


Fig 6.36 Thermal Conductivity (K) vs. Alumina Concentration, Volume % (V_f).

Comparison between Experiment and Hamilton and Crosser Equation.

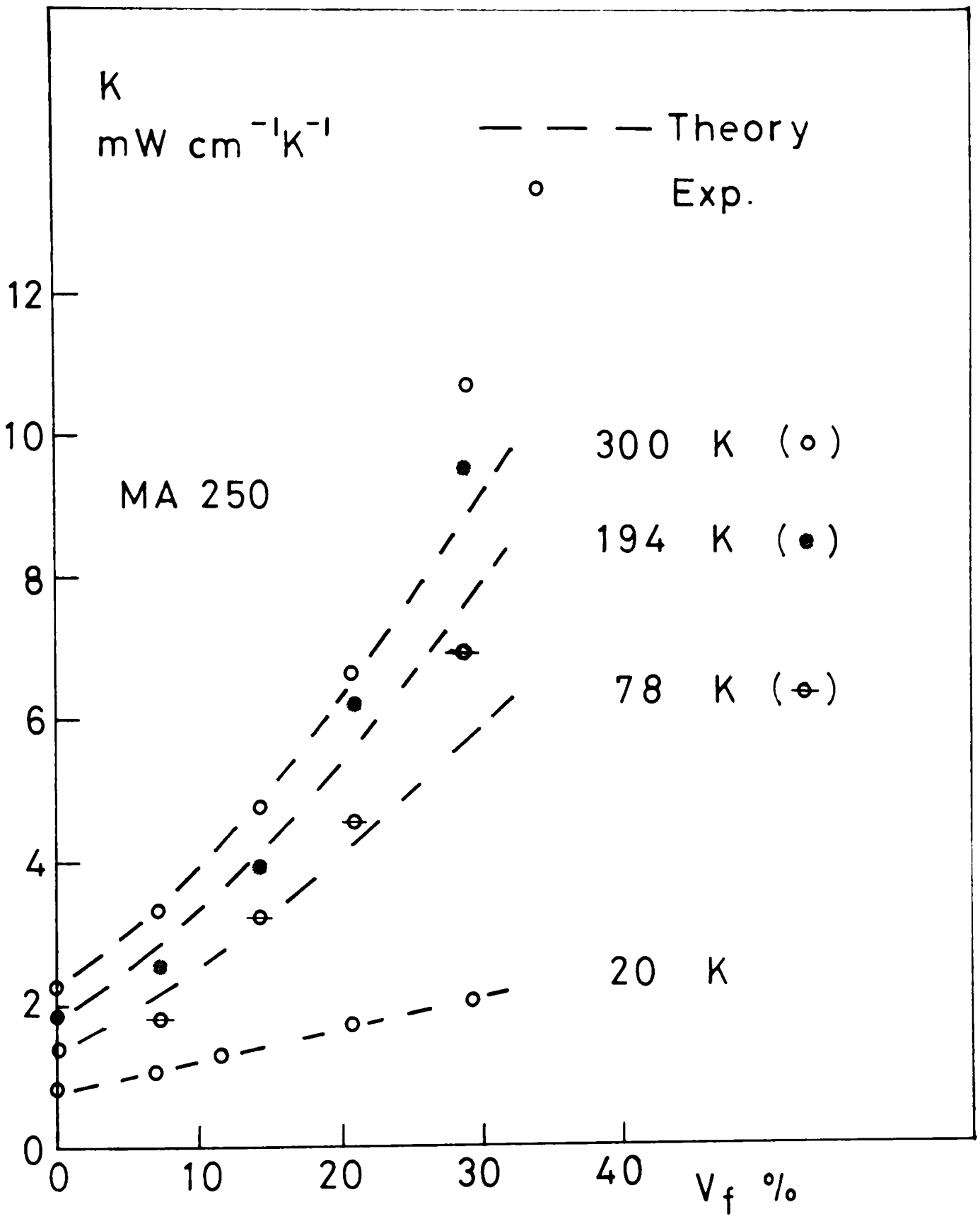


Fig 6.37 Thermal Conductivity (K) vs. Alumina Concentration, Volume % (V_f).

Comparison between Experiment and Hamilton and Crosser Equation.

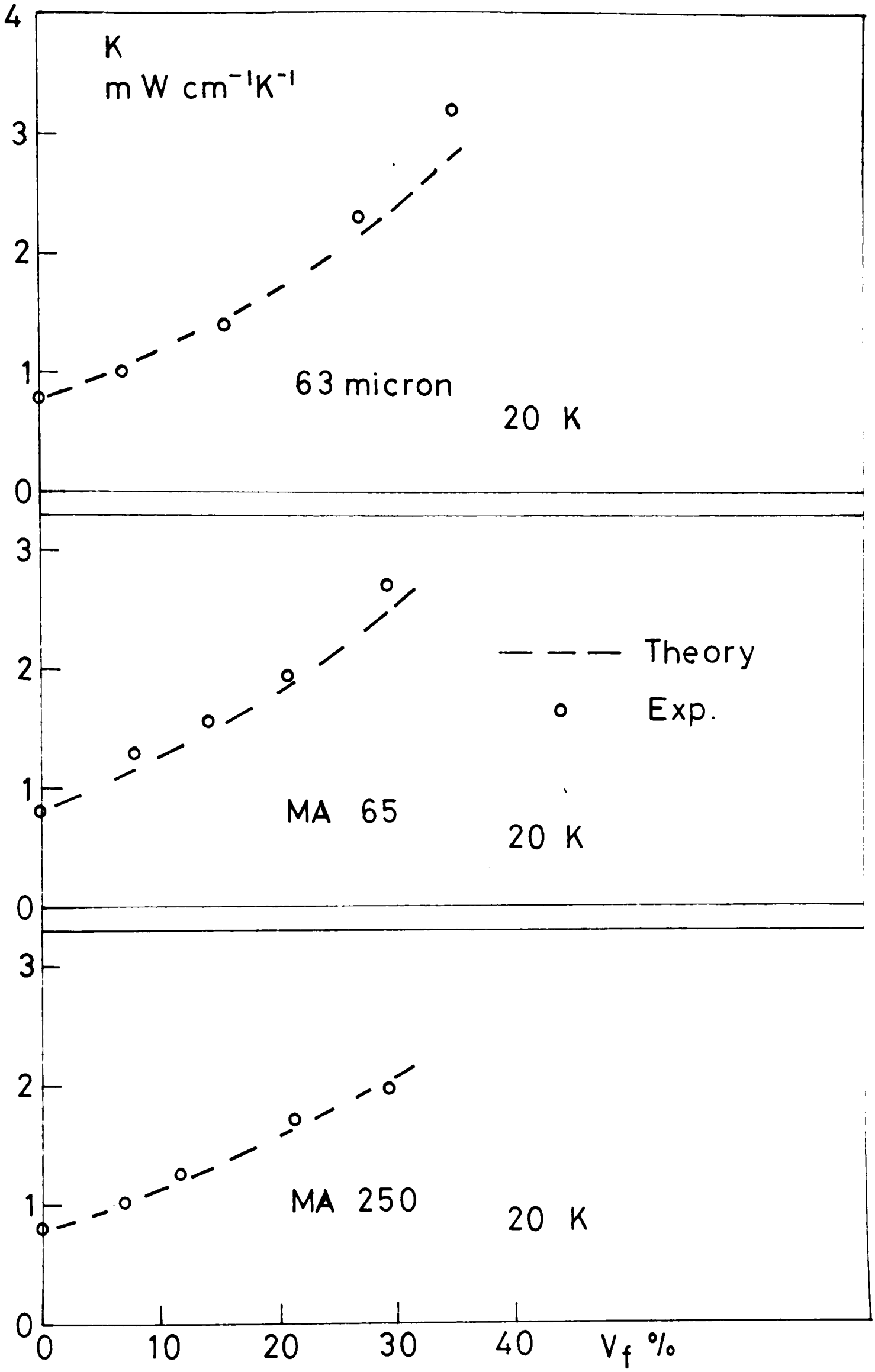


Fig 6.38 Thermal Conductivity (K) vs. Alumina Concentration, Volume % (V_f).

Comparison between Experiment and Hamilton and Crosser Equation.

T A B L E 6 . 4

TK	R_k K mW^{-1}	K_f $mW\ (cm\ K)^{-1}$	K_{fe} $mW\ (cm\ K)^{-1}$
4	$\frac{24 \times 10^{-4}}{A}$	34	1.25
2.5	$\frac{75 \times 10^{-4}}{A}$	11.5	0.40

The values of K_{fe} are applied to the Hamilton and Crosser equation and compared with the experimental results in fig. 6.39. Above 20% filler volume concentration the agreement is not very good. At 2.5 K the measured thermal conductivity decreases with increasing filler content as predicted up to about 20% by volume. However above this filler concentration the reverse is true, although the values are less than those predicted if there were no thermal contact resistance. It is possible that a small amount of particle contact will cause this. The particle conductivity at 2.5 K is about 30 times that of the resin and any short circuiting of the large thermal contact resistance will have a profound effect on the measured thermal conductivity of the composite.

For the MA 65 and MA 250 composite the analysis of the results is complicated by the platelet shape of the particles. An effective

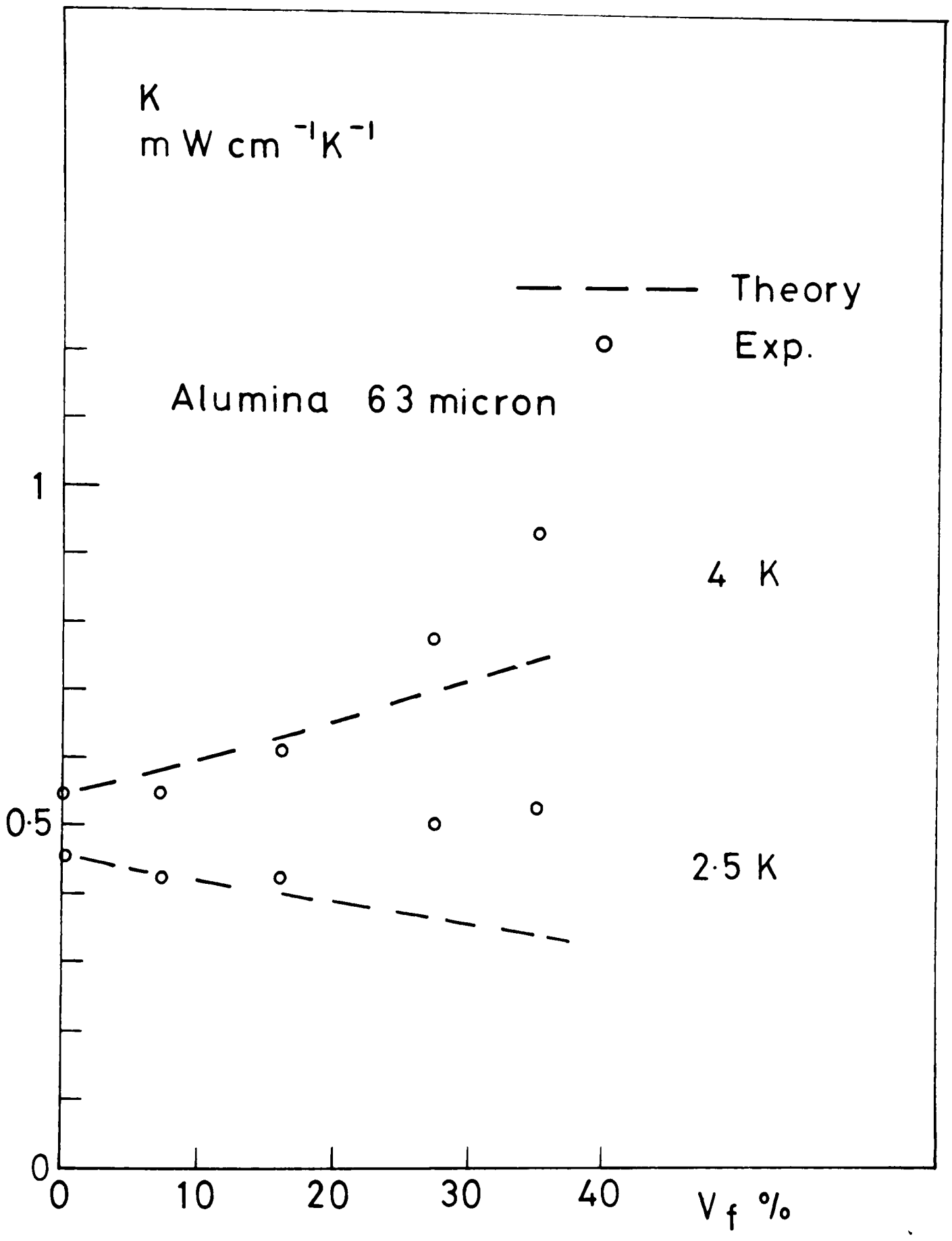


Fig 6.39 Thermal Conductivity (K) vs. Alumina Concentration, Volume % (V_f).

Comparison between Experiment and Hamilton and Crosser Equation.

particle conductivity can be obtained in the two cases when the plate is perpendicular to the direction of heat flow and when it is parallel to the heat flow. An average of the three orientations, one perpendicular and two parallel to the heat flow, can be taken for use in the Hamilton and Crosser equation.

T A B L E 6 . 5

	TK	R_k K mW $^{-1}$	$K_{fe\perp}$ mW (cm K)$^{-1}$	$K_{fe/\!/}$ mW (cm K)$^{-1}$	K_{fe} mW (cm K)$^{-1}$
MA 65	4	$\frac{24 \times 10^{-4}}{A}$	0.02	0.11	0.08
	2.5	$\frac{75 \times 10^{-4}}{A}$	0.01	0.04	0.03
MA 250	4	$\frac{24 \times 10^{-4}}{A}$	0	0	0
	2.5	$\frac{75 \times 10^{-4}}{A}$	0	0	0

The predictions of the Hamilton and Crosser equation using the average values of K_{fe} from table 6.5 are compared with the experimental results in figs. 6.40 to 6.43. The agreement is not very good except for the 4 K results for MA 65. The predicted

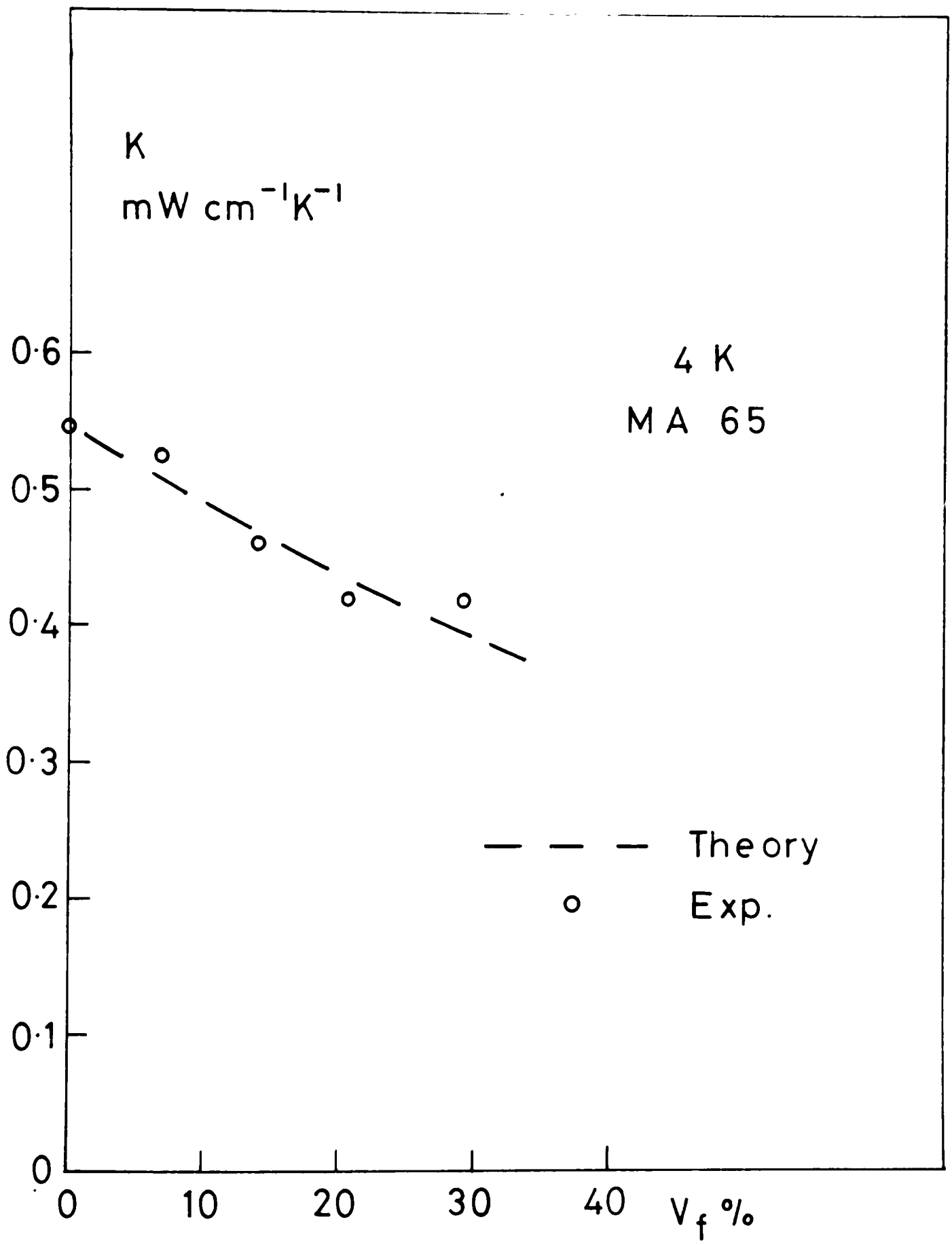


Fig 6.40 Thermal Conductivity (K) vs. Alumina Concentration, Volume % (V_f).

Comparison between Experiment and Hamilton and Crosser Equation.

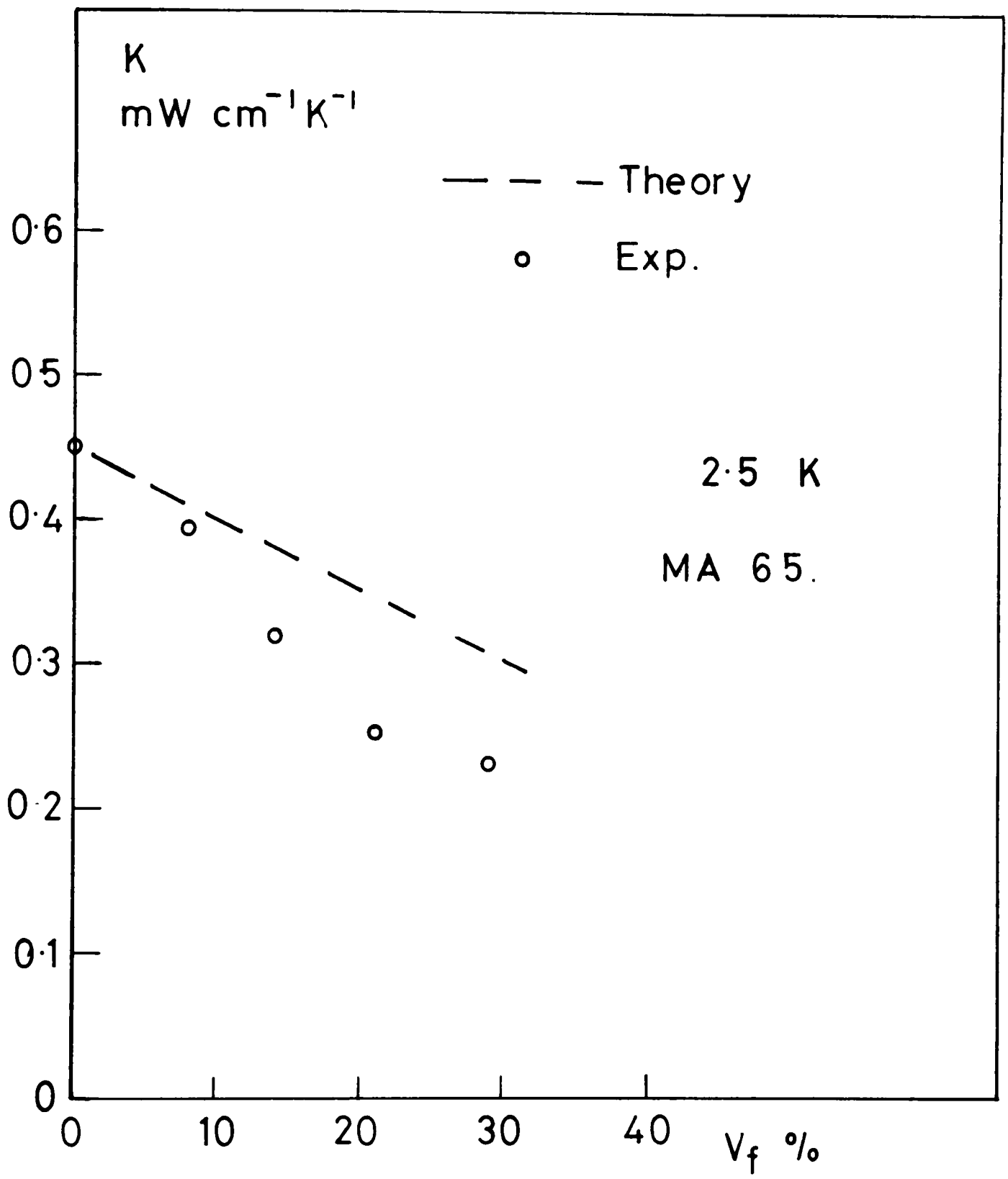


Fig 6.41 Thermal Conductivity (K) vs. Alumina Concentration, Volume % (V_f).

Comparison between Experiment and Hamilton and Crosser Equation.

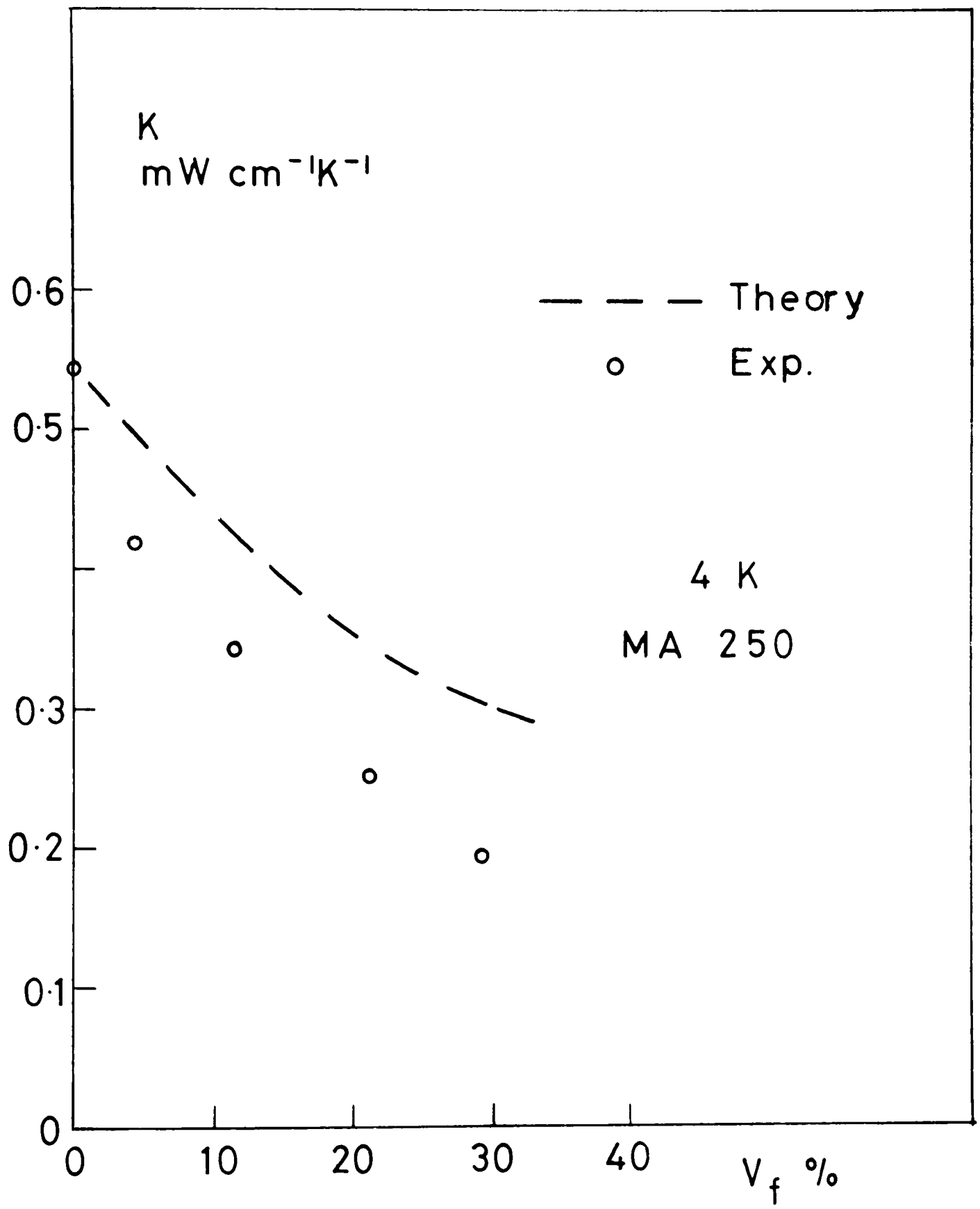


Fig 6.42 Thermal Conductivity (K) vs. Alumina Concentration, Volume % (V_f).

Comparison between Experiment and Hamilton and Crosser Equation.

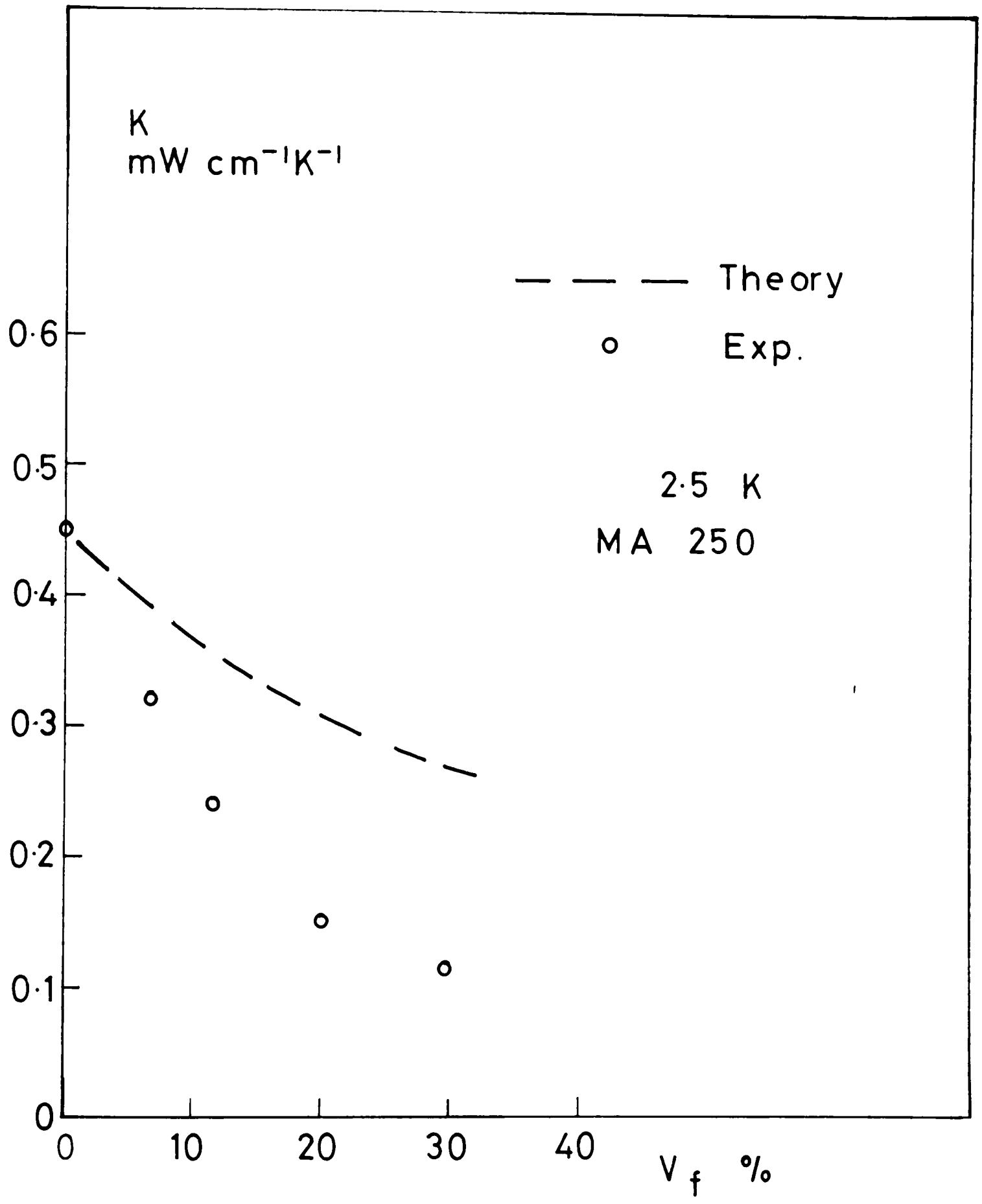


Fig 6.43 Thermal Conductivity (K) vs. Alumina Concentration, Volume % (V_f).

Comparison between Experiment and Hamilton and Crosser Equation.

conductivities are much higher than those measured. At 2.5 K the predicted conductivity is a factor of 2 higher than the experimental values at 30% concentration even when the effective particle conductivity used can be considered to be zero.

The discrepancy between the theory and the experimental results could be explained in one of two ways or a combination of both. The conductivity of the resin could be affected by the presence of the small size particles if at a certain concentration the average distance between particles is comparable to, or less than the phonon mean free path in the epoxy. The smaller the particle size the smaller the average distance between particles for a given concentration. In addition the theory might be inappropriate when the effective thermal conductivity of the particles is very low compared to that of the resin.

At 4 K and 2 K the average phonon mean free path in the epoxy is about 0.03 micron and 0.20 micron respectively. It is possible that at high concentrations the average mean free path could be comparable with the average distance between particles but even at a filler concentration of about 5% by volume at 2.5 K for the MA 250 composites the theory overestimates the thermal conductivity. So it appears that this is not the main effect.

It is possible to approach the problem from another angle. Consider a unit cube of composite of filler content V_f with a heat flux along the Z direction. We have an average projected area $\bar{A}$ perpendicular to the heat flux associated with each particle of volume V. There will be V_f/V particles in the unit cube. We can push all the particles together in the X - Y plane, leaving the

particle distribution undisturbed in the Z direction. The average projected area of the particles in the X - Y plane will be $\bar{A}\,(V_f/V)^{\frac{2}{3}}$, and the average number of layers of particles in the Z direction is $(V_f/V)^{\frac{1}{3}}$. The unit cube is now composed of two parts. One part of area $1-(V_f/V)^{\frac{2}{3}}\,\bar{A}$ in the X - Y plane and unit length in the Z direction composed only of epoxy, and the other of area $(V_f/V)^{\frac{2}{3}}\,\bar{A}$ in the X - Y plane and unit length in the Z direction, composed of resin and particles and with $2\,(V_f/V)^{\frac{1}{3}}$ complete layers of contact resistance. Assuming that the contact resistance is large compared with the resin-particle thermal resistance, and parallel heat flow, it is possible to calculate the effective thermal conductivity of the unit cube. This is given by

$$K_e = K_m\left[1-\left(\frac{V_f}{V}\right)^{\frac{2}{3}}\bar{A}\right]+\frac{\bar{A}}{2R_k}\left(\frac{V_f}{V}\right)^{\frac{1}{3}} \qquad 6.3$$

Equation 6.3 is compared with the experimental results of the MA 65 and MA 250 composites in fig. 6.44 to 6.47 at 4 K and 2.5 K. At 2.5 K fair agreement is obtained but at 4 K equation 6.3 underestimates the experimental results for the MA 65 composites. Equation 6.3 appears to be satisfactory for extreme cases where the contact resistance is very high and the effective particle conductivity can be considered to be zero.

In fig. 6.48 the experimental results of the alumina composites of the three particle sizes for concentrations of about 20% by volume are compared with the theoretical predictions for the temperature

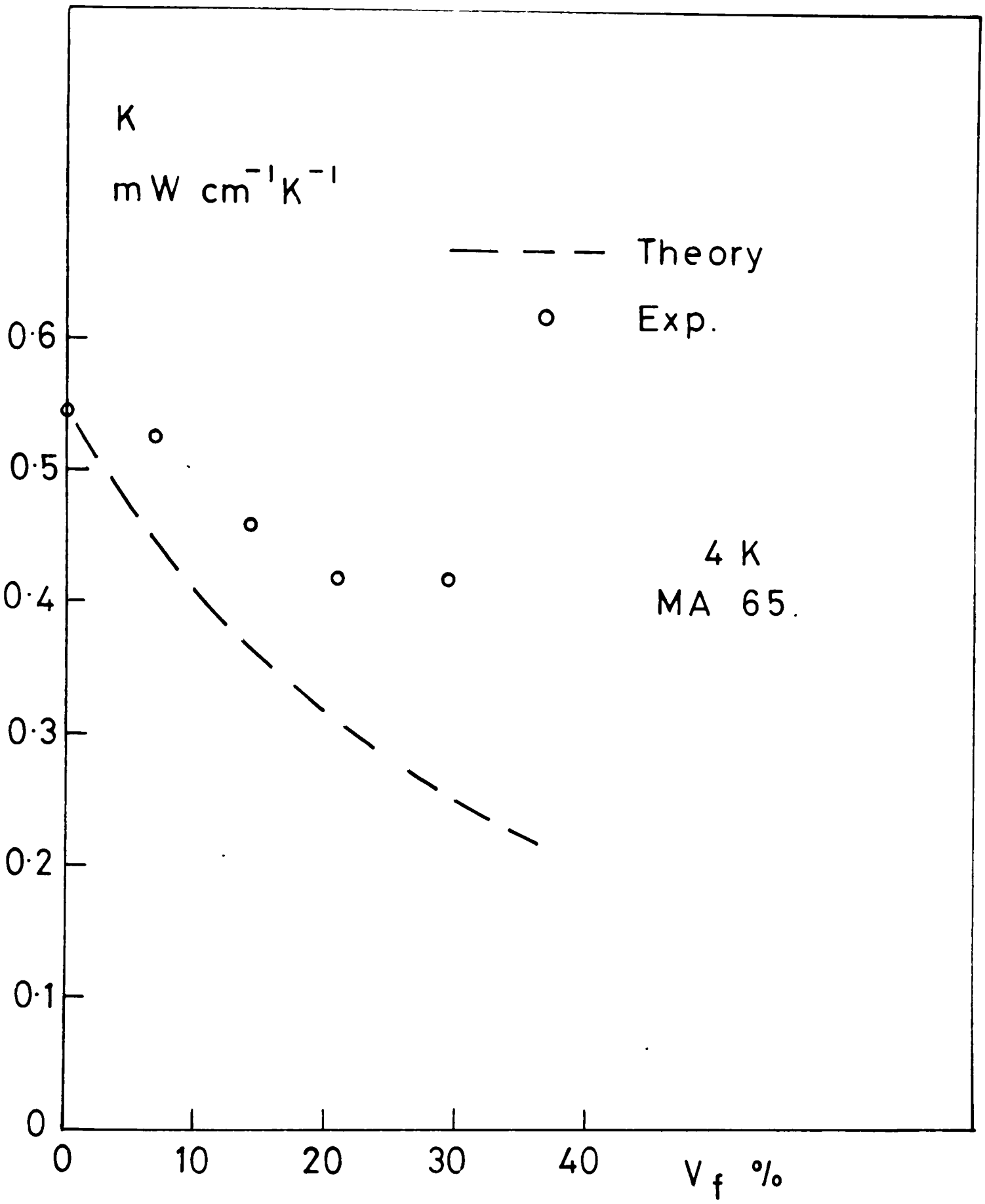


Fig 6.44 Thermal Conductivity (K) vs. Alumina Concentration, Volume % (V_f).

Comparison between Experiment and Equation 6.3.

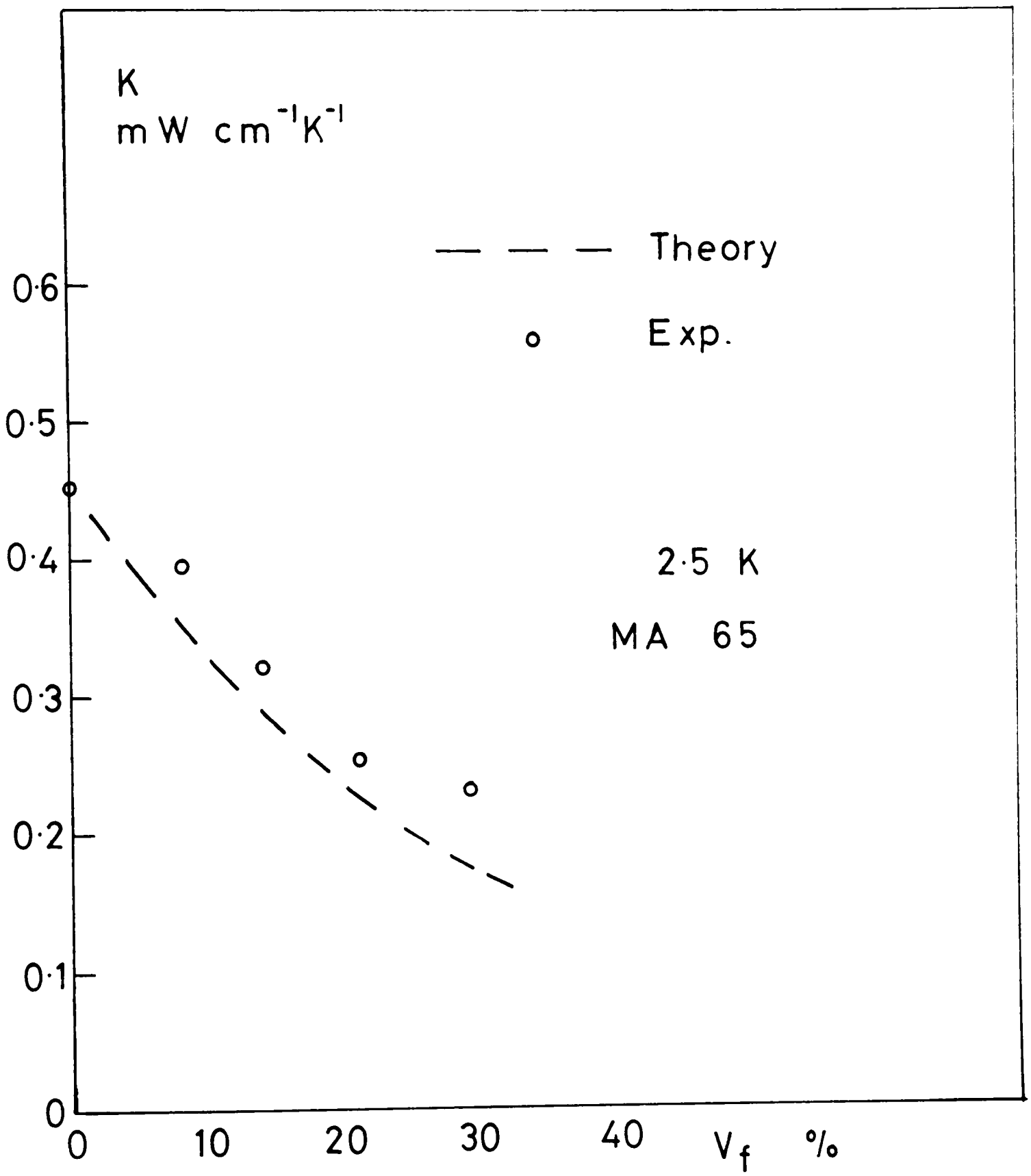


Fig 6.45 Thermal Conductivity (K) vs. Alumina Concentration, Volume % (V_f).

Comparison between Experiment and Equation 6.3.

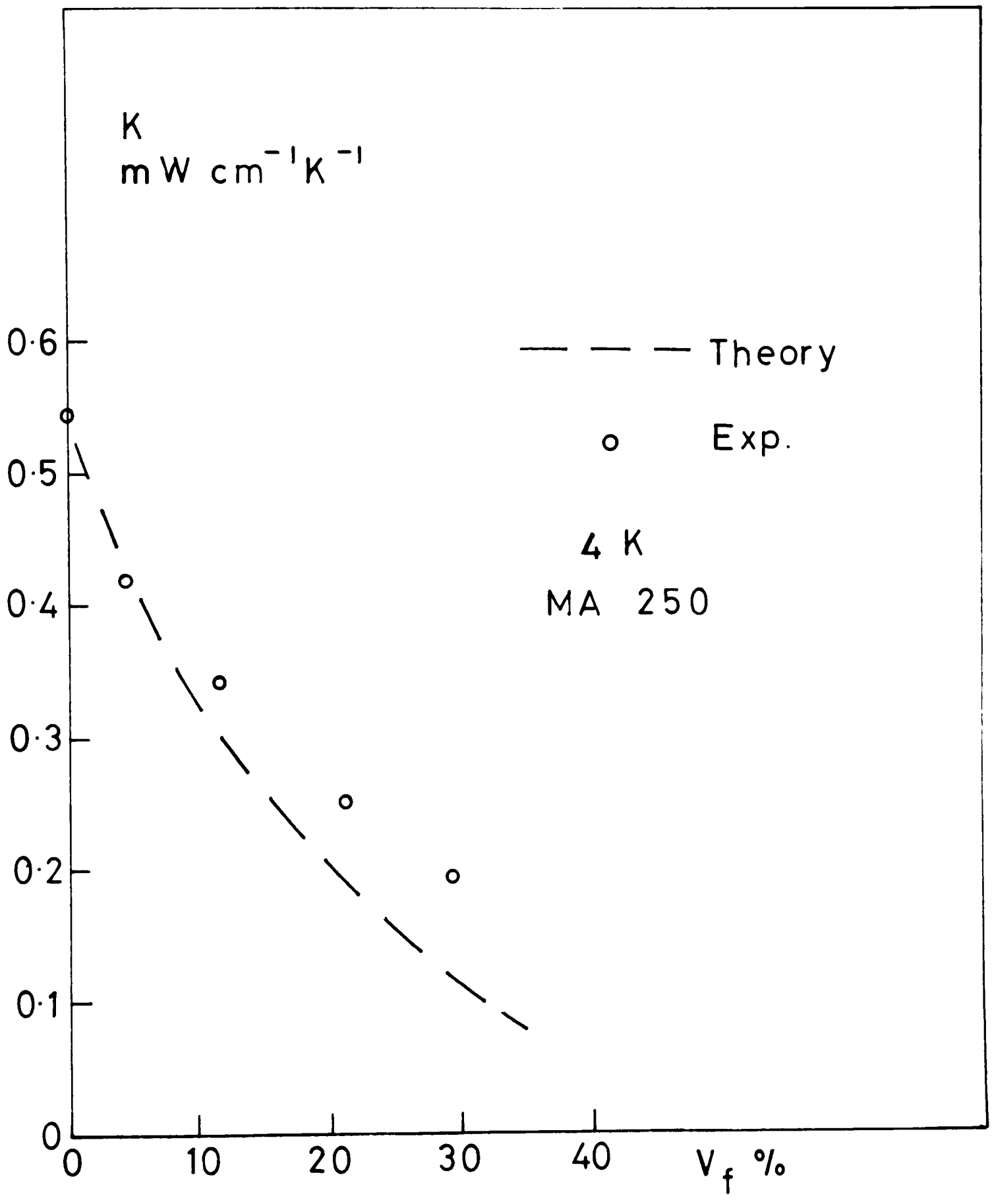


Fig 6.46 Thermal Conductivity (K) vs. Alumina Concentration, Volume % (V_f).

Comparison between Experiment and Equation 6.3.

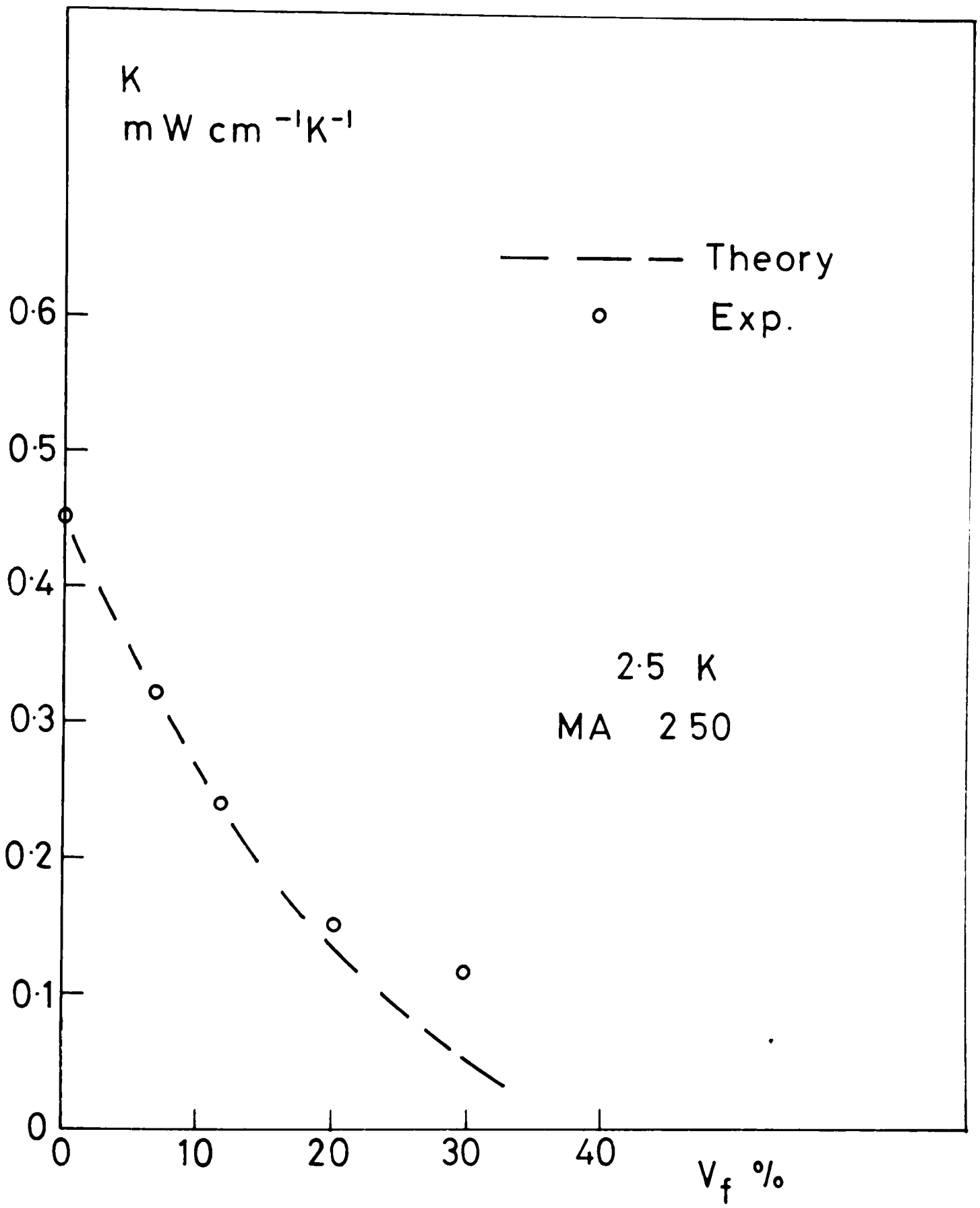


Fig 6.47 Thermal Conductivity (K) vs. Alumina Concentration, Volume % (V_f).

Comparison between Experiment and Equation 6.3.

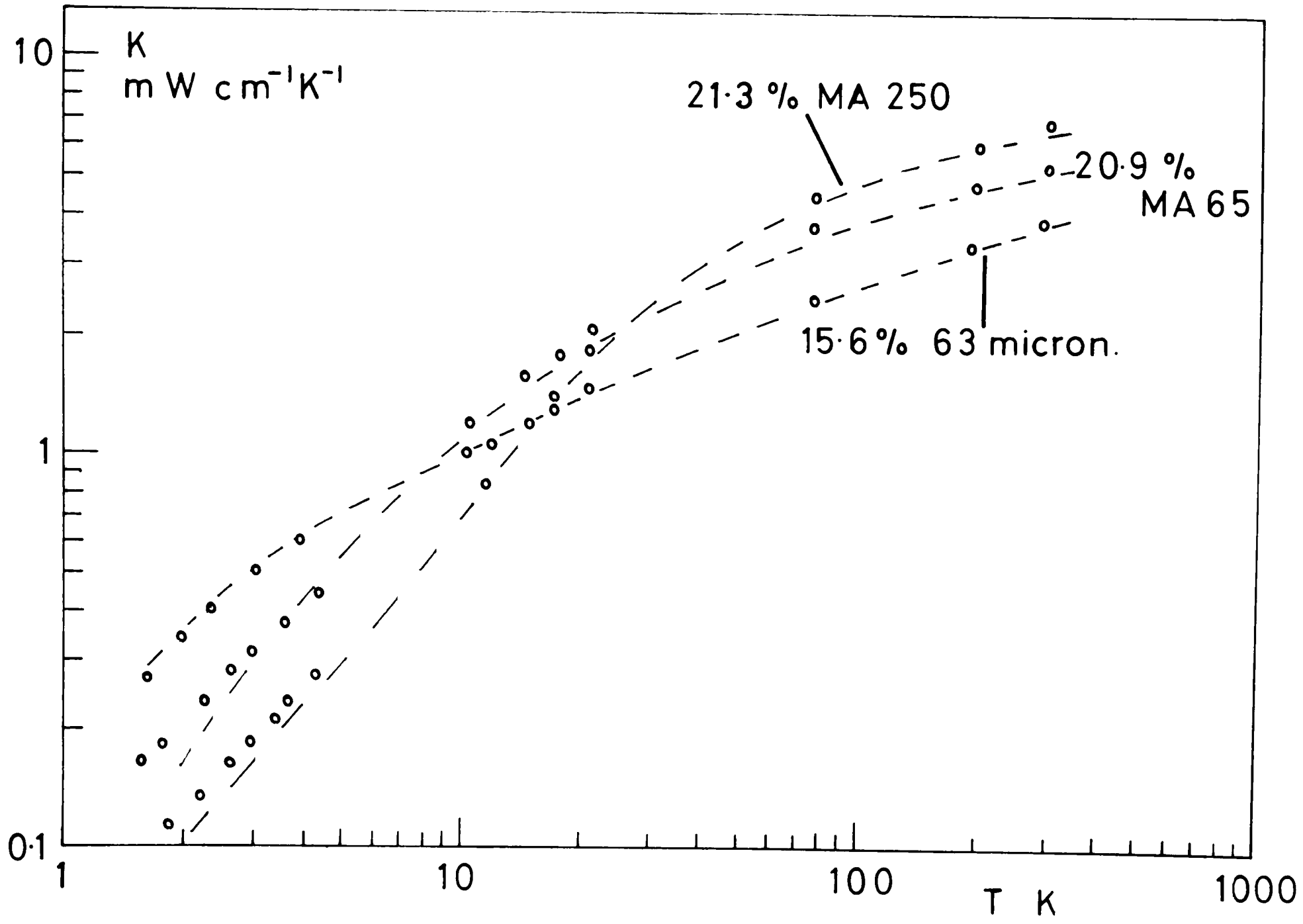


Fig 6.48 Thermal Conductivity (K) vs. Temperature (T). Comparison between Experiment and Theory.

range 2 K up to room temperature. At liquid hydrogen temperatures and above good agreement is obtained for these concentrations with the Hamilton and Crosser equation. At liquid helium temperatures using an effective particle conductivity, which includes the thermal contact resistance, the Hamilton and Crosser equation gives good agreement for the 62 micron and MA 65 composites. For the MA 250 composites, equation 6.3 has been used and good agreement is obtained.

DIAMOND FILLED EPOXIES

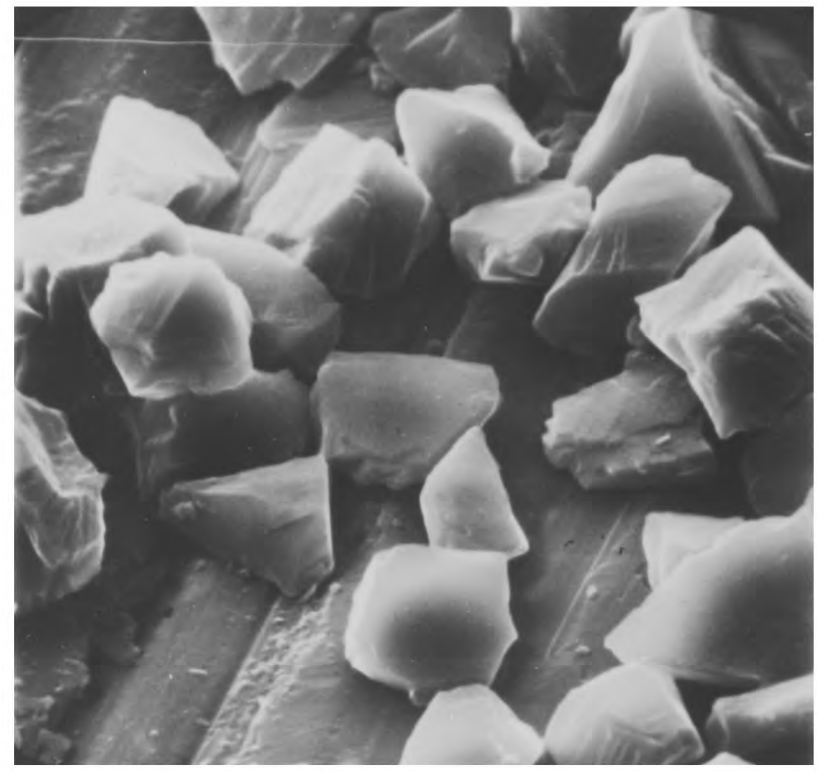
6.12 Specimens

Diamond filled epoxies might have little commercial value because of their high cost (except in small quantities), but since diamond has extreme thermal properties it is physically interesting to incorporate it into composites. Diamond has a Debye Θ of 2240 K and at room temperature its thermal conductivity is well above that of almost all other materials. The velocities of sound in diamond are high, and so, due to the acoustic mismatch, there should be a large thermal contact resistance at the diamond-epoxy interface at helium temperatures.

Industrial diamond powder in two size ranges, 8 to 15 micron and 1 - ½ micron, and type II A, gemstone quality, in size range 8 - 15 micron were used in the samples.

Scanning electron micrographs of the powders were taken and two of these are shown in plate 4. The powders consist of random, irregular particles. For the industrial diamond a volume weighted average cube length of 8 micron was obtained from measurements of the projected areas of the particles. For the type II A diamond a value of 8.5 micron was obtained. For the smaller industrial powder it was not possible to deduce this value because of the poor resolution of the micrographs.

The specimens were prepared as described in section 3.5 and filler concentrations up to about 17% by volume were employed. This was the highest filling factor possible with the amount of diamond powder available.



Industrial Diamond 8 micron

Plate 4

6.13 Experimental results and discussion

The thermal conductivity of the diamond filled epoxies are shown in figs. 6.49 to 6.52. In fig. 6.52 the industrial and type II A diamond composites are compared and no difference is found for the whole of the temperature range. At high temperatures, although the industrial diamond is expected to have a lower thermal conductivity than the pure type II A it will still be much higher than that of the epoxy and both types of diamond can be assumed to have an infinite conductivity compared with the epoxy matrix. At low temperatures because of the similar size of the two types of diamond, similar conductivities are to be expected for the composites.

The results exhibit properties akin to those of the alumina filled epoxies. At high temperatures increasing diamond content causes an increase in the thermal conductivity of the composites. At helium temperatures the reverse is true, the 8 micron conductivity curves cross over each other at about 7 K and the 1 - ½ micron curves at a higher temperature of about 20 K, and as before the composites of the smaller particles have a lower thermal conductivity for a given filler concentration.

To obtain a fit between the room temperature experimental results and the Hamilton and Crosser equation a sphericity of 0.4 is required. From the shape of the particles in the micrographs a sphericity of about 0.7 is more likely. At 78 K and 20 K a good fit can be obtained by using a sphericity of 0.7. At room temperature the thermal conductivity of the diamond will be about 4 orders of magnitude higher than that of the epoxy and it seems that the

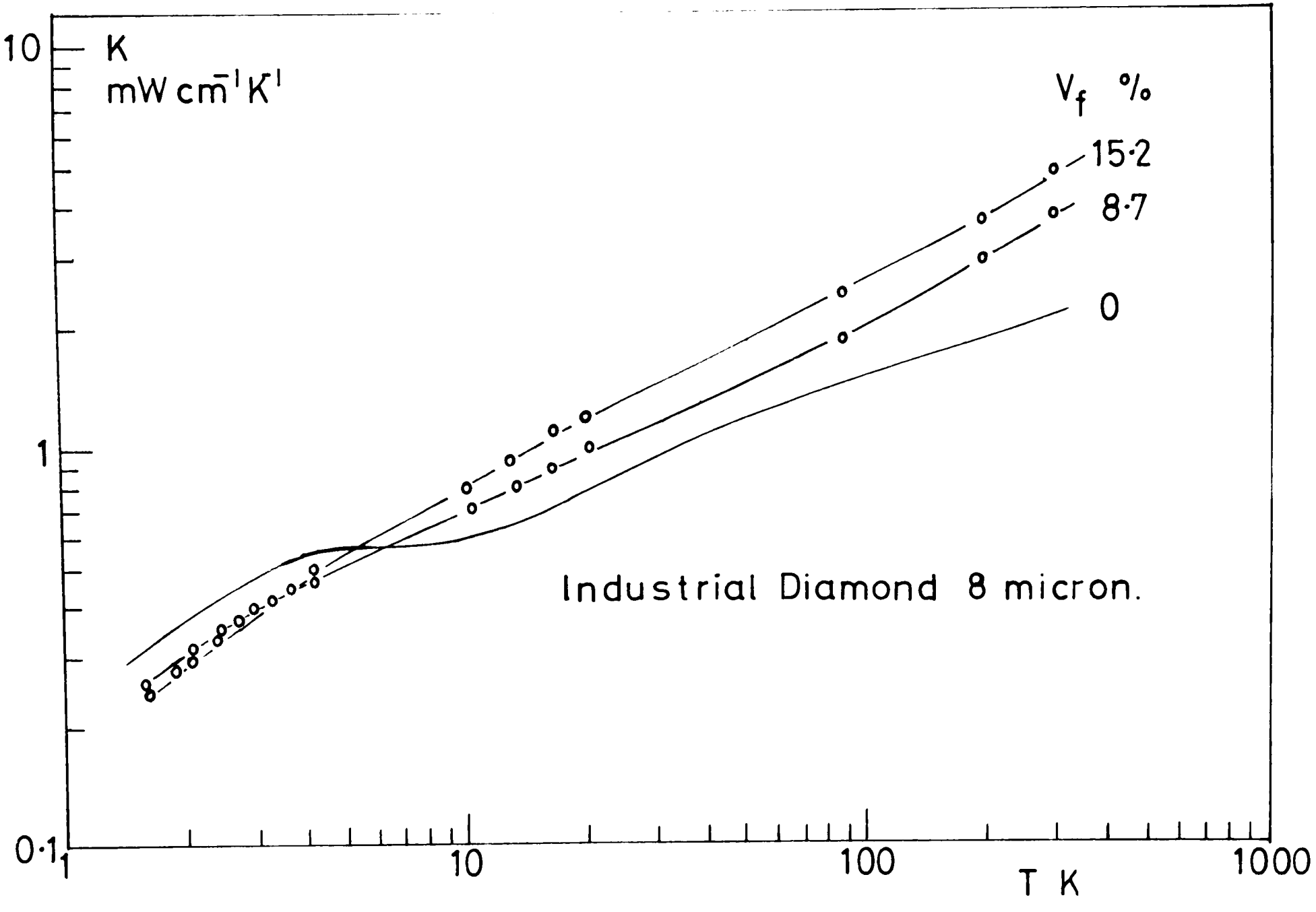


Fig 6.49 Thermal Conductivity (K) vs. Temperature (T).

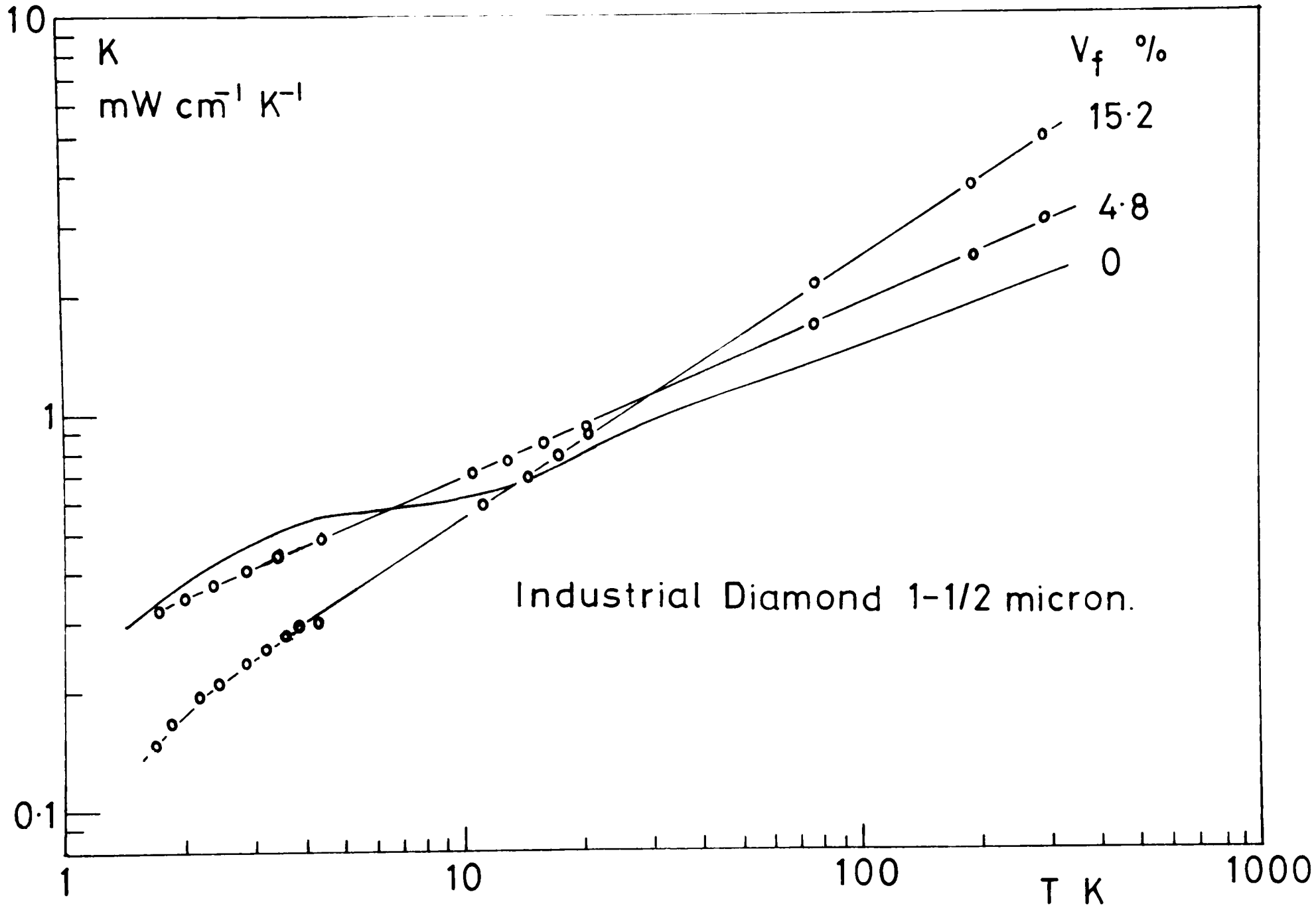


Fig 6.50 Thermal Conductivity (K) vs. Temperature (T).

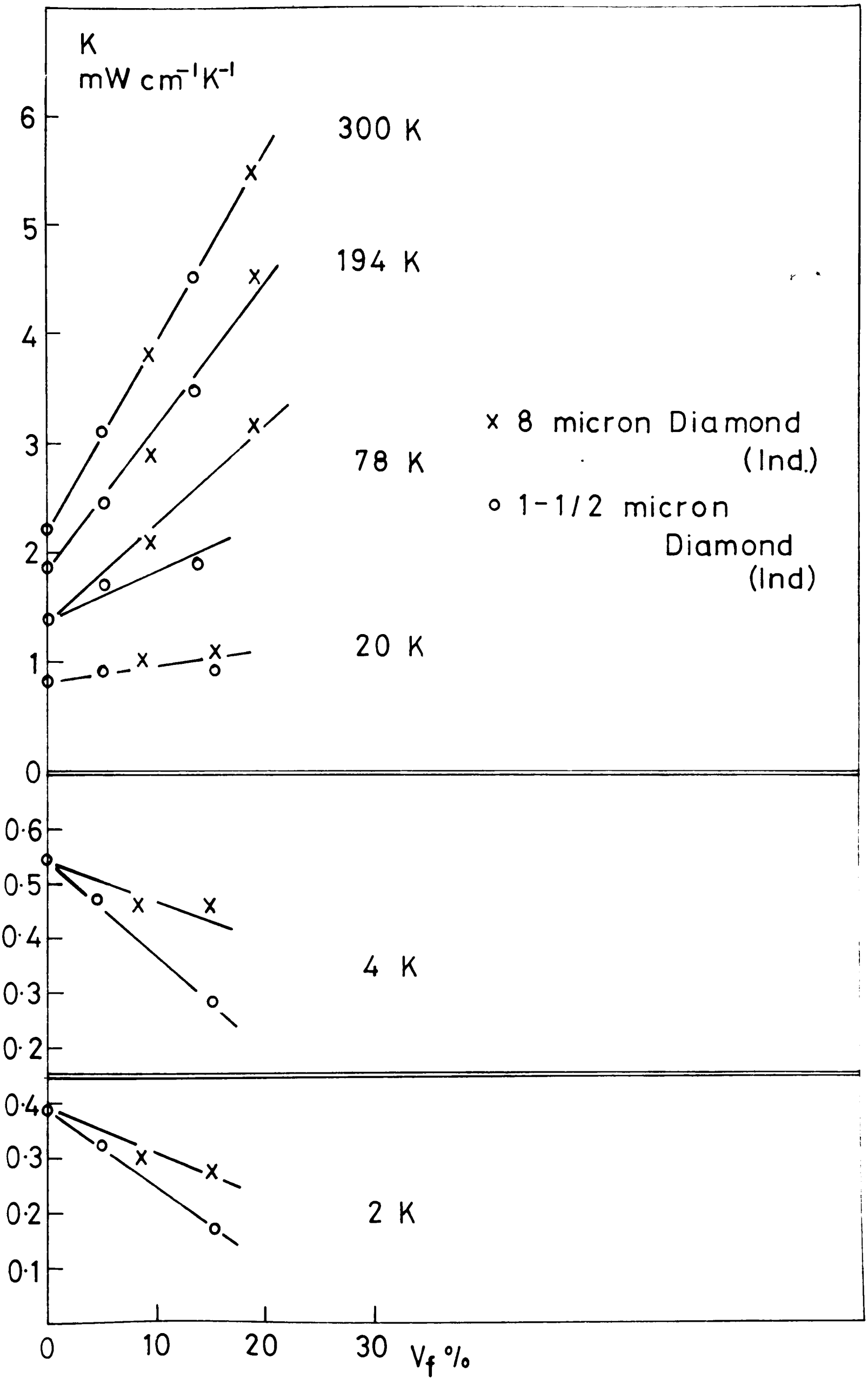


Fig 6.51 Thermal Conductivity (K) vs. Diamond Concentration, Volume % (V_f).

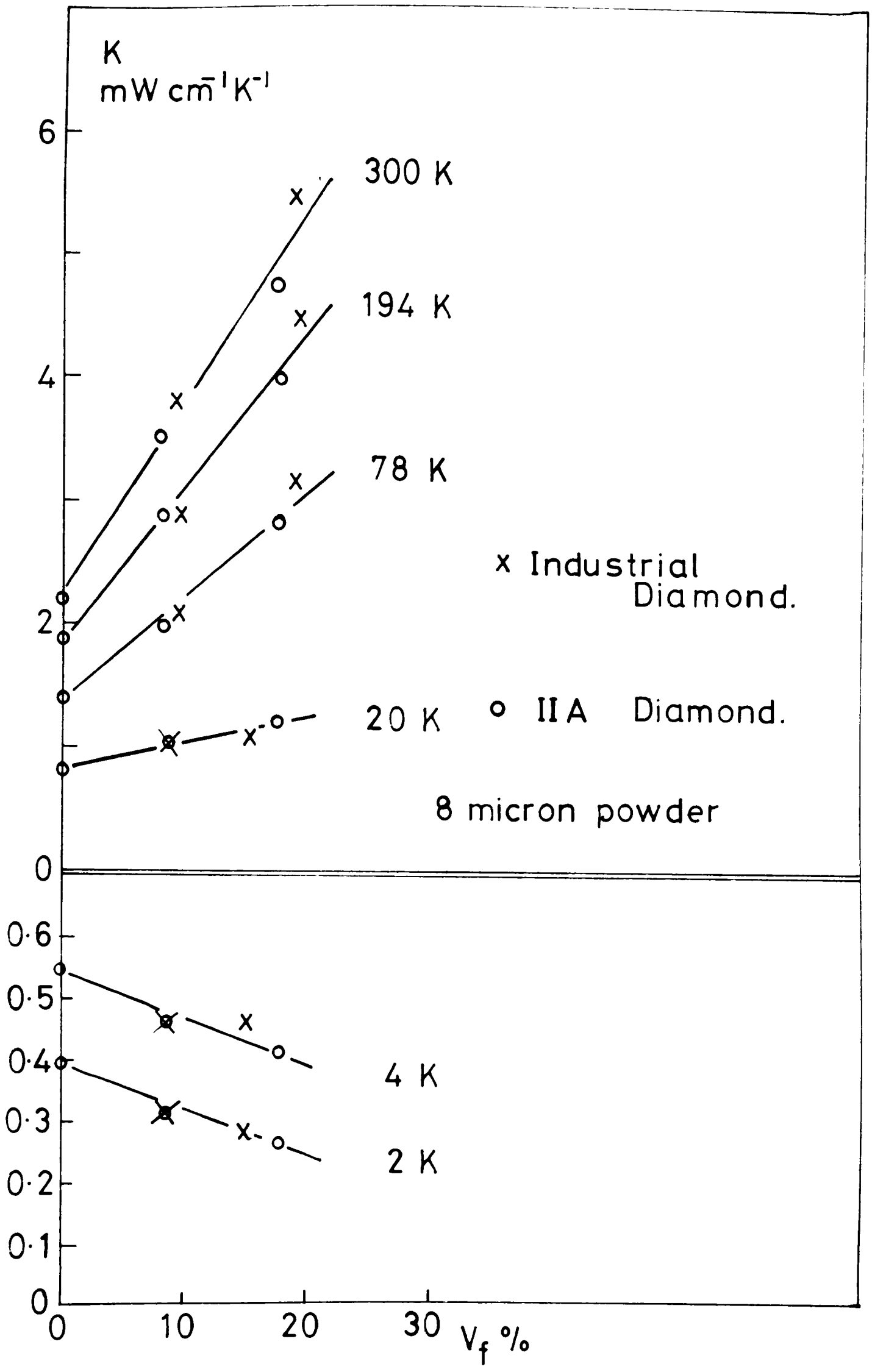


Fig 6.52 Thermal Conductivity (K) vs. Diamond Concentration, Volume % (V_f).

Hamilton and Crosser equation does not apply for composites whose fillers have a much higher thermal conductivity than that of the matrix even for the low concentrations used in the experiments. At 78 K and 20 K where the thermal conductivity of the diamond will be lower a fit can be obtained between the experimental results and the Hamilton and Crosser equation by using a reasonable value of the particle sphericity.

At helium temperatures the high value of the thermal contact resistance expected at the diamond-epoxy interface is demonstrated by the low values of the measured composite thermal conductivity. It was not possible to measure this contact resistance as no suitable bulk sample was available at the time, and also it was not possible to estimate it from Little's theory as the sound velocities are so much higher in diamond than those in the epoxy (Little's paper gives quantitative information only up to a ratio of 2 for the sound velocities in the two media and the smallest ratio for the diamond and epoxy media is about 5). If we assume that the thermal contact conductance to be zero compared with the matrix thermal conductance, equation 6.3 can be used to predict the 8 micron composite thermal conductivity. The comparison between the experimental values and the predictions of equation 6.3 is shown in fig. 6.53 and good agreement is obtained for the values at 2 K where the assumption made will be more valid than at 4 K.

The extreme thermal properties of diamond highlight the effect of fillers in an epoxy system even at the low filler concentrations

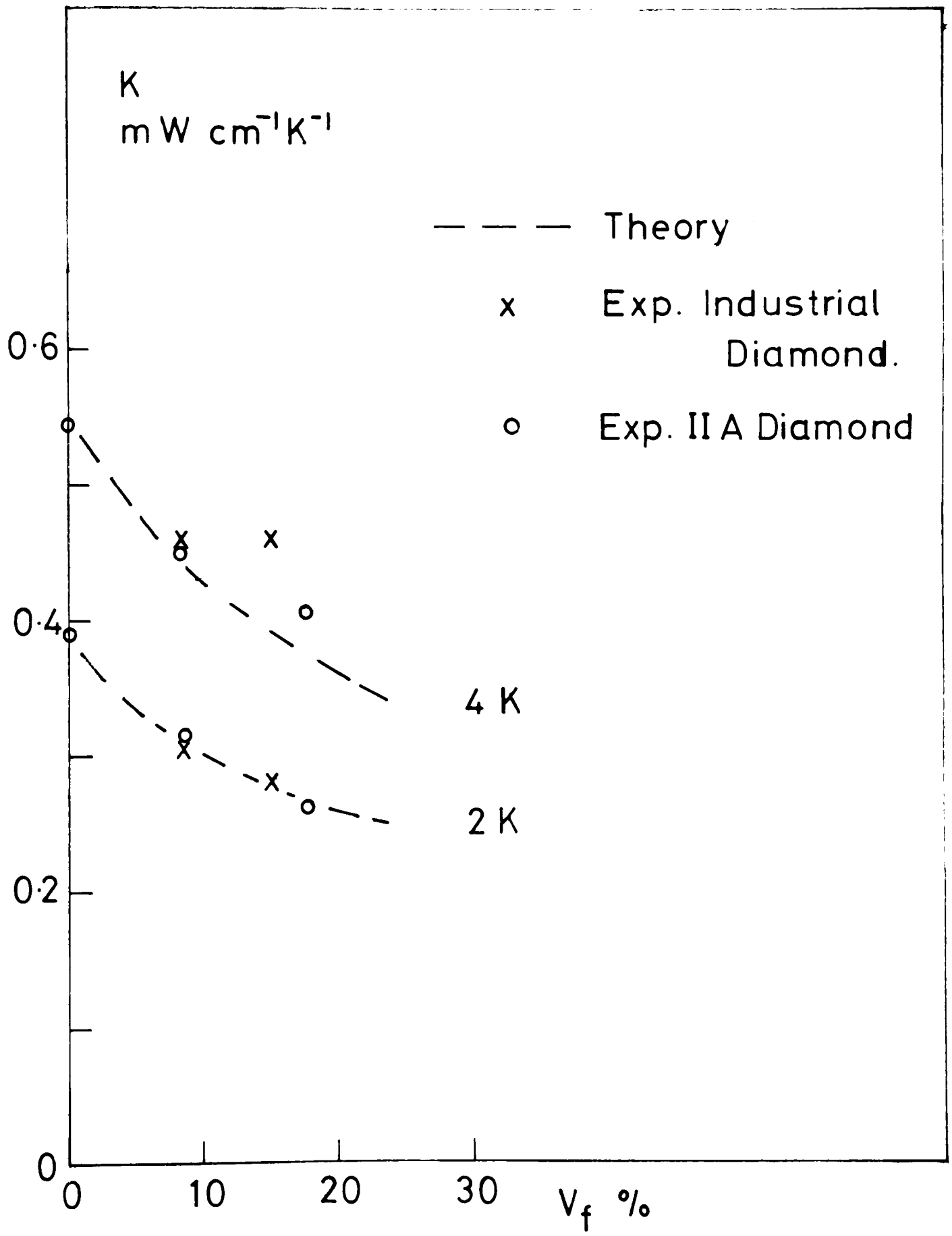


Fig 6.53 Thermal Conductivity (K) vs. Diamond Concentration, Volume % (V_f). Comparison between Experiment and Equation 6.3.

at which measurements were taken. At helium temperatures the large thermal contact resistance dominates any effect due to the good intrinsic conductivity of the diamond itself, even when limited by boundary scattering, and at high temperatures high thermal conductivity composites are produced because of the high conductivity of the diamond.

CHAPTER 7

CONCLUSIONS

Conclusions

It is well known that at room temperature, bulk displacement of a plastic with a particulate filler of a higher thermal conductivity results in a composite whose thermal conductivity is higher than that of the plastic. We have selected 4 types of non-metallic particulate fillers and a matrix of an epoxy resin and attempted to explain in detail the form of these changes, in the temperature range 2 K to room temperature.

At high temperatures we have been able to explain our results in terms of the bulk thermal conductivities of the matrix and the filler, the volume concentration of the filler and the shape of the filler particles. Generally agreement between theory and the experimental results is good except for high filler concentrations of high thermal conductivity filler. The high temperature results on the diamond filled composites cannot be explained satisfactorily with the theory, even for the low filler concentrations used in these samples. The high temperature thermal conductivity of diamond is large but the reason why the measured values are higher than those predicted by theory is not clear.

At helium temperatures we have been able to explain the experimental results in terms of a thermal contact resistance at the matrix filler interface and average particle size, in addition to the properties described above. By deducing an effective particle thermal conductivity incorporating the thermal contact resistance,

agreement between theory and experiment is generally good, although predictions of the Rayleigh Maxwell type of equations do not seem applicable when the contact resistance is so high that the effective particle thermal conductivity can be considered to be zero. For this case a simple model in which phonons are scattered by "planes" of contact resistance extending throughout part of the composite has been proposed.

At high temperatures significant increases in the composite thermal conductivity can be obtained by using a filler whose thermal conductivity is higher than that of the matrix. At helium temperature, particle size and the thermal contact resistance between the matrix and the filler greatly affect the composite thermal conductivity and values substantially higher or lower than that of the matrix can be obtained. Either type of behaviour may be useful in the low temperature application of composites.

REFERENCES

Anderson O.L., J. Phys. Chem. Solids 12 41 (1959)

Anderson A.C., Reese W., Wheatley J.C.; Rev. Sci. Inst. 34 1386 (1963)

Anderson A.C., Rauch R.B.; J. Appl. Phys. 41 3648 (1970)

Ashworth T., Bunting J.G., Smith S.J.; Cryogenics 8 167 (1968)

Ashworth T., Rechowicz M., Steeple H.; Cryogenics 9 58 (1969)

Athougies A.D., Peterson B.T., Salinger G.L., Swartz C.D.; Cryogenics 12 125 (1972)

Babanov A.A.; Soviet Phys. - Tech. Phys. 2 476 (1957)

Berman R.; Proc. Roy. Soc. A208 90 (1951)

Berman R., Foster E.L., Rosenberg H.M.; Brit. J. Appl. Phys. 6 181 (1955)

Berman R., Huntley D.J.; Cryogenics 3 70 (1963)

Berman R., Brook J.C.F., Huntley D.J.; Cryogenics 4 233 (1964)

Borelius G., Keesom W.H., Johnson C.H., Linde J.O.; Proc. Kon. Akad. Amsterdam 35 15 (1932)

Callaway J.; Phys Rev. 122 787 (1961)

Chang C.K., Jones R.E.; Phys. Rev. 126 2055 (1962)

Choy C.L., Salinger G.L., Chiang Y.C.; J. Appl. Phys. 41 597 (1970)

Dreyfus B., Fernandes N.C., Maynard R.; Phys. Lett. 26A 647 (1968)

Fricke H.; Phys. Rev. 24 575 (1924)

Godbee H.W., Ziegler W.T.; J. Appl. Phys. 37 56 (1966)

Gorring R.L., Churchill S.W.; Chem. Eng. Progr. 57 53 (1961)

Hamilton R.L., Crosser O.K.; Ind. Eng. Chem. Fundamentals 1 187 (1962)

Hirsch H., Koved F.; Modern Plastics 42 133 (Oct. 1964)

Hudson P.S.W.; Private Communication (1972)

Kapitza P.L.; J. Phys. (U.S.S.R.) 4 181 (1941)

Kittel C.; Phys. Rev. 75 972 (1949)

Klemens P.G.; Proc. Roy. Soc. A208 108 (1951)

Klemens P.G.; Solid State Physics 7 1 (1958)

Kline D.E.; J. Polym. Sci. 50 441 (1961)

Knudsen J.G., Wang R.H.; Ind. Eng. Chem. 50 1667 (1958)

Kolouch R.J., Brown R.G.; J. Appl. Phys. 39 3999 (1968)

Laubitz M.J.; Can. J. Phys. 37 798 (1959)

Lee H., Neville K.; "Handbook of Epoxy Resins" - McGraw - Hill p.6.32 (1967)

Little W.A.; Can. J. Phys. 37 334 (1959)

MacDonald D.K.C., Pearson W.B., Templeton I.M.; Proc. Roy. Soc. A266 161 (1962)

Maxwell J.C.; "A Treatise on Electricity and Magnetism" - O.U.P. 3rd ed., Vol. 1, p.440 (1892)

Meredith R.E., Tobias C.W.; J. Appl. Phys. 31 1270 (1960)

Powell R.L., Bunch M.D., Corruccini R.J., Cryogenics 1 139 (1961)

Lord Rayleigh; Phil. Mag. 34 481 (1892)

Reese W., Tucker J.E.; J. Chem. Phys. 43 105 (1965)

Reese W.; J. Appl. Phys. 37 864 (1966a)

Reese W.; J. Appl. Phys. 37 3227 (1966b)

Reese W.; J. Appl. Phys. 37 3959 (1966c)

Rosenberg H.M.; "Low Temperature Solid State Physics" C.U.P. p.43 (1963)

Rosenstock H.B.; J. Phys. Chem. Solids 23. 659 (1962)

Runge J.; Z. Tech. Physik 6 61 (1925)

Slack G.A.; Phys. Rev. 122 1451 (1961)

Sundstrom D.W.; Chen B.Y.; J. Composite Materials 4 133 (1970)

Tarasov V.V.; Zh. Fis. Khim. 24 111 (1950)

Tarasov V.V.; Phys. Stat. Sol. 20 37 (1967)

Woodside W., Messmer J.H.; J. Appl. Phys. 32 1688 (1961)